VYSOKÉ UČENÍ TECHNICKÉ V BRNĚ
BRNO UNIVERSITY OF TECHNOLOGY

FAKULTA STROJNÍHO INŽENÝRSTVÍ
ÚSTAV FYZIKÁLNÍHO INŽENÝRSTVÍ

FACULTY OF MECHANICAL ENGINEERING
INSTITUTE OF PHYSICAL ENGINEERING

FATIGUE PROPERTIES OF MAGNESIUM ALLOY AZ31
ÚNAVOVÉ VLASTNOSTI HOŘČÍKOVÉ SLITINY AZ31

DIZERTAČNÍ PRÁCE
DOCTORAL THESIS

AUTOR PRÁCE   Dr. Ing. ZUZANA ZÚBEROVÁ
AUTHOR

VEDOUCÍ PRÁCE   Prof. RNDr. PAVEL ŠANDERA, CSc.
SUPERVISOR

ŠKOLITEL SPECIALISTA   Prof. RNDr. LUDVÍK KUNZ, Dr.h.c.
SPECIALIST SUPERVISOR

BRNO 2009

Tato doktorská práce byla vypracována na Ústavu fyziky materiálů, Akademie věd České republiky, v. v. i., Žižkova 22, 616 62 Brno, Česká republika a na Ústavu materiálových věd, Technické univerzity Clausthal, Agricolastrasse 6, 38 678 Clausthal-Zellerfeld, Německo.

This doctor`s thesis has been performed at the Institute of Physics of Materials, Academy of Sciences of the Czech Republic, Žižkova 22, 616 62 Brno, Czech Republic and at the Institute of Material Sciences, Clausthal University of Technology, Agricolastrasse 6, 38678 Clausthal-Zellerfeld, Germany.

Abstract

Magnesium alloy AZ31 was studied in this work. Material was produced by three techniques, namely squeeze casting (SC), hot rolling (HR) and equal channel angular pressing (ECAP). ECAP is one of the methods of severe plastic deformation (SPD) suitable for production of materials with extremely fine microstructure. One of the goals of this work was to find optimal parameters of the ECAP process for the studied alloy.

The microstructure and texture of the three conditions of AZ31 significantly vary. Processing by ECAP results in the smallest grain size, whereas the SC material has extremely coarse-grained structure. The differences in texture and microstructure influence the mechanical properties of alloy AZ31 substantially.

Tensile and fatigue tests were performed and material responses for all three conditions of AZ31 were experimentally determined, mutually compared and discussed in terms of differences in microstructure and texture. The highest tensile strength was observed for HR material, while the highest ductility was found for material processed by ECAP. Material processed by ECAP and HR material has higher fatigue resistance and fatigue strength than the SC material. However, it was found that the fatigue lifetime is not further improved by ECAP process; HR material exhibits better fatigue performance. This up to now not published effect was discussed and explained. Research of fatigue notch sensitivity show that the SC material is notch insensitive while material processed by ECAP and HR material is strongly notch sensitive. No frequency effect on fatigue behaviour of magnesium alloy AZ31 was observed for all three conditions examined in very broad frequency range.

Results of this work show that for successful engineering application of Mg alloys it is necessary to choose the proper material condition for particular application.

Key words

Abstrakt

Disertační práce je zaměřena na hořčíkovou slitinu AZ31. Materiál byl zpracován třemi různými technologiemi, jmenovitě tlakovým litím (SC), válcováním za tepla (HR) a metodou označovanou „equal channel angular pressing" (ECAP). ECAP je jedna z metod využívající intenzivní smykovou plastickou deformaci k přípravě jemnozrnného materiálu. Jedním z cílů práce bylo naleznout optimální parametry ECAP procesu pro zpracování studované slitiny.

Mikrostruktura a textura zkoumaných tří stavů hořčíkové slitiny AZ31 se vzájemně výrazně liší. Mikrostruktura materiálu, který byl zpracován metodou ECAP, vykazuje nejmenší zrno, zatímco litý materiál má mikrostrukturu s největším rozměrem zrna. Velké rozdíly v mikrostruktuře a textuře výrazně ovlivňují mechanické vlastnosti hořčíkové slitiny AZ31.

Experimentálně byly stanoveny tahové a únavové charakteristiky všech tří stavů slitiny AZ31. Výsledky experimentů byly porovnány a diskutovány s ohledem na mikrostrukturní a texturní rozdíly. Nejvyšší pevnost v tahu byla zjištěna u válcovaného materiálu, zatímco nejvyšší tažnost u materiálu zpracovaného metodou ECAP. Válcovaný a ECAP materiál mají vyšší únavovou odolnost a únavovou pevnost než materiál litý. Novým zjištěním je skutečnost, že slitina AZ31 zpracovaná metodou ECAP nevykazuje žádné další zlepšení únavových charakteristik ve srovnání s válcovaným materiálem, který má nejlepší únavové vlastnosti. Toto zjištění je v práci diskutováno a vysvětleno. Výzkum únavové vrubové citlivosti prokázal, že litý materiál je vrubově necitlivý, kdežto válcovaný materiál a materiál zpracovaný metodou ECAP vykazují vysokou vrubovou citlivost. Experimentální pozornost byla věnována vlivu frekvence zatěžování na únavové charakteristiky. Bylo zjištěno, že změna frekvence zatěžování ve velmi širokém intervalu nemá vliv na únavové charakteristiky.

Výsledky této práce ukazují, že materiál s nejmenším zrnem nemusí nevyhnutelně znamenat nejlepší volbu pro inženýrskou praxi. Úspěšná praktická aplikace hořčíkové slitiny AZ31 vyžaduje velmi zevrubné posouzení vlastností použitého stavu materiálu ve vztahu ke konkrétnímu způsobu namáhaní konstrukčního dílu.

Klíčová slova

Únavové vlastnosti, jemnozrnné materiály, hořčíková slitina, AZ31, ECAP, intenzivní plastická deformace, textura.

Prohlášení

Prohlašuji, že tato doktorská práce byla vypracována samostatně a že všechny použité literární zdroje jsou spravně a úplně citovány.

V Brně 21.01.2009

podpis autora

Acknowledgements

To my grandparents

Content

1 Introduction

Since many decades, the requests on materials and their properties have been continuously increasing. The efficiency of components and the safety parameters have to be higher but on the other hand, the prize as well as components weight have to be lower. Broad variety of structural applications is used rather under cyclic loading than static one. This leads to demands of good knowledge of fatigue performance of engineering materials. Fatigue is a general phenomenon of material failure, which appears after repeated cycles of loading at a stress level below the ultimate tensile stress [1]. Material fatigue is defined as a loss of strength due to microstructural damage that is created step by step during cyclic loading. Indeed, it is necessary to avoid such damage. To fulfil this demand, research of fatigue damage of materials and in some cases also the whole structural components is unavoidable. Deep knowledge of fatigue may save high costs of reparations and even more important, not risk health or life of humans.

Since the last years, due to increasing demands of fuel savings, the main interest of the industries is to decrease the weight of components. The magnesium alloys start to be a very interesting and important material. It is because of the high strength/weight ratio of magnesium alloys. For example, the density of magnesium is of 1/4 of that of iron and 2/3 of aluminium. Magnesium alloys have other positive properties as for example high dimensional stability, high damping ability and good machinability. These characteristics of magnesium alloys speak for applications in automotive and aerospace industry as well as in computer and mobile phones branches. Magnesium is also easily reachable. It may be exploited from the oceans because 0.13 wt. % of oceans is composed from magnesium. Further, approx. 1.93 % by mass is in the earth crust. It makes magnesium the eight most abundant element on the earth. As everything in real life also magnesium and its alloys have undesirable properties. Here belong poor wear, creep and corrosion resistance. These disadvantages may be a limitation for some applications. However, if magnesium alloys should be used in real engineering applications, it is essential to know their fatigue behaviour. It is necessary to know and understand the material damage processes and the responses during their employment. Very important is, that material properties strongly differ in dependence on production processes.

One of the oldest and basic magnesium alloys, namely AZ31, was used for purpose of this work. This magnesium alloy contents approx. 3 wt.% of aluminum and 1 wt.% of zinc. The magnesium alloy AZ31 was produced by three following techniques: first the very well known and commonly used squeeze casting. The second production technique is also well known and it is hot rolling. The third technique is new, and till now used only in research laboratories. This technique is equal channel angular pressing (ECAP). ECAP is a quite promising technique of severe plastic deformation which enables to produce homogeneous material with extremely fine microstructure. This is promising from the point of view of improvement of mechanical properties. In order to make deeper understanding of fatigue properties of these three conditions of AZ31, the microstructure and texture observations have to be done. Results of these observations were compared, evaluated and discussed. Further, the monotonic tensile properties of all three conditions of AZ31 were examined with the aim to find out and explain which of the three conditions of AZ31 has the best strength and straining characteristics. However, the main focus of this work is given on fatigue behavior of all three conditions of AZ31. The fatigue endurance and fatigue strength as well as notch sensitivity and frequency effects are determined, compared and discussed. Cyclic plastic response of the material in all three conditions was examined too. This brings new information not only about properties of AZ31, which was up to now a matter of research in

some papers, but also about ECAP condition of AZ31. This is essential, because the data dealing with fatigue properties of magnesium alloys processed by equal channel angular pressing are completely missing in the open literature. There is also no work comparing different conditions of magnesium alloys as regards fatigue notch sensitivity, influence of loading frequency and cyclic plastic response. It is proving important for engineers to take into account differences among these three conditions. In this work the differences in properties of particular materials are tried to be explained on the basis of microstructure and texture details.

The results of this work show that different processing techniques lead to substantially different material properties of magnesium alloy AZ31. It is not possible unambiguously to say which of the three conditions of AZ31 has the "best" properties over the others. However, the results should help to decide which particular condition is suitable for a certain application. The appropriate technique has to be chosen by considering the specific demands of the application. Thus, the goal of this work is to build a small data base that may help to make a proper decision for engineers.

2   Severe plastic deformation and conventional production methods

2.1   Severe plastic deformation

Methods of severe plastic deformation (SPD) are interesting due to one main reason – they can create very fine grained structures. Materials processed by methods of severe plastic deformation have ultra-fine grained microstructure, which means that grains are in range of 100 – 1000 nm. It is not possible to obtain such grain size by any conventional production methods, as for example rolling, extrusion or casting. The fine grained materials are very interesting due to their better mechanical properties. It is expressed by the Hall-Petch equation. The tensile strength increases with decreasing grain size. This is the main driving force for extensive research and development of severe plastic deformation techniques. Presently, in the scientific world, there is a broad variety of SPD techniques (in alphabetical order):

- Accumulated Roll-Bonding (ARB); cf. Fig. 2.1, [2]
- Cyclic Extrusion Compression (CEC), cf. Fig. 2.3, [3]
- Equal Channel Angular Pressing (ECAP)
- Friction Stir Processing (FSP), [4]
- High Pressure Torsion (HPT), cf. Fig. 2.2, [5]
- Multi-Axis Forging / Deformation (MAD), [6]
- Multi Directional Forging (MDF), [7]
- Multipass Coin-Forging (MCF), cf. Fig. 2.4, [8]
- Repetitive Corrugation and Straightening (RCS), cf. Fig. 2.5, [9]
- Twist Extrusion (TE), cf. Fig. 2.6, [10].

These techniques differ in deformation level and in deformation mode. They lead to materials having not only different grain size, but also texture, final shape or size. The choice of the best technique strongly depends on the application objective.
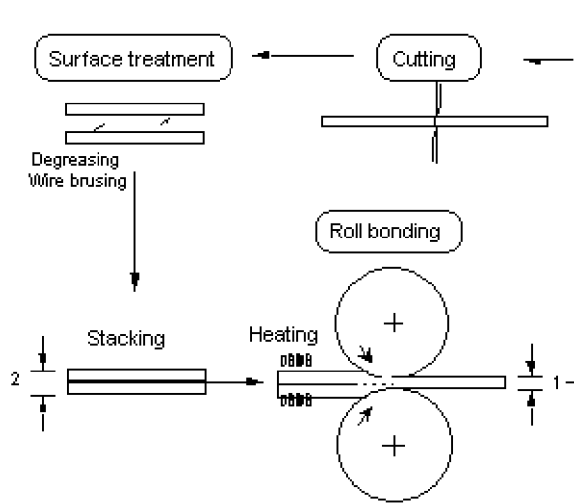
Fig. 2.2 Accumulative Roll Bonding (ARB), [11]
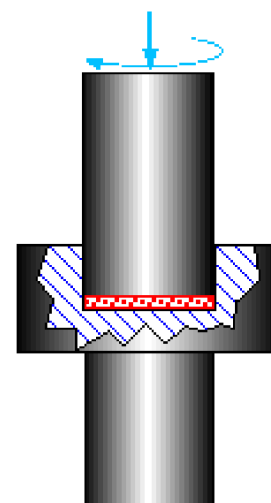
Fig. 2.1 High Pressure Torsion (HTP), [5, 12, 13]
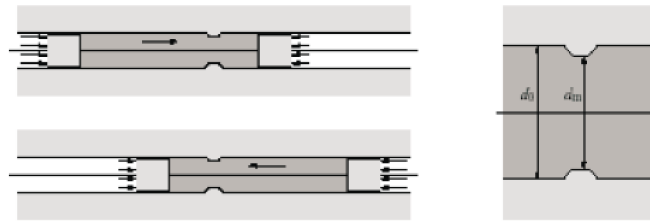
Fig. 2.3 Cyclic Extrusion Compression [3]
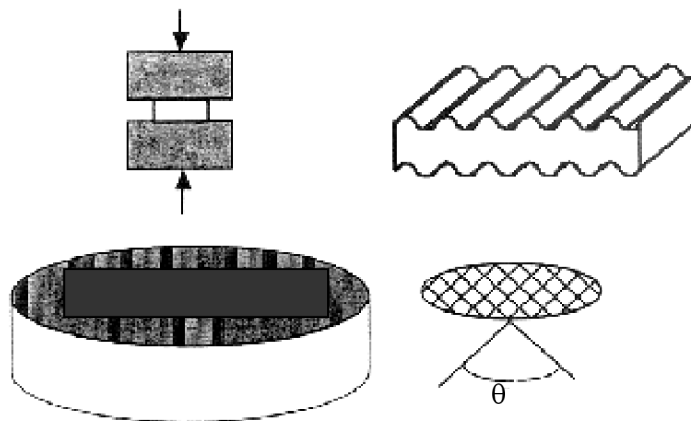
Fig. 2.4 Multipass Coin-Forging (MCF), [8]
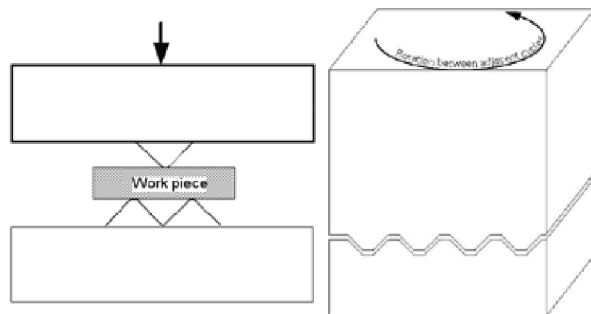
Fig. 2.5 Repetitive Corrugation and Straightening (RCS), [9, 14 - 16]
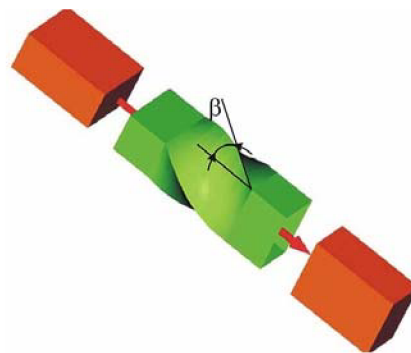
Fig. 2.6 Twist Extrusion (TE), [10]

The most used and for engineering practice the most suitable method is equal channel angular pressing (ECAP). By using this process bulk samples can be produced. Samples of approx. 25 mm in diameter can be processed. The production of a big bulk sample is one of the advantages of ECAP process when compared to other SPD techniques. For example the size of a specimen produced by HPT is usually only 10 mm in diameter and less than 1 mm in length. It is too small for many real applications. Further, the microstructure of ECAP specimens is uniform and homogenous in the whole bulk. The next advantage of ECAP is the possibility of its incorporation into continuous production operations, such as:

- Conshearing, cf. Fig. 2.7, [17]

- Continuous Confined Strip Shearing (C2S2), cf. Fig. 2.8, [18, 19]
- ECAP-Conform Process, cf. Fig. 2.9, [20].
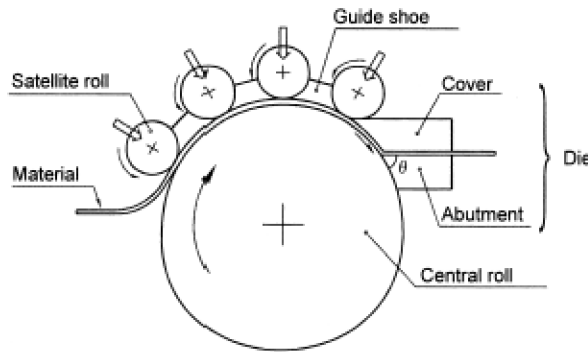
Fig. 2.7 Conshearing Process [17]
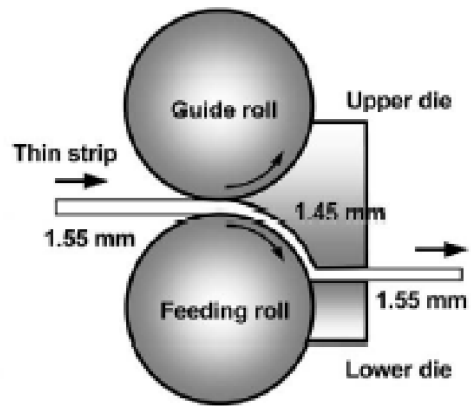
Fig. 2.8 Continuous Confined Strip Shearing (C2S2), [19]
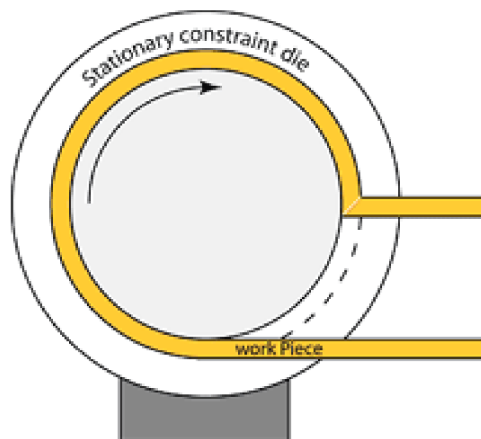
Fig. 2.9 ECAP-Conform [20]

Many scientific groups on the world have been focussing their research on SPD since the last decade. This may be the reason why the terminology in the literature associated with ECAP is not clearly defined yet. The same procedure has been designated as equal channel angular extrusion (ECAE), channel angular forging (ECAF) and equal channel angular pressing (ECAP). However, the International NanoSPD Steering Committee (www.nanospd.org) has approved the last acronym for general use [21]. Thus ECAP acronym will be used throughout this work.

During the last decade, the applications of severe plastic deformation (SPD) on bulk solids have become an established procedure for production materials with submicrometer or nanometer grains [22 - 28]. However, the knowledge of microstructural details and their influence on mechanical and especially fatigue properties of the materials processed by SPD are still quite poor and sometimes even contradictory. The main task of scientists is to develop a SPD method for specimen mass production with well defined and characterized material properties. Further, the SPD method has to be also easy reproducible. Only then, this production method and the materials produced by it, may find broad use in real engineering applications. The materials produced by SPD should meet these requirements: a) most of the

grain boundaries should be with high angle missorientation; b) homogeneous and uniform microstructure in the whole volume of the specimen and c) no cracks or any other defect in/on the specimen.

Equal channel angular pressing

As it was already pointed above, ECAP is a well established SPD method for producing ultrafine grained materials. ECAP won the attention over the more conventional industrial processes, such as rolling, extrusion or drawing due to several advantages. The sample is deformed without changes in cross-sectional dimensions. It is relatively easy to set up and use ECAP equipment. Further, the ECAP samples can be scaled up to produce relatively large bulk material. These characteristics of the ECAP technique are useful for real applications as for example in the medical or aircraft industry [29].

ECAP process is based on plastic deformation by simple shear. A coarse grained material deformed through ECAP die due to the very large strains results in fine grained microstructure with majority of high angle boundary grains. This process has been examined by many authors [5, 23, 28 - 40].

The ECAP idea is relative easy. A schematic illustration of the ECAP procedure is shown in Fig. 2.10. The ECAP rig consists of a die and a plunger. The die comprises of a channel that is bent at an angle. The channel geometry can be a circular or rectangular in cross-section. A sample is machined in a way to fit into the entrance channel that is in the most cases the vertical one. Consequently, the specimen geometry depends on the channel geometry. For the rectangular channel, the specimen has to be rectangular as well and opposite, for the circular channel the specimen has to be circular. The sample is pressed through the die into the exit channel (horizontal one) using a plunger. And since the cross-sectional dimensions of the sample are not changed during this process, it gives the possibility of a repetitive pressing process (see below). It permits accumulating very large strains [23, 30, 41 - 43]. It is very important as this leads to further refinement of microstructure and increment of high angle boundary grains.
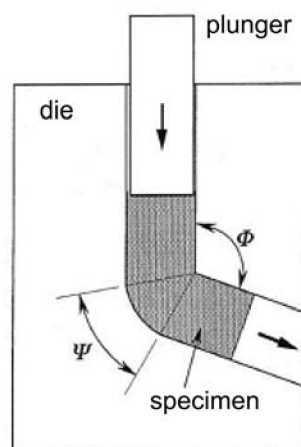
Fig. 2.10 ECAP angles $\Phi \neq 90°$ and $\psi \neq 0°$ [26].

The strain imposed on the sample in each pass through the die depends mainly on the angle, Φ, between the two channels of the die (Figs. 2.10) and also to a minor extent upon the angle of curvature, ψ, representing the outer arc of curvature where the two channels intersect. To achieve optimum results, ECAP is generally conducted using the die with a channel angle

of $\Phi = 90°$. With this geometry it can be shown that the imposed strain in each pass is approximately equal to 1 with only minor and almost negligible, dependence upon the arc of curvature ψ, see Eq. 2.1 [44]. The angle between the channels is one of the aspects, which influence the final microstructure [26, 45].

$$\varepsilon = \frac{1}{\sqrt{3}}\left[2\cdot\cot\left(\frac{\Phi}{2}+\frac{\Psi}{2}\right)+\Psi\cdot\mathrm{cosec}\left(\frac{\Phi}{2}+\frac{\Psi}{2}\right)\right] \qquad (2.1)$$

The repetitive ECAP process means that the sample is rotated about the longitudinal axis between each pass. Four processing routes are commonly used for ECAP, see Fig. 2.11. In Route A the specimen is pressed repetitively without any rotation, in Route B_A the specimen is rotated by 90° in alternate senses after each pass, Route B_C involves rotation by 90° in the same sense after each pass and finally Route C in which the sample is rotated by 180° between passes. It is very important to distinguish between these routes, since each route introduces different shearing patterns into the sample. It leads to a variation of the macroscopic distortions of the individual grains in polycrystalline matrix and in the capability to develop a reasonably homogeneous and equiaxed ultrafine or fine-grained microstructure. Required structures and textures are influenced by chosen route [23, 35]. Additionally, the properties of the materials differ strongly regarding to the applied route [25, 26 and 41]. In many cases the route B_C is used because so processed material shows the most homogeneous structure [26, 30, 38 and 46]. The important consequence of repetitive ECAP pressing is that the grain size decreases with increasing number of passes [47].
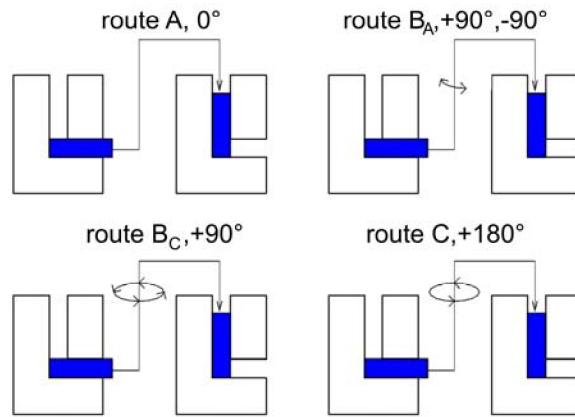
Fig. 2.11 Schematics of the ECAP routes.

Additionally, the ECAP process forms equiaxed fine grains with a large proportion of high-angle grain boundaries and it also introduces into the material a high dislocation density and internal stresses [5, 27, 38]. It is true that the grain size decreases with increasing strain, but only to a certain minimum size. This size strongly depends on the SPD conditions as a method, process temperature and a pressing speed. Even, when the minimum grain size is reached then a further increase of the fraction of high-angle grain boundaries is observed. It means that with further straining the amount of grains with high angle boundaries increases [5].

The ECAP process may be conducted at different temperatures. ECAP process at room temperature runs without any problems for many materials as for example Cu, Fe, aluminium alloys as Al6082 and etc. On the other hand, many materials due to their lattice

structure or chemical composition are difficult or not possible to process by ECAP at room temperature and an application at an elevated temperature is necessary for a successful process. Otherwise cracks or other defects may appear in the material. One group of these materials are magnesium alloys. They require processing at elevated temperature. The reason for it is their hexagonal structure. This gives certain limitations to obtain fine grained structure in materials processed at elevated temperatures. Small grains are achieved, when ECAP is performed at the lowest possible temperature [47, 48]. This is due to dynamic grain growth or dynamic recrystallization because they are more pronounced at higher temperatures.

2.2   Conventional production methods

Hot rolling

Rolling is well known, old and established deformation process. It belongs to the conventional production techniques and simultaneously, it is one of the applied production techniques on material used in this work. During the rolling process, the material is deformed between a set of work cylinders, Fig. 2.12. The material after deformation has sheet geometry. It means large size in two dimensions and very tiny in one dimension. Generally, rolling process is classified according to the temperature. If the temperature is above the recrystallization temperature then the process is referred to as a hot rolling. If the temperature of the process is below the recrystallization temperature the process is termed a cold rolling.

Most wrought magnesium alloys are processed at elevated temperatures because of their very low ability to shape [49]. Hot rolling of magnesium alloys requires a large number of rolling cycles with a small reduction step. Generally, by hot rolling, homogeneous microstructure with grain size in the range of 10 - 30 µm can be reached. However, magnesium alloys with much larger grain size after hot rolling are observed as well. Also here, as in the case of ECAP process, the grain size of deformed material decreases with decreasing rolling temperature [50].
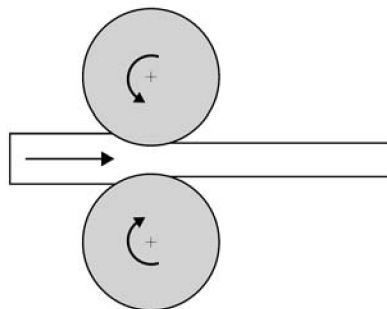
Fig. 2.12 Principle of hot rolling.

Mechanical properties of materials in their final as-rolled state depend, as in case of ECAP, on many factors: material chemistry, reheating temperature, rate of temperature decrease during deformation, rate of deformation, heat of deformation, total reduction, recovery time, recrystallisation time and subsequent rate of cooling after deformation [51]. These are a variety of aspects that influence the material microstructure. They lead to extremely diverse grain size.

Squeeze casting

Squeeze casting is one of the often used casting methods. Its main advantage is a low porosity of the material when compared to other cast techniques. Low porosity normally improves the mechanical properties of materials. Squeeze casting is described as a combination of casting and forging process. The principle of this casting is shown in Fig. 2.13. Prior to casting, a die is pre-heated. Only then, the molten metal is poured into the bottom half of the die. As the metal starts to solidify, the upper half closes the die. Consequently, during the solidification process, pressure on the material is applied. This amount of applied pressure is significantly less than that used in forging. By squeeze casting hollow parts may be produced. To do that a coring is used.
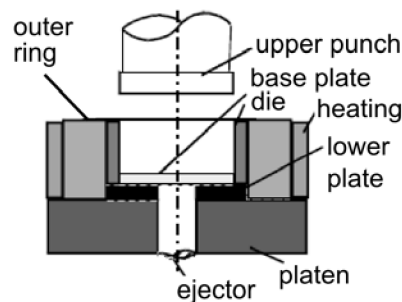
Fig. 2.13 Principle of squeeze casting [52].

Apart of low porosity, this process has also other advantages when compared to other casting processes. The grain size of materials after squeeze casting is generally smaller then after processing by other casting techniques (sand casting, gravity casting and etc.). This is the positive effect of the applied pressure during casting. For example grain size of magnesium alloy after squeeze cast has approximately 300 μm [53, 54]. However, the positive result in microstructure depends on many factors as for example: the chemical composition of materials, if the material has a grain growth refiner or grain growth impeder during solidification, casting temperature and cooling rate.

As by every casting also by squeeze casting, casting defects may appear during the process. The formation of casting defects often depends on the solidification. The large solidification range leads to the formation of micro shrinkage, which is additionally favoured by the dendritic structure [55]. Materials, as for example Mg-Al alloys, display a wide freezing range. They are therefore susceptible to a range of casting defects including segregation, porosity and hot tearing [56]. In the case of magnesium alloys the amount of porosity is strongly affected by the Al content. The highest porosity was observed for Mg-Al alloy with the Al amount of 9 wt. % [56]. Another reason for introducing casting defects may lie in the processing route used. For example under high casting speed the melt flow is non-laminar and trapped air can cause porosity when the melt solidifies [55].

All introduced methods have advantages and disadvantages. It is important to choose the proper technique and processing parameters for each material depending on its purpose.

3   Magnesium alloys and their mechanical properties

3.1   Magnesium alloys

Magnesium itself and magnesium alloys are the lightest metallic structure materials with a high specific strength. This makes them very attractive for a broad variety of applications in automotive, aerospace and other branches of industry [49, 57 - 59]. Magnesium alloys are used e.g. in airbag housings, door frame/inner, oil/water housings, for clutch and brake pedals, support brackets, computer housings but also in luggage, ladders and etc.

Two letters and two numbers designate magnesium alloys. The letters represent two elements in the material with the highest amount. The numbers mean weight percentage of those two elements. For example, magnesium alloy AZ91 means that aluminium and zinc are the two main elements present in the alloy. There is 9 wt.% of Al and 1 wt.% of Zn.

Generally magnesium alloys can be divided in four main groups:

1   Zirconium free alloys
          Magnesium-aluminium system
          Magnesium-zinc system
          Magnesium-zinc-copper
          Magnesium-rare-earth-zinc

2   Zirconium containing alloys
          Magnesium-zinc-zirconium alloys
          Magnesium-rare-earth-zinc-zirconium
          Magnesium-thorium system
          Magnesium-silver system
          Magnesium-yttrium-system

3   Amorphous magnesium alloys

4   Metal matrix composites

This work is focussed on one magnesium - aluminium system. There are many groups of these systems; the following belong to the most important: AZ (Mg-Al-Zn), AM (Mg-Al-Mn), AS (Mg-Al-Si-Mn), AX (Mg-Al-Ca), AJ (Mg-Al-Sr) and ZACE (Mg-Zn-Al-Ca-RE). This work is focused just on AZ system, and, particularly on AZ31. The Mg-Al series is the oldest and the mostly used magnesium alloy system since the World War I. The typical aluminium content of Mg-Al alloys is in range of 1 – 9%. The Mg-Al-Zn alloy system (AZ31, AZ61, AZ81 and AZ91) is typically used for wrought products. AZ alloys can be extruded at temperatures in the range of 300 to 450°C. Both the solid and hollow profiles are produced. Forging represents just a small volume of wrought magnesium products. The reason for it is that they can be fabricated only from fine-grained magnesium alloys. Forging is often applied to produce components of intricate shape and when strength higher than that achievable with cast material is required [49]. Still, over 90% of magnesium alloys are produced by casting [60].

Magnesium alloy AZ31 was selected as studied material of this work. AZ31 is one of the mostly examined magnesium alloys; thus a broad literature data exists. However, as it will

be shown in the next, there are still many aspects of the mechanical behaviour that are not clearly and completely understood yet.

General properties of magnesium alloy AZ31 are the following:

- high strength / weight ratio
- very easy machinability in mean of a depth of cut, speed, tool wear and relative amount of
  power required for the equipment being used [49]
- good casting properties
- moderate creep resistance up to ca 110°C (for AZ31)
- low and moderate corrosion resistance
- low formability at room temperature
- low thermal stability
- suitable for bio-degradable implants
- weldable
- possibility of strengthening by strain hardening.

Properties of magnesium alloys are influenced by many internal and external parameters. The internal factors are hexagonal crystallographic lattice structure and chemical composition. The external ones are manufacturing way, fabrication details, and heat treatment.

$\{0001\}<11\bar{2}0>$ $\{1\bar{1}00\}<11\bar{2}0>$ $\{1\bar{1}01\}<11\bar{2}0>$ $\{11\bar{2}2\}<11\bar{2}3>$

Basal plane   Prismatic plane   Pyramidal planes
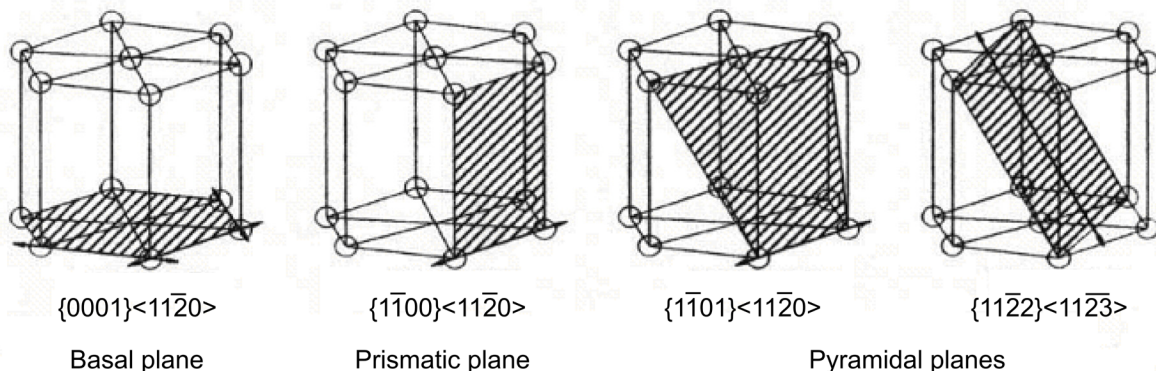
Fig. 3.1 Slip planes and slip directions in a hexagonal close packed crystal [61].

The formability of magnesium alloys is strongly affected by lattice structure. The hexagonal lattice structure of magnesium alloys means limitation of slip and twinning modes at room temperature [62]. Mg alloys do not have sufficient number of active slip systems at room temperature. Since, the formability of the materials is given by the number of independent slip systems; the texture has a big influence on mechanical properties [63, 64]. In Mg and Mg alloys only basal slip systems $\{0002\}$, with a slip direction $\langle 11\bar{2}0 \rangle$ are available for deformation at room temperature. Those are only two independent active slip systems available, cf. Fig. 3.1. It means the material does not match the required five independent slip systems for general ductility [59, 63, 65 - 68]. Thus twinning is very important for formability of Mg alloys [63, 65, 69 - 71]. Twinning occurs in crystallites that are unfavourably oriented for dislocation glide. Twinning in $\{10\bar{1}2\}$ $<10\bar{1}1>$ is favoured when the tensile load is perpendicular to the basal plane or a compression load is parallel to the basal plane cf. Fig. 3.2 [65, 67, 72, 73]. By contrast, $\{10\bar{1}1\}$, $\{11\bar{2}1\}$, and $\{11\bar{2}2\}$ twins are activated in opposite

direction [65]. The non-basal slip systems; prismatic slip system $\{10\bar{1}0\}\langle11\bar{2}0\rangle$, and pyramidal slip $\{10\bar{1}1\}\langle11\bar{2}0\rangle$, $\{10\bar{1}2\}\langle11\bar{2}0\rangle$ or $\{11\bar{1}2\}\langle11\bar{2}3\rangle$ are active at elevated temperatures [67, 68, 74 - 76]. The prismatic slip gives two independent slip systems. Those together with two of basal slip systems give still only four independent slip systems. When pyramidal slip systems are activated as well then next four independent slip systems are present [77]. The role of twins is not only to provide additional deformation system. Twins act as barriers for dislocation slip and give rise to work hardening [66]. Additionally, twins may be seen as a source of dynamic recovery.
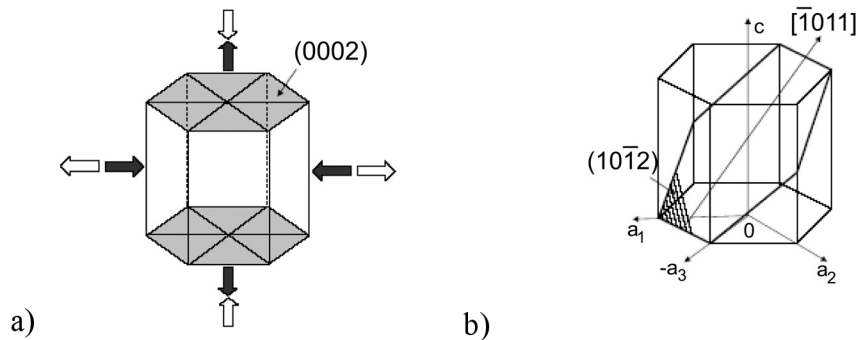
Fig. 3.2 a) Relationship between the orientation of favourable $\{10\bar{1}2\}$ twinning and the applied loading directions with respect to the c-axis of hcp-Mg. The black arrows indicate the applied loading directions for favourable twinning; the white arrows indicate the applied loading direction for unfavourable twinning; b) The $\{10\bar{1}2\}$ tensile twinning system [67].

Since the slip system scarcity in hcp metals at room temperature, plastic forming is difficult. Extrusion, rolling and ECAP have to be performed at elevated temperatures. Consequently, different production methods result in development of different microstructures and textures. In a great deal the texture variety of magnesium alloys strongly influences the mechanical properties [58]. The mechanical properties as the yield locus, tensile and compressive strength, are generally anisotropic. This effect is well seen in the case of tensile and compressive behaviour of magnesium alloy AZ31, cf. Fig. 3.3.
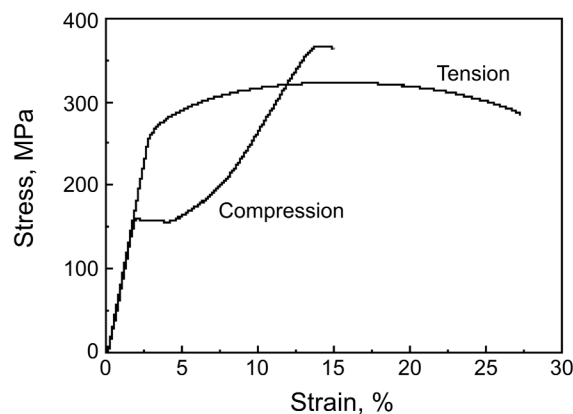
Fig. 3.3 Engineering compressive and tensile stress vs. strain curves, AZ31 extruded, loaded parallel to the extrusion direction [67].

3.2   Texture and grain size of magnesium alloys

In next, the influence of production techniques on the final microstructure of magnesium alloys in terms of texture and grain size will be briefly introduced.

Texture

Extrusion leads to orientation of the basal planes normal and the $<10\bar{1}0>$ directions approximately perpendicular to the direction of extrusion. This texture is called fibre or cylindrical [69]. The grains of material after extrusion are commonly small and elongated in the extrusion direction.
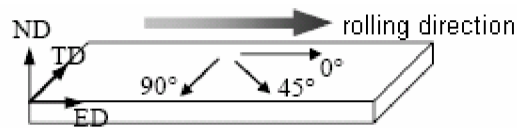
Fig. 3.4 Considered direction of the specimen related to rolling or extrusion direction [65].

Rolling process of magnesium alloys tends to orient the basal planes parallel to the surface of sheet with the $<10\bar{1}0>$ direction in the rolling direction [58, 71, 73 -75, 78 - 80]. This texture is named centre type. The basal plane prefers to align in the higher deformation direction, cf. Fig. 3.4. The basal planes are oriented parallel to the sheet plane [58]. The grain size of the magnesium alloys after rolling is relatively small ca. 20 - 50 μm. However the influence of dynamic recrystallization (DRX) due to the elevated temperature during the rolling process has to be considered.
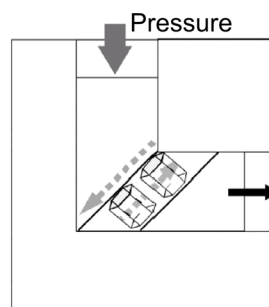
Fig. 3.5 The basal plane orientation in Mg developing in the ECAP process [81].

Equal channel angular pressing is a new production method. It can be expected that it results in a special texture. However, until now, this effect was not studied in sufficient details. Generally, texture can be of significant interest for modifying the material properties. It is important to say that the majority of the texture observation was done on cubic metals as Al, Cu, Fe and their alloys. Information about hexagonal materials is not very broad [59, 72]. The available literature data show that the texture of deformed magnesium alloys by ECAP has the basal plane (0002) parallel to the shear plane. It means, the basal planes are tilted ~45°

to pressing direction, cf. Fig. 3.5 [31, 42, 59, 81 - 84]. Consequently also the prismatic planes are inclined about 45° to the ECAP direction. The grain size of magnesium alloys after ECAP is extremely small but also here, as in the case of rolling or extrusion, the effect of DRX cannot be forgotten.

Casting process tends to create no particular texture or better to say it leads to a random texture. It means there is no major orientation. Consequently, the material after casting does not show any significant anisotropy of the properties. The grain size of the cast magnesium alloys is commonly large and it is in a range of several hundreds μm till mm.

Above described types of textures are however simplified. The final texture is influenced by c/a-ration of each particular magnesium alloy, chemical composition, strain rate and temperature. These factors influence the activity of different deformation modes [65, 69]. The material textures developed by conventional deformation methods are limited. Due to it the possibly positive effect of ECAP texture on the properties of magnesium alloys is very interesting. The first research works dealing with the influence of ECAP texture on material properties of magnesium alloys are reported by Mukai et al. [81] and Agnew et al. [72].

Grain size

It is well known that the fine-grained microstructure improves strength at ambient temperature as well as plastic formability of Mg alloys [85]. As it was mentioned in Sec. 2, there are different techniques to reduce the grain size of materials. It is expected, the ECAP process provides a much smaller grain size when compared to hot rolling and squeeze casting. It is due to the intensive plastic shear deformation and lower processing temperature of ECAP. The microstructure refinement by ECAP will be explained more closely.

(A)   (B)   (C)   (D)
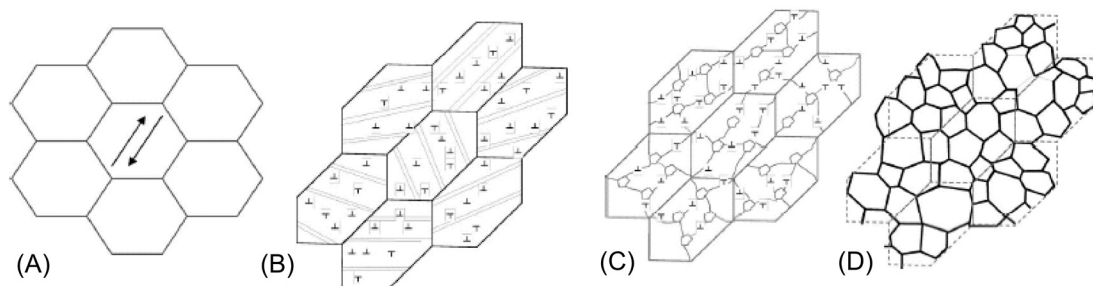
Fig. 3.6 A dislocation cell structure formation that gradually transforms to a new grain structure during ECAP of Mg above room temperature showing: A) equiaxed and coarse-grained microstructure; B) immediately after shear deformation; C) shortly after deformation; D) recrystallized grains [68].

The grain refinement model of Mg alloy is schematically shown in Fig. 3.6 [68]. During the deformation dislocations are generated and accumulated in the initial grains. Due to dislocation accumulation the driving force for recrystallization is high. The next effect helping to recrystallization is an elevated temperature of ECAP process. It leads to a rearranging of dislocations and nucleating strain free grains. The new grains nucleate within shear bands and along grain boundaries. The dislocations are rearranged via glide and climb. The rearranged dislocations form new sub-grain structures within the grains and so they lead to a gradual formation of new grain boundaries. This transformation appears directly after shearing due to the high stored strain energy that is accelerated by heat during the process.

The new grain boundaries transform into high angle boundaries as a results of trapped dislocations at the low angle boundaries trying to pass through them.

The temperature of ECAP process is closely related to the grain refinement. Low processing temperature and short time result in more effective grain refinement when compared to processing at high temperatures and long processing times. A process at a high temperature causes rapid grain growth in material. Grain refinement is more pronounced when deformation processes are conducted at low temperature.

3.3   Tensile properties

The tensile properties of magnesium alloys are influenced by material and external loading parameters. Texture and microstructure are inherent material factors, whereas to the external parameters belong testing temperature [33, 60, 86 - 100], strain rate [5, 59, 60, 63, 82, 87, 92, 101 - 117] and loading mode [118, 119]. The focus of this work will be given on tensile properties at room temperature.

Tensile properties of magnesium alloys with different texture

The tensile properties of extruded or rolled magnesium alloys depend strongly on the loading direction. They show a strong anisotropy of the properties. This anisotropy is well seen in Fig. 3.7, showing results of experiments on three specimens tested in three directions. The tensile loading direction 0° denotes that the longitudinal axis of the specimen was in the extrusion direction. It means, the basal plane (0002) was perpendicular to the tensile loading direction. Direction 90° corresponds to the loading direction (LD) perpendicular to the extrusion direction. In this case the basal planes were parallel and perpendicular to LD. The loading direction of 45° means that the specimen was tilted 45° to the loading direction. Here, the texture is a combination of basal planes and prismatic planes inclined at about 45° to LD [65].
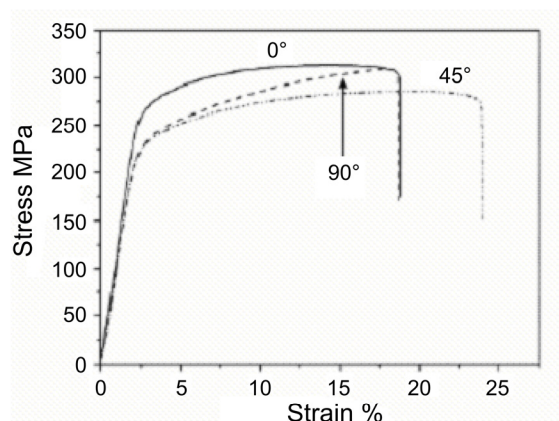
Fig. 3.7   Tensile   stress-strain   curves   for extruded AZ31 [65].

The 0° sample shows the highest yield strength as well as the ultimate tensile strength. The lowest value of ultimate tensile strength was determined for the 45° sample. The highest strain was observed for the 45° specimens [65]. This behaviour was explained by different intensity of particular deformation modes for these three loading directions [51, 53 and 65]. In

0° oriented sample the hexagonal c-axis is normal to the tensile loading direction. In this case no slip and twinning can be activated easily. To activate these deformation modes a high stress is necessary [72, 75 and 120]. For this reason the high yield strength is observed in this sample. The specimen with basal planes oriented 45° to the loading direction has a favourable position for slip. It explains the lower yield stress and higher ductility when compared to the 0° specimen. When the specimen basal planes are oriented 90° to the loading direction, then the twinning is activated easily. It leads to lower yield stress as in the case of 0° sample. But due to the hardening effect of twins, the 90° specimen has lower ductility as the specimen oriented 45° to LD [65].

The strong texture effect is shown in Fig. 3.8, where results on extruded and ECAP materials are compared. In the case of ECAP material the basal planes were inclined 45° to the loading direction, which is a favourable orientation for easy activation of the deformation modes when compared to the extruded material. The ductility is considerably improved after ECAP. Further, a higher strain hardening of ECAP material as compared to the extruded alloy was observed [81]. It is important to note that these two conditions of AZ31 (extruded and ECAP+annealed) did not differ in grain size but did in texture. Thus the different behaviour of those two conditions of AZ31 is really influenced only by different texture [81].
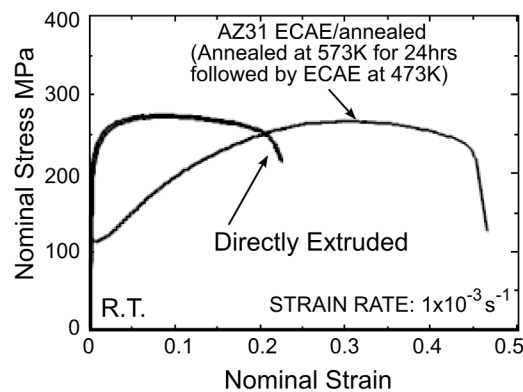
Fig. 3.8 Tensile curves of AZ31 extruded and ECAP+annealed [81]. In both cases the grain size was 15 μm.

The available data clearly show that the proper modification of texture may lead to an enhancement of the ductility of magnesium alloys despite its hcp structure. The magnesium alloys formed by ECAP show an improvement in ductility without deterioration of the ultimate tensile strength. On the other hand, their yield stress is lower than that of extruded or hot rolled alloys.

Tensile properties of magnesium alloys with respect to grain size

The grain size of the materials has a strong influence on mechanical properties. This effect is described by the well-known Hall-Petch relation [95, 121 and 122]:

$$\sigma = \sigma_0 + K d^{-1/2} \qquad , \qquad (3.1)$$

where σ_0 is the flow stress in the absence of grain boundaries, K is a constant and d is the grain size. According to this equation the fine grain structure leads to high strength [50, 81]. The ductility of fine-grained material is also generally higher than that of coarse grained

structures. Just these are the reasons why the interest of engineers and material researchers is focused on the ultrafine-grained materials.

Since the cast materials have a coarse grain structure it is expected that their mechanical properties will be the lowest when compared to the extruded structures or structures produced by ECAP. Fig. 3.9 confirms this behaviour. Generally, cast magnesium alloy show ductility of ~10 % at room temperature [59, 81]. The reason why cast materials have a relatively low formability is that the large grains do not permit easy accommodation of plastic strain incompatibility between adjacent grains. Cast hcp Mg alloys show slip anisotropy and difficulty of cross-slip within the grains [123]. In the cast materials the effect of grain size is dominant and other influences, particularly texture effects, do not play any significant role. Further, cast magnesium alloys contain defects as larger inclusions and porosity, which is not the case of extruded materials. They naturally negatively influence the mechanical properties of cast magnesium alloys [64, 124].
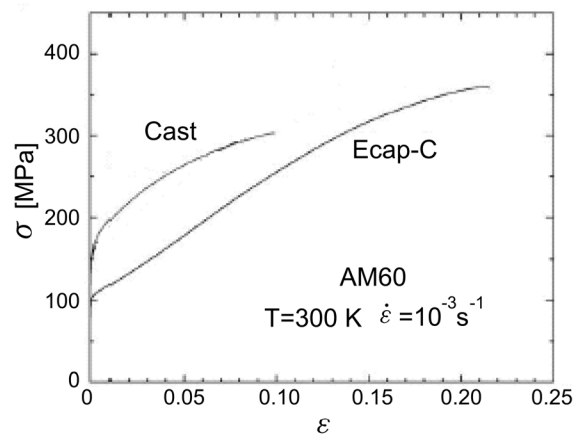
Fig. 3.9 Tensile curves of AM60 cast and ECAP processed [59].

Thus, the extruded, rolled and ECAP magnesium alloys have better mechanical properties not only because of structure with smaller grain size, but also because of absence of large defects in material itself.

The positive effect of small grain size on mechanical properties was observed by Yongjun et al. [31]. Higher tensile yield stress, ultimate tensile strength and elongation (290 MPa, 350 MPa and 10 %, respectively) was reported for $Mg_{97}Zn_1Y_2$ ECAP when compared to the cast one (yield stress of 120 MPa and elongation of 4 %). Similar results were reported in [48, 59, 66, 81 and 125].

Positive influence of small grains size together with the suitable ECAP texture on ductility of magnesium alloy is shown in Fig. 3.10. However, in this case, the material strength is not improved [83]. Similar results were published also in [84, 90, 98 and 126]. The reason of this behaviour is not fully clear yet, but a possible explanation could be in texture effect.
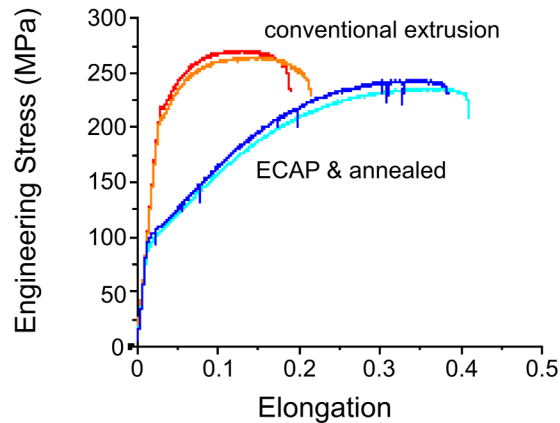
Fig. 3.10 Tensile curves of AZ31B extruded with
GS = 49 μm and ECAP with GS = 19 μm [83].

Texture vs. grain size and relation to tensile properties

The grain size effect on mechanical properties of Mg alloys is known. However, it seems that in some cases the texture effect can be more significant. This has been demonstrated on AZ91 extruded and processed by ECAP and having the same grain size and different texture [51]. The higher tensile strength and yield stress were observed for extruded material. Contrary to that, the better ductility was found for material after ECAP. This effect can be explained by favourable texture orientation of ECAP material for easy plastic deformation. Similar results were found also by Mukai et al. [81]. Their results show that the texture has most probably the dominant effect over the grain size effect on mechanical properties of magnesium alloys. When the texture of the materials is identical then the grain size effect on the mechanical properties is dominant. This tendency was shown by Somekawa et al. [82]. In this study the magnesium alloy AZ31 did not differ in texture but in grain size. As it is expected the better tensile properties were observed for small grained condition of AZ31.

So far, there is no agreement if texture or grain size has stronger effect on the mechanical properties of magnesium alloys. The majority of research papers indicate that the texture has most probably predominant effect on the properties of Mg alloys. However, further study is necessary to answer this question completely.

3.4 Fatigue

Due to increase of the exposed load on the structural parts in the engineering practice, the demands on materials increase. The load has in many cases cyclic character. This results in microscopic and macroscopic damage of material and consequently to failure of the whole component. For this reason the materials and structural parts are tested under cyclic loading. These tests are called fatigue tests.

The fact that the magnesium alloys are very attractive due to their low weight for many structural applications is not fully sufficient for their real use. The safety requirements have to be fulfilled as well. Since, applications of magnesium alloys under cyclic loading escalate, the fatigue testing of magnesium alloys and deeper understanding of the fatigue damage process are necessary [127 - 129]. A broad variety of tests is used to determine the fatigue characteristics.

The oldest and still the most used test is the determination of Wöhler curve, Fig. 3.11. The Wöhler curve is a diagram stress amplitude vs. number of cycles to failure. It is often called S – N curve. The S - N curve is a basic material characteristic, which is used for description of lifetime and endurance of fatigue limit.
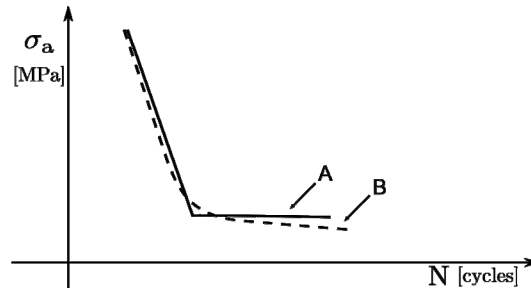
Fig. 3.11 Wöhler curve.

Not only the S-N curve, but other material characteristics can be established under cyclic loading. Material changes as cyclic softening or hardening may be measured. Results of cyclic hardening/softening determination are schematically shown in Fig. 3.12. The values of stress or strain amplitudes are determined from hysteresis loops. There are two ways to carry out this type of tests; namely at constant amplitude or at constant plastic deformation. The results of such experiments characterize the cyclic mechanical and physical behaviour of material. The knowledge of this behavior is necessary for prediction of the fatigue lifetime of components under cyclic loading. Except of S-N curve, particularly in the low cycle fatigue region, the Coffin-Manson curve, i.e. the dependence of number of cycles to failure on plastic strain amplitude is experimentally determined [55, 130 - 141].
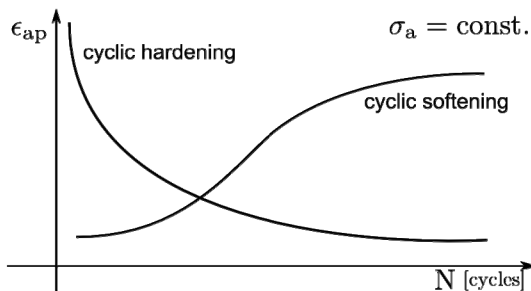
Fig. 3.12 a) Cyclic softening and hardening at constant amplitude load
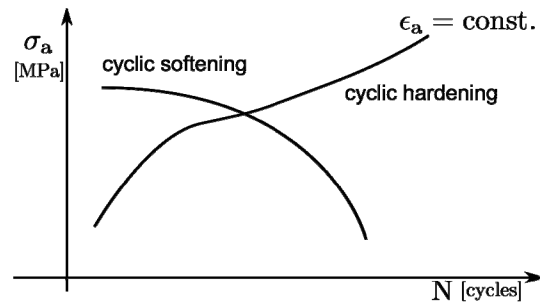
Fig. 3.12 b) Cyclic softening and hardening at constant plastic deformation

Another important material characterization is the so-called fatigue crack propagation curve, Fig. 3.13. This dependence correlates crack growth rate with stress intensity factor. It is called also the fatigue crack propagation law for long cracks. The curve asymptotically tends to the threshold value of the stress intensity factor for low crack growth rates. In the central region, the dependence is linear in the log-log plot. This part of the curve is called Paris region. In the third stage, the crack propagation rate increases rapidly and the final fracture of the remaining ligament of takes place. The crack propagation in Mg alloys has been studied relatively extensively, e.g. [15, 55, 127, 137, 142 - 154].
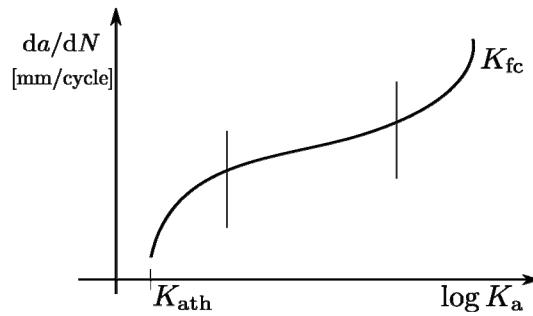
Fig. 3.13 Crack propagation curve

Since the main experimental interest of this work is concentrated on the examination of cyclic hardening/softening behaviour and on S – N curves and lifetime, these characteristics will be discussed in more detail.

Engineering materials strongly differ in their fatigue behaviour and characteristics. Materials as steel and cast iron show a fatigue limit at "constant" number of cycles of 10^6 - 10^7 range [155]. If the material under the testing reaches this number of cycles, then lifetime during further loading at this stress amplitude is considered to be infinite, c.f. 3.11-A. Magnesium alloys do not show such behaviour. The fatigue endurance decreases with increasing number of cycles up to gigacycle region, c.f. Fig. 3.11-B. For this kind of materials the given number of cycles determines the endurance limit - fatigue strength [147, 156 - 159]. Decreasing fatigue endurance of magnesium alloy with increasing number of cycles was reported by Papakyriacou et al. [142]. In this paper AZ91HP alloy was examined. It was found that the endurance limit at 10^7 cycles is 50 MPa. This value is substantially higher than the endurance limit of 38 MPa found for the number of cycles equal to 10^9. This type of behaviour was observed also for wrought magnesium alloys AZ61HP AZ80HP, forged AZ80HP and cast AZ91HP [128].

Many material, technological and testing factors in great extent influence the fatigue properties [144, 160]. Some of them are listed in Tab. 3.1.

Tab. 3.1 Factors with influence on fatigue properties

Factors		
Material	**Technological**	**Testing**
chemical composition	production	loading frequency
microstructure	size	load amplitude
texture	surface condition	asymmetry ratio
	heat treatment	environment
	thermo-mechanical treatment	

For broader engineering use and safer lifetime prediction of magnesium alloys, more thorough knowledge of fatigue properties such as fatigue strength for constant amplitude loading, the influence of notches and the frequency effect is necessary [131]. Because of that, the main focus of this work will be given on the influence of the grain size and texture on fatigue performance of AZ31 alloy. Because the notch sensitivity and frequency influence on fatigue properties are also of engineering importance and because the knowledge of these effects is very poor, the study performed in this work was focused on both these effects.

3.4.1 Hardening/softening of magnesium alloys

As already mentioned above, from the strain changes under the stress-controlled tests, the cyclic hardening or softening of the magnesium alloys could be determined. If these processes are in equilibrium during cycling, then a saturated stage is reached [55, 132, 161 and 162]. If softening or hardening appears, it depends strongly on the material itself and on the production technique of the material. Different behaviour is expected in the material strongly deformed prior to fatigue testing and in the material annealed prior to fatigue testing. It is due to the fact that in the initial stage of loading the dislocation density changes, the dislocation structures form and interact mutually. This stage is usually still crack-free. The dislocation movement in magnesium alloys is not easy and twinning influences the cyclic behaviour in a large extent. Twinning may contribute to the cyclic hardening; twins can play a role of obstacles for dislocation movement. Simultaneously, also softening can be observed, when twins help to rearrange and free the dislocations and so create a free path for dislocation movement. It is not clear and understood which of the mechanisms appear in magnesium alloys.
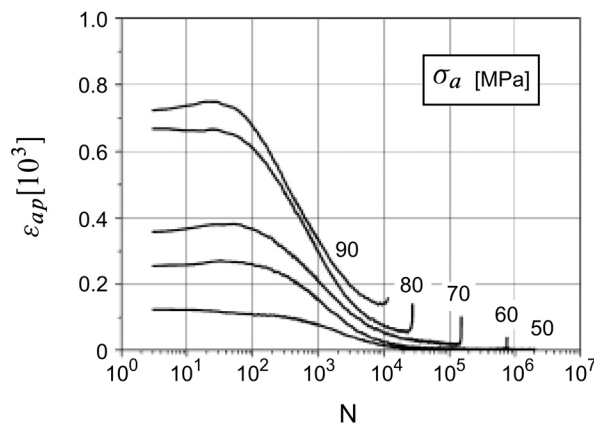
Fig. 3.14 Cyclic deformation curves of cast AZ91D, tested at RT, [161].

Despite of the importance of knowledge about the cyclic behavior, there are very limited data of this kind in literature. The comparison of deformation behaviour for materials prepared by different techniques is missing completely. Some data are available for conventionally prepared materials. However, data for materials prepared by SPD techniques are not available. As regards the AZ alloy system, the cyclic hardening has been reported. This effect is explained by increasing dislocation density due to cyclic plastic deformation. Since this alloy has incoherent precipitates, also pinning of dislocation may appear and help to strengthening [55, 132]. This statement is supported by results of Lamark et al. [163], who observed cyclic hardening of high pressure die cast AS21. In Fig. 3.14 [161], the cyclic deformation behaviour for cast AZ91 is shown. The material was fatigued by symmetrical loading at a frequency of 5 Hz and at asymmetry ratio of -1. At the beginning of the test the saturation or very weak softening was determined. After less then 100 cycles the pronounced hardening was found. The hardening is typical behavior for the prevailing part of the lifetime. At the end of the test, shortly before fracture, the softening is again detected. This is explained by extensive crack growth.

3.4.2   S – N curve

The S – N curve of magnesium alloys shows a typical knee point. For magnesium alloys this knee is approximately at 10^5 cycles. It points out the transition from low to high-cycle fatigue. This behaviour has been reported by Sonsino et al. in [131], who found the knee around 10^5 cycles for cast AZ91HP, AM50HP and AM20HP. Identical tendency was found also by Nan et al. [164] for extruded AZ31 and Eifert et al. [165] for cast WE43A. The appearance of sharp knee on S - N curves may be related among others to the presence of inherent material defects.

Influence of grain size on fatigue behaviour

Generally, the fatigue endurance increases with decreasing grain size. The endurance limit is higher for materials with finer microstructure when compared to materials with coarse microstructure. This trend is kept also in the case of magnesium alloys. Extruded alloys show better fatigue properties when compared to cast ones. This behaviour was confirmed by Sajuri et al. in [150] for cast and extruded AZ91, cf. Fig. 3.15. The identical tendency is expected also for fine-grained magnesium alloys processed by ECAP. However, the literature data regarding fatigue behaviour of ECAP magnesium alloys are very scarce and unambiguous conclusions cannot be made [146, 153, 166 and 167]. So far, most of the experimental tests were done on ECAP-prepared Cu, Al and Al-alloys, Ti, Fe-Ni and carbon steel [141, 168 - 183].
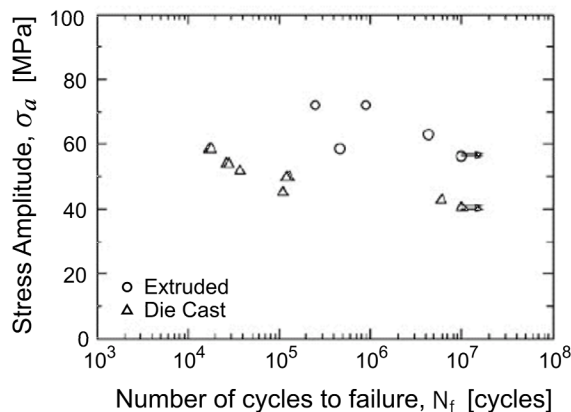
Fig. 3.15 S – N curves, die-cast vs. extruded AZ91D [150].
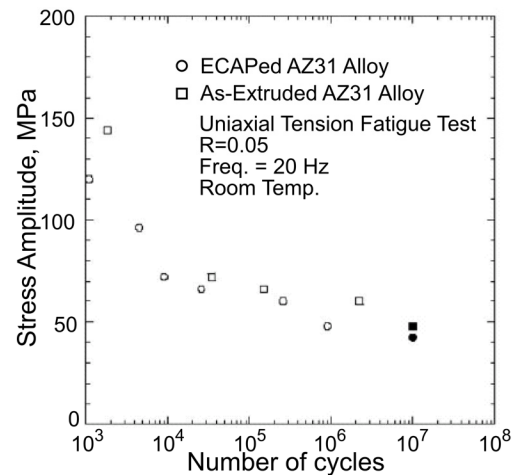
Fig. 3.16 S - N curves, extruded vs. ECAP AZ31 [146].

However, the expected behaviour, that the fine-grained ECAP magnesium alloy would have better fatigue endurance when compared to the extruded one, was not confirmed in the paper by Kim et al. in [146]. They observed that extruded AZ31 has slightly higher fatigue endurance and strength when compared to AZ31 after ECAP, cf. Fig. 3.16. This behaviour is typical both for low cycle region as well as for high cycle region. The authors conclude that the ECAP material has lower resistance to crack nucleation and propagation. The tensile properties of ECAP alloy studied in the work of Kim et al. [146] were lower when compared to the extruded material. This suggests that there may be a certain correlation between tensile and fatigue properties.

However, not only the grain size has influence on fatigue behaviour. As it was already mentioned above, there are more factors that influence fatigue life and they have to be considered as well. In cast alloy, the casting defects have a main influence on the fatigue properties. On the other hand, in the wrought alloys, the texture influence has to be taken in account.

Influence of casting defects and texture on fatigue behaviour

Casting defects form during solidification of the melt. Among casting defects belong porosity, flaws, shrink holes, cavities and inclusions. They can negatively influence the mechanical properties of Mg alloys [55, 127, 128, 130, 134, 137, 142 – 143, 148 - 150, 161, 184 - 192]. They reduce substantially the fatigue endurance; the effect is most pronounced in high cycle regime. Defects result in scatter of fatigue data. Generally, if casting defects are presented in material, the cracks start to nucleate from them [143, 186 and 191]. For cast magnesium alloys this was confirmed by Mayer et al. [189] who examined die cast magnesium alloys AM60HP, AS21HP, AE42HP. An example of crack initiation from a pore is shown in Fig. 3.17. A similar effect was observed in many other works [128, 142, 143, 147, 149, 150, 161, 186 - 190]. Crack initiation does not have to start only on casting defects. It may start also on the grain boundaries. This mechanism was confirmed for cast magnesium alloys in [127, 161 and 188].
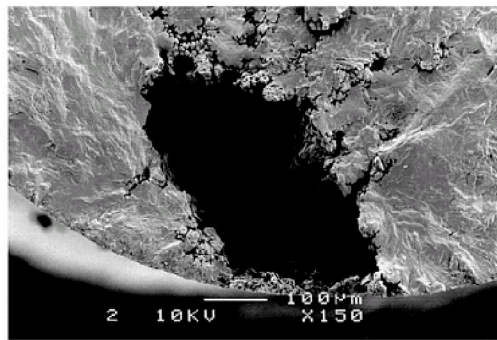
Fig. 3.17 Pore in cast AZ91HP, σ_a = 42 MPa, N_f = 1.92 x 10^6 [189].

Magnesium alloys produced by wrought techniques, as extrusion and rolling, show generally better fatigue resistance when compared to cast ones. This is not only due to the smaller grain size, but also because no casting defects are present in material [132, 145]. However, other types of defects, as for example inclusions, can influence the fatigue behaviour of magnesium alloys. The inclusions are generally stress raisers that help to induce slip bands during loading and so help to promote the crack initiation [55, 145, 152, 157 and 166]. The negative effect of defects is more pronounced under low stress. This behaviour was reported by Uematsu et al. in [152], where in extruded AZ80 cracks initiated at interfaces between an inclusion and matrix. Further, Sajuri et al. [150] observed the cracks initiation from slip bands on the specimen surface of extruded AZ91D.

The fatigue performance of materials depends on the fatigue crack initiation and crack propagation. Generally, the fatigue properties of fine-grained materials are superior to those having coarse grains. In fine-grained structures the dislocation movement is more restricted because of the high amount of grain boundaries, which serve as obstacles for dislocation slip.

Thus, in fine grained materials the resistance to crack initiation and propagation is improved. This behaviour was observed by Uematsu et al. in [152], where the coarse grained and fine-grained AZ31 were examined.

Texture, which is another important internal factor, may also influence the fatigue behaviour of wrought magnesium alloys. Unfortunately, in the literature does not exist many studies dealing with this issue [146, 153, 167 and 193]. The problem of the relation of texture and fatigue performance of ECAP processed magnesium has not been studied at all.

The fatigue results in Fig. 3.16 show, that ECAP material does not have better fatigue endurance when compared to extruded ones. This cannot be attributed to the grain size effect, because ECAP material has smaller grains than the extruded alloy. This indicates that texture influences the fatigue behaviour of magnesium alloys [146, 153 and 167]. However, the detailed information concerning texture effect on fatigue properties is missing. It could be only speculated that in materials with texture favourable oriented for easy slip, the crack initiation and propagation would have more favourable conditions than in materials with texture unfavourable for slip [146, 152 and 153]. From the fragmentary data it seems that the texture effect may have even stronger influence on fatigue resistance than the grain size. The strong texture effect on fatigue behaviour of hot rolled AZ31 was reported by Chino et al. [193]. They tested material properties of two sets of specimens with directions (0° and 90°) to loading direction. Higher endurance limit was found for the specimen with texture unfavorable for easy slip. The fatigue strength of 90°-specimens was 95 MPa whereas for 0°-specimens was only 90 MPa.

The already nucleated cracks can propagate in Mg alloys in two ways; transcrystalline and intercrystalline. Which of the mechanisms occurs, depends on material and testing conditions. In magnesium alloys, mostly transcrystalline crack propagation is observed. This type of fatigue crack propagation was found in AM50, AZ91HP, AS21HP, AE42HP and AZ91D [128, 132, 149, 161 and 189]. On the other hand, in [55, 188] the intercrystalline propagation in AZ91 was reported. The intercrystalline propagation is more frequently observed in material with higher porosity. Tokaji et al. [145] reported both transcrystalline and intercrystalline modes in rolled AZ31.

Fatigue notch sensitivity

The decisive majority of structural parts contain stress concentrators. They are substantially influencing the fatigue strength. Since notches can influence the fatigue behaviour in large extent, their impact on fatigue lifetime has to be examined. The susceptibility of material on notch presence in a loaded body is expressed by a fatigue notch factor. Notch sensitivity of materials depends on material as well as on the notch geometry itself. Different notch shape and size have different impact on the fatigue strength. Indeed, this issue is very important for engineering practice; however, only scarce literature data are available [131, 186, 194 and 195].

Each notch can be characterized by a theoretical stress concentration factor K_t, which can be computed using standard finite element procedures or to find for many of frequent cases e.g. in [196]. Notches have generally negative effect on fatigue lifetime. The fatigue strength decreases with increasing theoretical stress concentration factor [131]. This was experimentally proved many times for various alloys, among them also for magnesium alloys [131, 195]. However, the real influence of notches, characterized by the fatigue notch factor K_f, is usually weaker than indicates the theoretical stress concentration factor. In the case of magnesium alloys it has been reported that they have generally lower notch sensitivity than

aluminium, cast iron or wrought steel [131]. However, a pronounced notch sensitivity of magnesium alloys was reported in papers by Sonsino et al. and Tsujikawa et al. [131, 197]. They show that the notch influence on fatigue properties is more noticeable in the fine-grained materials than in coarse-grained ones [197]. Sonsino et al. [131] compared fatigue strength of cast specimens with two different stress concentration factors. In the first case, the stress concentration factor K_t of smooth specimen was 1. On the other hand, the stress concentration factor of notched body was 2.5. The magnesium alloy AZ91HP was used for tests. The fatigue strength for smooth specimens with lower stress concentration factor was 77 MPa. In the case of notched specimens with higher stress concentration factor, the fatigue stress of 56 MPa was determined. The fatigue strength increased with decreasing stress concentration factor. As regards the fatigue crack initiation mechanism, in the notched specimens cracks initiate on the surface [127, 187].

Materials having internal defects, as for example porosity or inclusions, may have higher internal stress concentration factor than the external artificial notch. Due to this, the degradation influence of internal defects is over the external one. The external artificial notch does not have any negative effect on fatigue endurance in this case. Berger et al. in [191] confirmed this fact experimentally. Cast material due to high porosity showed a higher internal stress concentration factor than that caused by external notch. The result is then the apparent artificial notch insensitivity.

Frequency effect on fatigue behaviour

Loading frequency influences fatigue behaviour of materials because the cyclic plastic deformation is a strain rate dependent process. Further, this influence is driven by time-dependent processes, as corrosion and creep [142, 190 and 198]. Testing at low frequency means that the material is exposed under a given environmental conditions for longer time than in the case of loading at higher frequency (for the constant number of cycles to failure). Only a few comparative studies dealing with frequency effect are available. Results of testing under ultrasonic and conventional frequency can be found in papers by Papakyriacou et al. and Mayer et al. [142, 128 and 189]. However, these results are related only to conventionally prepared magnesium alloys. The observed effect of frequency in the case was not significant. In [142] three cast magnesium alloys AM60HP, AZ91HP and AS21HP were tested. Two loading frequencies of 100 Hz and 10 kHz were applied. The endurance limit at both frequencies was nearly the same, though very different frequencies used. Identical behaviour was reported by Mayer et al. [189] for AZ91HP, AS21HP, AM60HP and AE42HP tested at 20 kHz and 50 Hz. From these results it can be concluded that the frequency does not have substantial influence on lifetime of conventionally produced magnesium alloys loaded in air. Experimental data concerning magnesium alloys prepared by ECAP are missing completely. Confirmation of low sensitivity of Mg alloys prepared by ECAP would be an important result, because the high frequency experimental data may be used then for fatigue life predictions of parts that are loaded at much lower frequencies [128]. It means a saving of testing-time, energy and consequently expenses.

Influence of stress ratio on fatigue life

In engineering practice materials are prevailingly loaded under action of mean stresses. The asymmetry of loading cycle is expressed by a stress ratio. Mean stresses substantially influence the fatigue lifetime. Asymmetry ratio R is defined as

$$R = \sigma_{min} / \sigma_{max} \qquad , \qquad (3.1)$$

where σ_{min} is minimum stress amplitude and σ_{max} is maximum stress amplitude in a loading cycle.

Generally, the fatigue lifetime decreases with increasing R ratio. This holds also for magnesium alloys. For example, for extruded AZ31 tested at asymmetry R = 0.1, the fatigue strength of 94 MPa was found [197]. The fatigue strength corresponding to the loading in stress symmetrical cycle, i.e. with R =-1 was higher, namely 123 MPa [164].

Effect of environment on fatigue behaviour

Many engineering materials, among them also magnesium alloys, are sensitive to the environment conditions. Aggressive environments as chlorides, nitrates and phosphates, lead to deteriorations of fatigue properties [160, 185, 199 and 200]. In the case of Mg alloys tap and even distilled water mean aggressive environment. If Mg alloys are exposed to water or any other moisture environment then their fatigue life is significantly reduced [55].

The deterioration of fatigue resistance due to humidity, water vapour and elevated temperature was reported for majority of magnesium alloys, AZ61, AZ91HP, AS21HP and AE42HP, in many works [55, 143, 144, 149, 150, 165, 184, 191, 201 and 202]. Mayer et al. [149] reported 90 % degradation of fatigue strength for magnesium alloys tested at temperature of 120°C when compared to testing at 20°C. Hilpert et al. and Papakyriacou et al. [142, 160] reported the negative influence of air on fatigue properties when compared to vacuum.

In aggressive media, the fatigue cracks initiate from corrosion pits, pores and on secondary particles as $Mg_{17}Al_{12}$ and Mg_2Si [199, 200 and 203]. Crack propagation in magnesium alloys is in aggressive media faster than in vacuum [144, 184], which results in decrease of lifetime [149].

The wrought magnesium alloys are more susceptible to fatigue life reduction in an aggressive environment than cast alloys. It is probably due to the more extensive deformation during production of those materials. High residual stresses in wrought materials play probably important role [199, 200]. Consequently it means a higher chemical potential of the metal atoms and so higher chemical reactivity. Despite of that, the wrought magnesium alloys (extruded, rolled) show better fatigue resistance than cast ones.

Surface treatment effect on fatigue behaviour

Surface treatment may improve but also deteriorate fatigue properties of magnesium alloys. It strongly depends on surface treatment technique and naturally the type of environment [55, 160, 185 and 204]. For example Wendt et al. [185] reported that the shot peening and roll-burnishing lead to an improvement of fatigue strength of magnesium alloys when compared to electropolished condition. However, this is valid only when magnesium alloys are tested at room temperature and in neutral environment. The shot peening introduces high density of near-surface dislocations and high compressive residual stresses. It helps to reduce crack initiation and crack growth by reducing the dislocation mobility. On the other hand, the surface roughness is increased. In aggressive media it may result in early crack initiation and growth [55, 160 and 185] and so to the deterioration of fatigue performance.

4   Goals of this work

The goals of this work result from the deficient knowledge of the mechanical behaviour of Mg alloys, which are of increasing utilization in many branches of industry. This research was driven by specific needs and general reasons, which can be grouped into the following three main categories.

1   Magnesium alloys are the lightest metallic structural materials used in engineering applications. To further extend their use, an intensive study of their mechanical properties is necessary. At present, the magnesium alloys are produced by standard production techniques as casting and rolling. The grain size of rolled and cast Mg alloys is typically 15 and 500 µm, respectively. These microstructural parameters limit the mechanical properties and consequently restrict the use of magnesium alloys. New productions methods are nowadays searched with the vision of further improvement of mechanical properties. Severe plastic deformation seems to be very promising procedure for successful achievement of this goal.

2   Not all of the SPD techniques are suitable for magnesium alloys. The proper SPD technique has to be chosen for particular alloys. One of them is equal channel angular pressing (ECAP), which enables to obtain ultrafine-grained microstructure in bulk. Since the magnesium alloys have hexagonal lattice, the simple forming processes used for f.c.c. materials are impracticable. Also the application of equal channel angular pressing on magnesium alloys is not without problems. The task of this work was to find the proper conditions for the application of equal channel angular pressing for conventional and fine-grained Mg alloys.

3   The mechanical properties of coarse grained magnesium alloys are mostly known, but on the other hand the data of fine grained magnesium alloys are very scarce and in many cases even completely missing. The field of mechanical properties is very broad and it is not possible to focus on all their areas within this work. That is why this study concentrates on one important field, namely on fatigue properties. Fatigue behaviour and material data of ultrafine-grained alloys will be compared with coarse-grained ones. It is necessary to note that these data, which are of utmost importance for the future proper engineering application of Mg alloys, are completely absent in the literature.

The research performed in this work was focussed also on the problem of notch sensitivity of Mg alloys. The literature data on this behaviour are practically missing. Very limited information can be found for notch sensitivity of extruded alloys. No information at all is available for ultrafine-grained structures. This state of knowledge is naturally insufficient for engineering practice, where not only smooth-body components are applied. Due to it the fatigue behaviour of notched as well as smooth specimens will be examined and mutually compared.

Another piece of knowledge important for engineering applications is the influence of loading frequency on fatigue behaviour of magnesium alloys. There is very limited information in the open literature concerning SC and HR materials. The data on ultrafine-grained magnesium alloys are completely missing. In this work, the frequency influence on fatigue behaviour of coarse and fine-grained magnesium alloys as well as frequency influence on notched behaviour will be examined and discussed from the point of view of microstructure of particular alloys.

General knowledge based on the Hall-Petch relation gives the idea that the fine-grained material should have better mechanical properties when compared to the coarse

grained material. However, also the opposite behaviour was reported in some papers. The tensile strength and yield stress as well as fatigue endurance limit of fine grained materials in certain cases are lower when compared to coarse grained ones. The reason of this behaviour is not clear. The answer and clarification of this specific behaviour is very desirable. These contradictory effects try to be explained in this work as well.

5 Material production processes

Magnesium alloy AZ31 was chosen as experimental material for the purpose of this work. Three production techniques were applied. These are squeeze casting, hot rolling and equal channel angular pressing. Processing conditions of these procedures will be described in the next chapters.

5.1 Processing conditions of squeeze casting

Magnesium alloy AZ31 was heated up to casting temperature of approx. 720°C. Prior to casting the cast die was pre-heated to a temperature of 200°C. After, pouring the material into the preheated die, a two-step pressure was applied. The first loading step was of 80 MPa with a loading time of 15 s. The second pressure was 140 MPa for 90 s. The squeeze casting run under a protective gas atmosphere of Ar-SF$_6$. This process was carried out in ZfW GmbH in Clausthal-Zellerfeld, Germany. The final size of the cast disc was of 250 mm in diameter and 60 mm in high.

5.2 Production conditions of hot rolling

The cast block of magnesium alloy was used for rolling process. The rolling was carried out at a temperature of 370°C. Since rolling of magnesium alloys requires a high number of rolling cycles with a small reduction, the process was done in the following way. The magnesium alloy AZ31 was rolled in several steps with thickness reduction of max. 10 % per each step. The total reduction was 85% and the final thickness of the sheet was 18 mm. After each rolling step, the sheet was rotated by an angle of 90°. The rolling process was performed at MgF GmbH in Freiberg, Germany. The final size of the rolled sheet was 320 mm x 470 mm x 18 mm.

5.3 Production conditions of equal channel angular pressing

At the material science department of Clausthal University of Technology several ECAP die geometries were designed and tested. After optimizing ECAP equipment, a split ECAP die pictured in Fig. 5.1 was used for purpose of this work. The die angle Φ between two channels was 90° and the outer arc of curvature ψ was zero. The channels have rectangular shape. The die material was the tool steel X38CrMoV5-1. Tool steels X40CrMoV5-1 (DIN 1.2344) and X3NiCoMoTi 18-9-5 (DIN 1.2709) were used as plunger materials. The tools were hardened to 48 HRC.
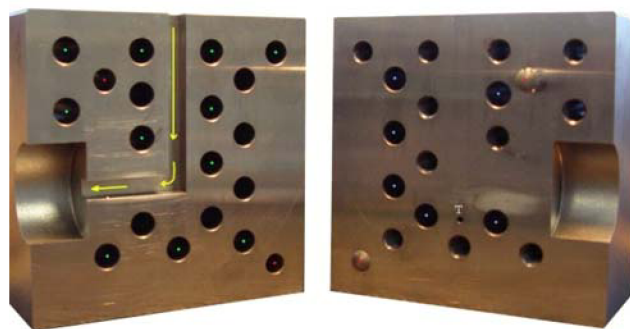
Fig. 5.1 Split ECAP die.

The dimensions of the rectangular billets were 10 mm x 10 mm in cross section and 100 mm in length. They were machined from the hot rolled AZ31 that was produced in the way described above. The longitudinal axis of the billet was parallel to the last rolling direction. For ECAP pressing of this work route B_C was applied. It means a rotation about the longitudinal axis by 90° between each passes. The specimens passed through out the ECAP channels for four times. These pressing conditions lead to a strain ε of 1.15 per pass. A servohydraulic testing machine Instron 8502 with ± 200 kN maximum load capacity was used.

ECAP process is relatively young. Though theoretically this process is very simple the practical use of ECAP brings certain problems. To avoid them some pre-conditions have to be fulfilled. As for example, a proper temperature of the pressing has to be found as well as a proper pressing speed. The pressing load has to be adjusted to possibilities of the equipment. The length of the specimen had to be optimised. To avoid a negative effect of friction a lubricant had to be used. When the ECAP pressing temperature is too high then an undesirable flow of the magnesium alloy around the plunger appeared, cf. Fig. 5.2. Consequently, the friction between plunger and channel increased. It leads to an increase of temperature and the pressing forces. Further, at high temperature a welding of two specimens may occur, cf. Fig. 5.3. On the other hand, when the pressing temperature is too low then heavy cracking on the specimen occurred, cf. Fig. 5.4. This is because at low temperature the formability of magnesium alloy is low.

The ideal conditions for ECAP pressing of the magnesium alloy AZ31 were found at pressing temperature of 200°C and speed of 5 mm/min. To reduce a friction during the pressing a temperature resistant lubricant Molykote MoS_2 was used.

Fig. 5.2 Flow of AZ31 around the plunger.

In the case that the optimal conditions of ECAP pressing are not found, then the pressing under inappropriate conditions may lead to the damage of tools. Such a case is shown in Fig. 5.5, where two bent plungers are pictured. In the worse case, the ECAP die may be destroyed. Such a case is shown in Fig. 5.6. A heavy crack across the whole die and cut off of heating elements are visible. Such damages are necessary to avoid due to the high cost of new equipment and in order to assure a continuous material production.
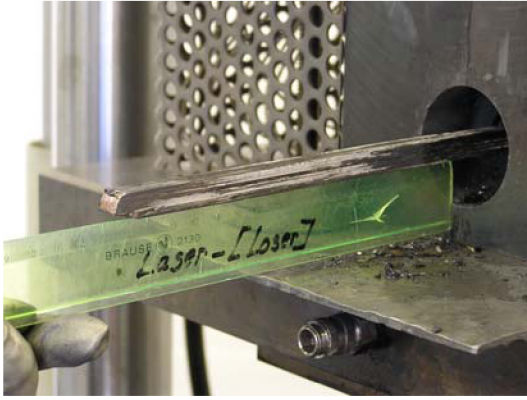
Fig. 5.3 Two welded ECAP specimens
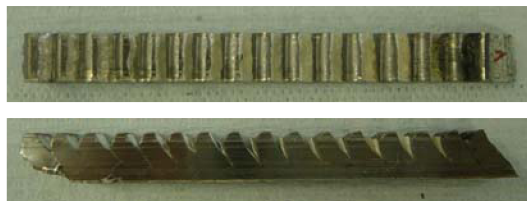
Fig. 5.4 Heavy cracks on ECAP specimen.

a)

b)

Fig. 5.5 Bent plungers
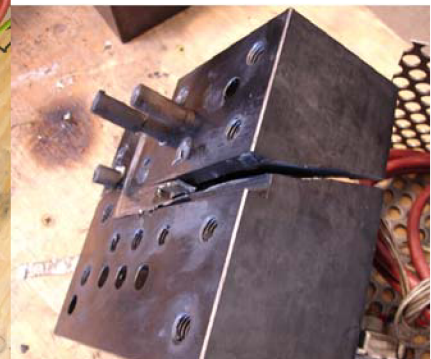
Fig. 5.6 Completely broken die. a) A crack through the entire die and cut heating elements are seen, b) not pressed specimen in the vertical channel is visible as well as the material that oozed out from the die.

6 Results and experimental

The magnesium alloy AZ31 produced by three techniques; squeeze casting, hot rolling and equal channel angular pressing, was examined. The examinations were divided in three parts. First, the microstructure and texture characteristics of the alloy were determined. Second, the tensile properties of AZ31 were investigated and third, the focus was given on the fatigue properties of the magnesium alloy AZ31. The results are presented in this chapter by reason of extent of the thesis together with the necessary brief description of specimens, experimental facilities, procedures and methods which have been used.

6.1 Microstructure and texture

Since the magnesium alloy AZ31 was produced by three different techniques, its microstructure and texture obviously diverse. These differences were examined, compared and discussed. The light microscopy, transmission electron microscopy, electron backscatter diffraction EBSD and the neutron diffraction were applied for microstructural examinations. The light microscopy was used for grain size determination. The transmission electron microscopy was done to establish more precisely the grain size and dislocation density of the materials. The electron microscopy yields more information about small grain character and misorientation angle between grains. The neutron diffractions were used to determine the global texture of the material.

Microstructure observations were carried out with a ZEISS Axioplan light microscope, at TU Clausthal, IWW in Clausthal-Zellerfeld, Germany. For the observations the sample had to be prepared in the following way. The first step was grinding on SiC paper with grits in range of 320 – 1200. Then mechanical polishing was done with 1 μm diamond suspension. To reveal the grain microstructure, etching with Picric acid was performed. Picric acid compounds from solution of 100 ml. distilled water, 100 ml. ethanol and 5 g Picric acid. This etchant was used because of its good reactivity with grain boundaries of magnesium alloy AZ31 [205]. Consequently, the visible grains were measured by the linear intercept method.

A microscope Philips CM200 was used for the transmission electron microscopy. Thin foils were prepared for material examinations. They were mechanically polished with following electropolishing. Electropolishing was performed in a Tenupol 5 double jet polishing unit in a LiCl + Mg perchlorate + methanol + buthyloxyethanol solution at – 45°C. These observations were performed at TU Clausthal, IWW, Clausthal-Zellerfeld, Germany.

A LEO 1530 electron microscope with electron backscatter diffraction was used for determination of microstructure. The microscope operated at 20 kV. These observations were carried out at RWTH Aachen, Germany. The misorientation angle distributions were analysed using a standard computer program for EBSD analysis. The step magnitude of the analyzer was adjusted and optimised to the material conditions and to save time. For fine grained material, small steps are necessary for precise analysis. On the other hand for coarse materials the step of analyzer may be bigger. Since in ECAP material, the smallest grain size may be expected, a smallest step of 0.1 μm was used. Contrary, in coarse cast material a step of 5 μm was applied. The capacity and accuracy of the EBSD equipment allowed to measure the misorientation angle of 2.5° as the smallest value. Examined samples were prepared by grinding on SiC paper in the same way as in the case for the light microscopy.

A TEX-2 four-circle diffractometer with neutron diffraction system was used for the global texture determination. The neutron wave length was 1.332 Å. These measurements were performed in GKSS Geesthacht, Germany.

For a complete characterisation of the magnesium alloy AZ31 further tests were performed. Hardness was measured in Vickers units using Duramin micro hardness equipment. A load of 981 mN ($HV_{0.1}$) was applied for a duration of 10 seconds. For each measurement over 20 dips were performed. Consequently an average value was calculated as the representative value of the hardness. The density of the three conditions of AZ31 was determined by the Archimedes law. The chemical composition of hot rolled and cast AZ31 was determined on a Spectro analytical instrument (Spectro Analytical Instruments GmbH, Germany) based on optical emission spectrometry.

Microstructure and texture of squeeze cast material

The cast material was used without casting skin. Specimens were cut without any specific direction. The result of the chemical analysis of the cast magnesium alloy AZ31 is given in Tab. 6.1. The measured Vickers microhardness of the material was 60 $HV_{0.1}$. The measured density was 1777 kg/m^3. Since the measured density is close to the ideal one, the material does not show any significant porosity or any internal casting cracks.

Tab. 6.1 Chemical composition of AZ31SC in wt.%.

Al	Ca	Cu	Fe	Mn	Ni	Pb	Si	Sn	Zn	Zr
3.6230	>0.1800	0.0044	0.0027	0.2916	0.0015	0.0137	0.0145	<0.0200	1.3610	<0.0100

Balance 94.5 wt.% of Mg.

Four cast discs were used for the purpose of this work. Some material characteristics vary a bit in particular discs. Light microscopy revealed a strong dendrite structure in all casting discs. Grains size was homogeneous in each particular cast disc. However, the average grain size was different in particular castings. The grain size was in range of 150 to 450 μm. No twins were observed. An example of microstructure of cast AZ31 with a grain size of 450 μm is pictured in Fig. 6.1.1.

500 μm
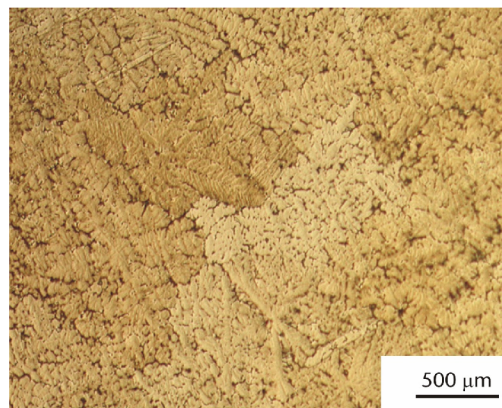
Fig. 6.1.1   Optical   micrograph   of   AZ31SC,
dendrite structure, average grain size of 450 μm.

In Fig. 6.1.2, the misorientation distribution histogram for AZ31SC is shown. It gives information about the nature of the grains of cast AZ31. Two peaks are visible. One peak is at very low misorientation angle below ca 7°. It could mean a high amount of low angle boundaries. But most probable it is only an artefact resulting from surface preparation imperfection that frustrates the grain boundary map. The second peak corresponds to high misorientation angle. This peak has maximum at 86°. It clearly indicates the presence of twins in the matrix. In the area of high angle boundaries (misorientation angle > 15°), the volume fraction of grains increases with increasing misorientation angle.
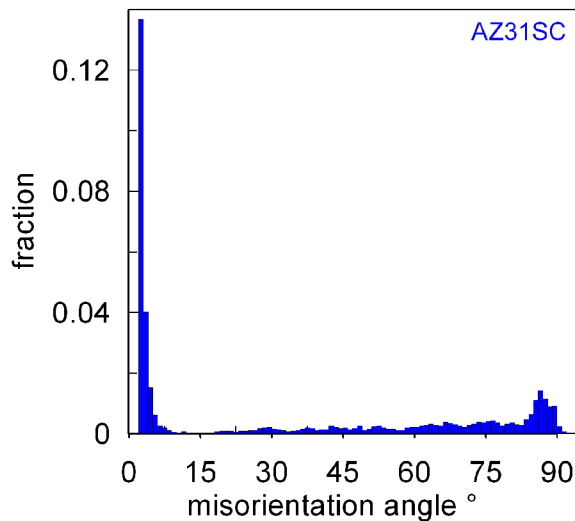
Fig. 6.1.2 Distribution of misorientation angles for AZ31SC. Two peaks are visible, one for low angle and second for high angle misorientation.
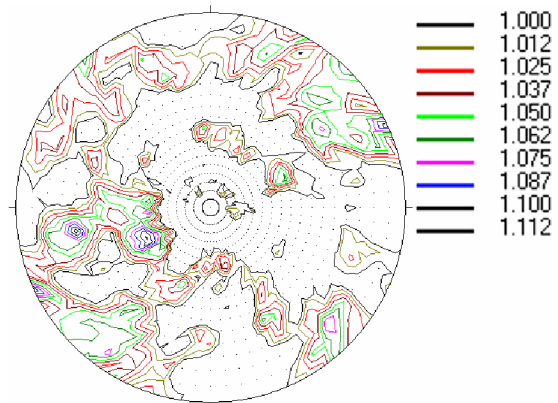
Fig. 6.1.3 Pole figure of AZ31SC, (10.0), pole figure intensity (P_{max}) of 1.1 m.r.d. indicates a nearly random texture.

The result of texture analysis for squeeze cast AZ31 is shown on pole figure (10.0) in Fig. 6.1.3. The nearly random texture is visible. The maximum pole figure intensity of 1.1 m.r.d. (multiple random distribution) was determined and it is close to ideal random texture intensity defined as 1.0 m.r.d. of (10.0) pole figure.

Microstructure and texture of hot rolled material

The chemical composition of hot rolled material is given in Tab. 6.2. A Vickers microhardness of 64 $HV_{0.1}$ was found. The measured density of AZ31HR was 1782 kg/m^3. This density value is close to the ideal density of magnesium and so it could be stated that no internal defects of the material were indicated.

Tab. 6.2 Chemical composition of AZ31HR in wt.%.

Al	Ca	Cu	Fe	Mn	Ni	Pb	Si	Sn	Zn	Zr
3.7440	0.0272	0.0034	0.0028	0.3844	<0.0005	0.0099	0.0386	<0.0020	0.8710	<0.0100

Balance 94.9 wt.% Mg.

The microstructure of hot rolled material is shown in Fig. 6.1.4. The equiaxed and homogeneous grains are visible. The average grain size of 15 μm is observed. The microstructure is fully recrystallized. No twins are observed. To reveal the microstructure in more detail, TEM observations were done. On Fig. 6.1.5, an area of small grains is pictured. The grains are clear with low dislocation density. The present dislocations are accumulated at the grain boundaries. This microstructure suggests that the dynamic recrystalization DRX occurred in the material.
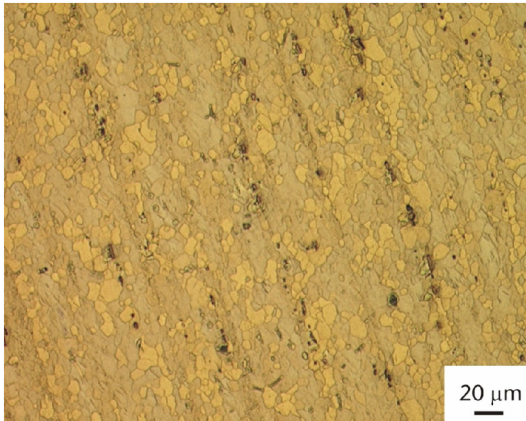
Fig. 6.1.4   Microstructure   of   AZ31HR (orientation   RD - TD),   recrystallized microstructure with grain size of 15 μm.
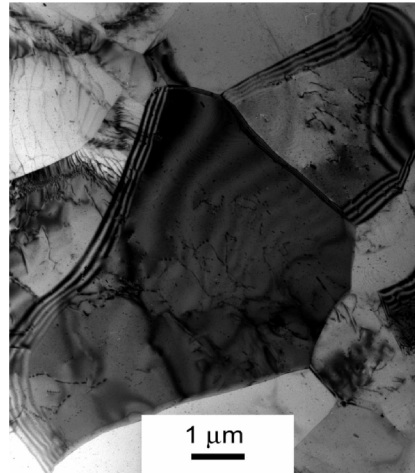
Fig. 6.1.5 TEM microstructure of AZ31HR (orientation TD –ND), a region of small grains.

The misorientation angle distribution of hot rolled AZ31 is shown in Fig. 6.1.6. One intense peak corresponding to the 30° misorientation angle is visible. This indicates, as it is stated in literature [88], that the recrystallization of the material took place.
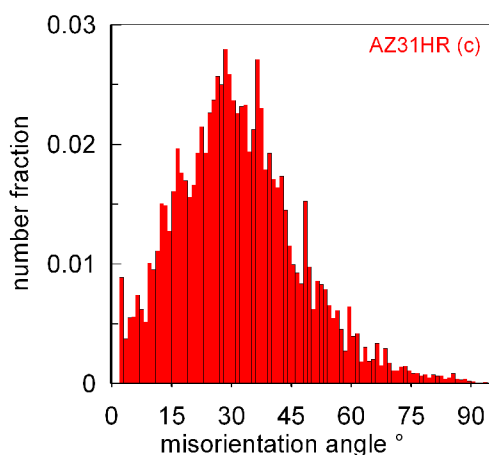
Fig. 6.1.6   Distribution   of   misorientation angles   of   hot   rolled   AZ31   with   a   peak intensity of ~ 30°.
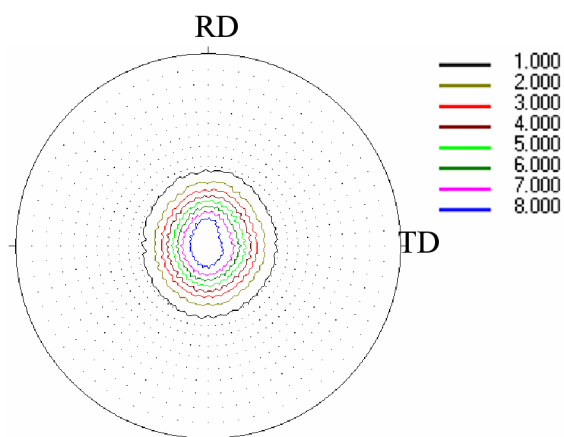
Fig. 6.1.7 Pole figure of AZ31HR, (00.2), with strong basal texture.

The texture observations revealed that the hot rolled AZ31 has a strong basal texture. The basal texture is shown in Fig. 6.1.7 for the pole figure (00.2). It means that the plane (00.2) lies parallel to the rolling direction and the c-axis is perpendicular to the rolling direction. The pole figure intensity P_{max} of 8.6 m.r.d was determined.

Microstructure and texture of ECAP material

The Vickers microhardness of ECAP specimens of 74 HV0.1 was determined. A density of 1834 kg/m^3 was measured for AZ31ECAP. The density of ECAP alloy is close to the ideal value; thus no porosity and cracks are present in the material.

The grains of ECAP material are equiaxed and well developed. The grain size is 2.5 μm. No twins were revealed by light microscopy as well as by TEM, see Figs. 6.1.8 and 6.1.9. The grain boundaries have a characteristic contrast of equilibrium boundaries. The dislocation density in the grains of ECAP material is low. This indicates that the recrystallization took place.
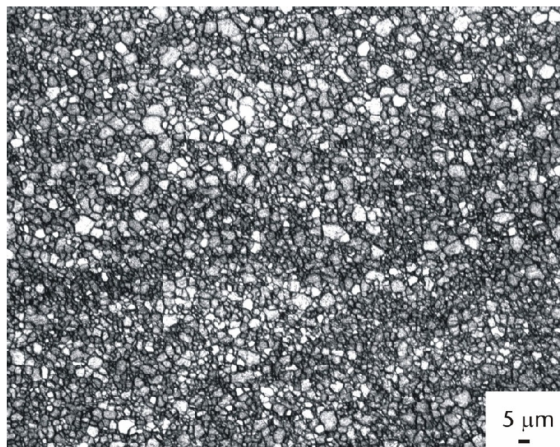
Fig. 6.1.8 Microstructure of AZ31ECAP (orientation TD – ND), recrystallized grains with size of 2.5 μm.
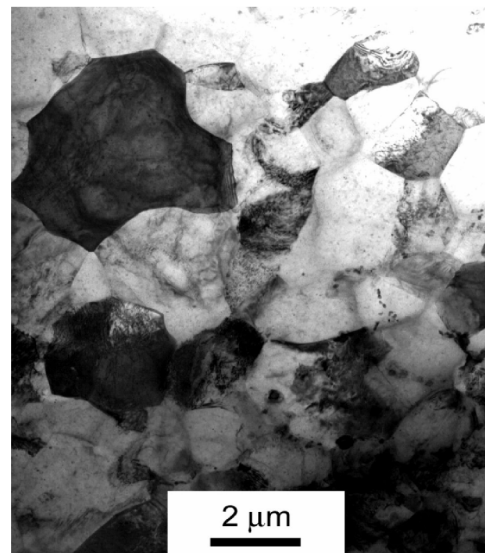
Fig. 6.1.9 TEM microstructure of AZ31ECAP (orientation TD – ND).

The misorientation angle distribution shown in Fig. 6.1.10 exhibits two main intensity peaks. The first peak is situated at 30° and the second one at 86°. Both peaks are in the high angle misorientation area. This means that the majority of the grains have high angle boundary character. The existence of a peak at 86° can be explained in two ways: The 86° misorientation may indicate twin formations in the microstructure. The second way of explanation is that the peak does not have any special meaning; there simply exist more grains with high angle boundary. Since none of the examinations revealed twins in the matrix, the more probable explanation is the second one. The peak of 30° misorientation speaks for dynamic recrystallization in the material.
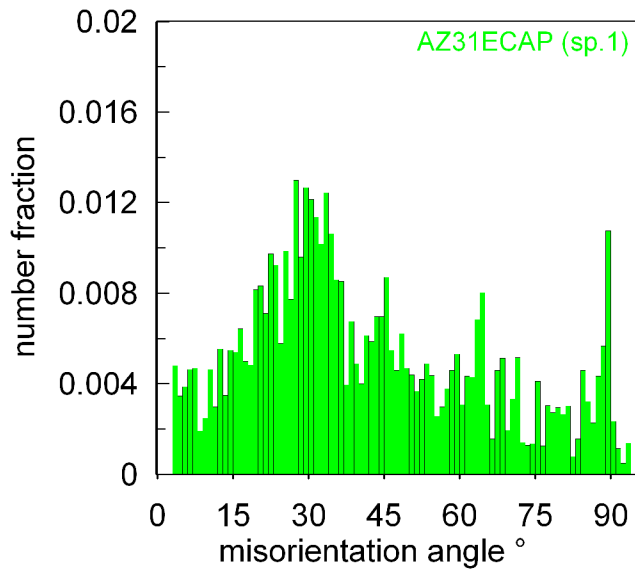
Fig. 6.1.10 Distribution of misorientation angle of AZ31ECAP, two peaks at 30° and ~86° are visible.
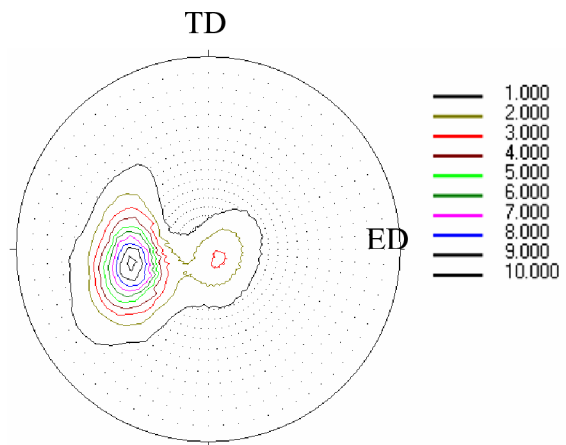
Fig. 6.1.11   Pole   figure   (00.2)   of AZ31ECAP, basal texture bounds about 45° to the pressing direction.

The pole figure (00.2) of AZ31ECAP is shown in Fig. 6.1.11. The basal planes are tilted 45° to the pressing direction. It means that the basal planes are parallel to the shear plane of ECAP. The pole figure intensity of ECAP material is 10.4 m.r.d. The ECAP specimen position for texture measurement is shown in Fig. 6.1.12.
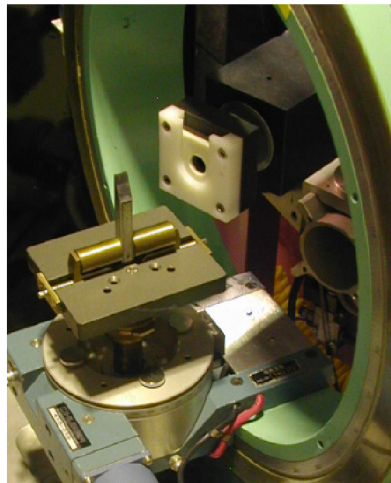
Fig. 6.1.12 ECAP sample and sample holder mounted in the Eulerian cradle of TEX-2

The ECAP material exhibits the smallest grain size when compared to hot rolled and squeeze cast AZ31. It results from the lowest processing temperature of ECAP and the high plastic deformation. The microstructure of ECAP and HR AZ31 is fully recrystallized with low dislocation density. No twins were observed. Contrary to that AZ31SC had coarse grained structure. The coarse grains result from cast process, during which material cools down slowly and thus the grain growth may occur. The density of all tested conditions of AZ31 showed that no internal defects as porosity are in the material. The highest hardness

was detected for ECAP material. It is due to its finest microstructure. The texture intensity of ECAP material was the strongest one when compared to hot rolled and cast material. This high texture intensity results from high strain involved in ECAP process as well as from low processing temperature.

6.2   Monotonic tensile tests

Cylindrical specimens were used for tensile tests. The specimen dimensions of SC and HR material were 5 mm in diameter and 25 mm in gauge length, cf. Fig. 6.2.1. The ECAP specimens, due to the size of ECAP processed billets were smaller. The specimen diameter was 4 mm with a gauge length of 20 mm. All specimens were without material skin. The SC specimens were cut without any regards to specific orientation. HR specimens were machined in such a way that the longitudinal axis of HR specimens was parallel to the last rolling direction. In the case of ECAP specimens the gauge length was parallel to the ECAP processing direction.

The three conditions of AZ31 were monotonically tested in tension. The specimens were loaded till failure occurred. The tests were run at room temperature in air. An Instron servohydraulic testing machine with load cell capacity of 5 kN was used. The machine operated at a constant rate of cross-head displacement. The tests were carried out with initial strain rate of 1×10^{-3} s^{-1}. All tensile tests were conducted at TU Clausthal, Clausthal-Zellerfeld, Germany.
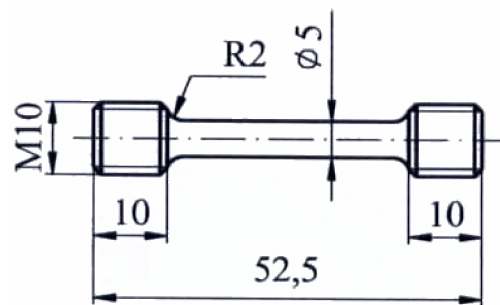
Fig. 6.2.1 Geometry of tensile specimen

The results of tensile tests for three conditions of AZ31 are shown in Fig. 6.2.2, where the true stress vs. true strain behaviours are pictured. For better readability the results and their comparison is given in Tab. 6.3. True stress and true strain were evaluated from the measured engineering stress - engineering strain curves using Eqs. 6.1 and 6.2 [121]:

$$\sigma_{true} = \sigma_{eng} (1 + \varepsilon_{eng}) \tag{6.1}$$

$$\varepsilon_{true} = \ln (1 + \varepsilon_{eng}) \tag{6.2}$$

Where σ_{true} - the true stress [MPa]

σ_{eng} - the engineering stress [MPa]

ε_{true} - the true strain

ε_{eng} - the engineering strain [%].
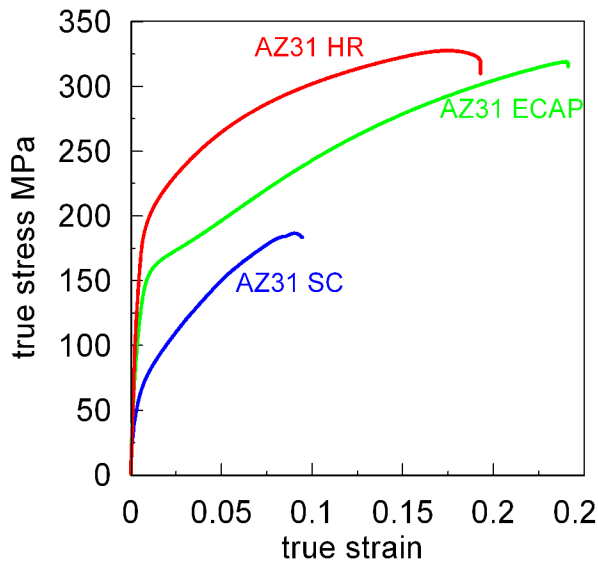
Table 6.3 Tensile properties of AZ31, (offset of 0.01 true strain)

AZ 31	SC	HR	ECAP
YS [MPa]	86.2	213.8	163.7
true UTS [MPa]	186.8	327.7	318.9
true strain at UTS	0.0905	0.1744	0.2398

YS – yield stress
UTS – ultimate tensile strength

Fig. 6.2.2 True stress *vs.* true strain curves for monotonic tensile tests of AZ31SC, HR and ECAP

The lowest tensile characteristics exhibits coarse grained SC material. The yield stress and tensile strength of the HR material were higher when compared to the ECAP material. This behaviour was not expected and is surprising, because ECAP material has the smallest grain size. Thus according to the Hall-Petch relation it can be predicted that ECAP material would show the best tensile behaviour. The situation is different when the straining of the HR and ECAP material is compared. The best formability was observed for ECAP material when compared to HR and SC alloy. This behaviour results not only from the grain size effect but significantly also from the texture.

For better understanding of strain hardening of three conditions AZ31, the strain hardening coefficient θ was calculated from monotonic true tensile curves. This strain hardening coefficient quantity is defined as:

$$\theta = \left(\partial\sigma / \partial\varepsilon\right)\Big|_{\dot{\varepsilon}}$$ (6.3)

Where: θ - the strain hardening coefficient [MPa]
σ - the true stress [MPa]
ε - the true strain
$\dot{\varepsilon}$ - the strain rate [s^{-1}].

The strain hardening coefficient was determined from piece-wise polynomial fittings through 5 data points of monotonic true tensile curves. Slope determination by the tangent to each local polynomial curve was used to determine the corresponding value of θ. A Matlab program was used for θ calculation using data of flow stress. The flow stress from yield stress (defined at off-set 0.01 of true strain) to ultimate tensile stress was considered for calculation, Eq. 6.3. The dependency of the strain hardening coefficient on the true stress, using the 5 data point base, is presented for AZ31SC, HR and ECAP in Fig. 6.2.3.
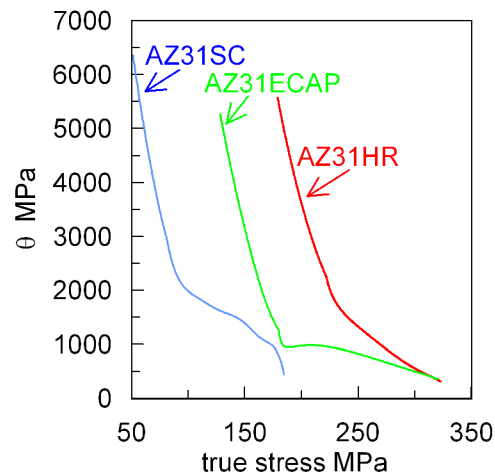
Fig. 6.2.3 Strain hardening coefficient vs. true stress for AZ31SC, HR and ECAP.

The highest strain hardening was determined for ECAP material followed by HR alloy. The lowest value was found for SC material. These findings show that the hardening mechanisms are the strongest in ECAP material.

6.3   Fatigue behaviour of AZ31

Examinations of fatigue behaviour of magnesium alloy AZ31 were focused on the determination of cyclic plastic response, fatigue endurance, fatigue strength and notch sensitivity of the material. Influence of loading frequency on fatigue behaviour was examined as well. Three conditions of AZ31 were tested and the results were compared to each other. Cyclic plastic response was determined from hysteresis loops. The hysteresis loops were measured only at the beginning of the cyclic loading. The fatigue endurance was determined in broad range from low to high cycle region. In the case of AZ31SC, the very high cycle region was studied as well. A broad range of stress amplitudes was applied and the fatigue responses were compared. The S – N curves and fatigue strength of smooth and notch specimens were determined and notch sensitivity factors were defined for all three conditions of AZ31.

Two types of specimens were used for fatigue testing. The specimen geometry was given by requirements of the testing facilities.

The smooth cylindrical specimens were used for hysteresis loop measurements. From these results the cyclic plastic response was established. Cylindrical specimens were machined in the same way as the specimens for tensile tests. The dimensions of SC and HR specimens were 5 mm in diameter and 25 mm in gauge length, cf. Fig. 6.2.1. The diameter of ECAP specimen was 4 mm and their gauge length was 20 mm.

Identical specimen geometries were used also for determination of smooth S – N curves and fatigue strength of SC material. Additionally, for these tests also hour-glass shaped specimens with 8 mm in diameter were used, cf. Fig. 6.3.1. In the case of HR material testing, the dimensions of the smooth hour-glass specimens with diameter of 3.5 mm were used. Additionally, also specimens with diameter of 8 mm, pictured in Fig. 6.3.1., were tested. Fatigue tests performance on ECAP material was done with the smooth hour-glass specimens with 7 mm in diameter. For testing of SC material, in the gigacycle regime, specimens with the geometry pictured in Fig. 6.3.2 were used.
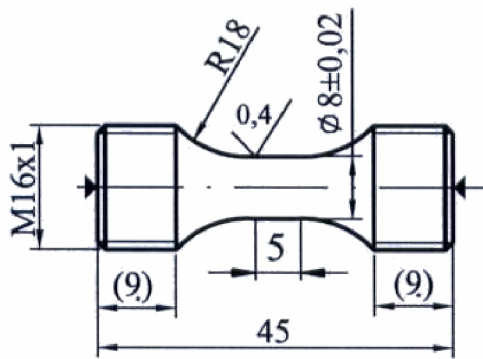
Fig. 6.3.1 Smooth specimen for fatigue testing
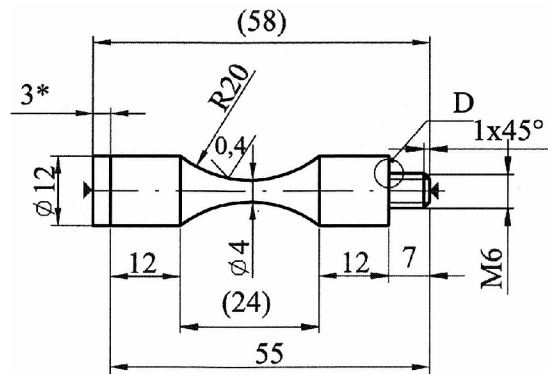
Fig. 6.3.2 Specimen geometry for testing in gyga-cycle regime

Notched specimens were prepared from smooth ones by machining of a circumferential notch in the centre of the gauge length. A notch specimen with two notch geometries is shown in Fig. 6.3.3. The notch specimen geometries and corresponding theoretical stress concentration factors K_t for different conditions of AZ31 are given in Tab. 6.4. The theoretical stress concentration factor was determined according to Peterson's diagrams [196].
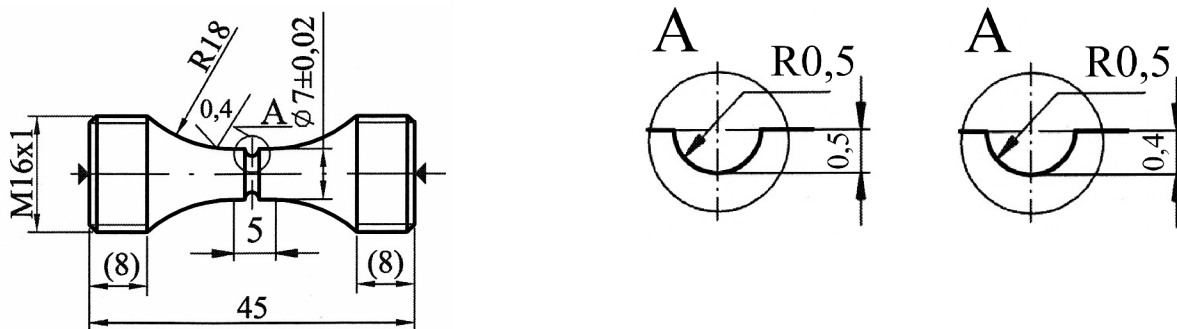
Fig. 6.3.3 Fatigue specimen with two notch geometries

Tab. 6.4 Geometry of notch specimens and theoretical stress concentration factors

	SC	HR	ECAP	ECAP
Diameter below the notch [mm]	7	7	6	6
Notch radius / r [mm]	0.4	0.4	0.4	0.5
Depth / h [mm]	0.5	0.5	0.5	0.5
Theoretical stress concentration factor / K_t	2.8	2.8	2.5	2.0

Specimens were used in the as machined conditions; no surface treatment was done. Only in some special cases when the surface observation had to be performed, the surface was polished with grit paper of 2400.

Fig. 6.3.4 Instron 8501 servohydraulic testing machine

Fig. 6.3.5 Servohydraulic testing machine Shimadzu EHF

Fig. 6.3.6 Resonant testing system Amsler HFP 5100

A number of testing machines was used for fatigue testing; Instron 8501 (servohydraulic testing machine of ± 10 kN load capacity), cf. Fig. 6.3.4 and Shimadzu EHF (servohydraulic testing machine with maximum load of ± 10 kN), cf. Fig. 6.3.5. Testing frequencies of 1 and 20 Hz were applied, depending on the kind of experiments. These machines belong to laboratories at TU Clausthal, Clausthal-Zellerfeld, Germany and Academy of Sciences, Brno, Czech Republic, respectively. Loading at higher frequency was performed on an Amsler HFP 5100 resonant testing system of ± 20 kN load capacity, cf. Fig. 6.3.6. The operating frequencies, which depend on the stiffness of the loaded body, were 60 and 100 Hz. These tests were done at the Academy of Sciences, Brno, Czech Republic. An ultrasonic testing machine with a frequency of 20 kHz was used for tests in the gigacycle region. Air-cooling during the ultrasonic tests was applied to keep the specimen temperature below 25°C. Ultrasonic tests were run at the University of Zilina, Zilina, Slovak Republic.

All tests were performed under load control and under symmetrical loading with a sine waveform. The asymmetry ratio R of -1 was applied. The fatigue tests were conducted at room temperature and in air.

Fatigue fracture observations were performed on a scanning electron microscope JEOL 6460. The observations were done at TU Clausthal, Clausthal-Zellerfeld, Germany.

6.3.1   Cyclic plastic response

The main purpose of the examination of cyclic plastic response from the hysteresis loops was the determination of softening and hardening mechanisms in the three conditions of AZ31 at the beginning of fatigue cycling. The hysteresis loops were measured on a servohydraulic testing machine Instron 8501.

A broad variety of stress amplitudes was applied for testing SC material. Namely, the stress amplitudes σ_a of 40, 50, 60, 70 and 80 MPa were used. It could be stated that cyclic hardening at the beginning of the cyclic loading was observed for all tested specimens. For a better transparency not all results are shown here. One example of a hysteresis loops of AZ31SC for the load amplitude of 80 MPa for the first approx. 150 cycles is shown in Fig. 6.3.7. It is clear that the hysteresis loops get narrower with increasing number of loading cycles. It indicates that the cyclic hardening occurs in the material during the initial loading. The cyclic hardening effect was more pronounced for higher load amplitudes.

In the case of HR material testing a broad variety of load amplitudes was used too. The following load amplitudes were applied; 100, 110, 120, 130, and 140 MPa. Also here, due to the place scarcity, only results of representative load amplitude are presented. An example of a hysteresis loop corresponding to the stress amplitude of 110 MPa is shown in Fig. 6.3.8. The cyclic hardening of HR material was observed at the beginning of the cyclic loading.
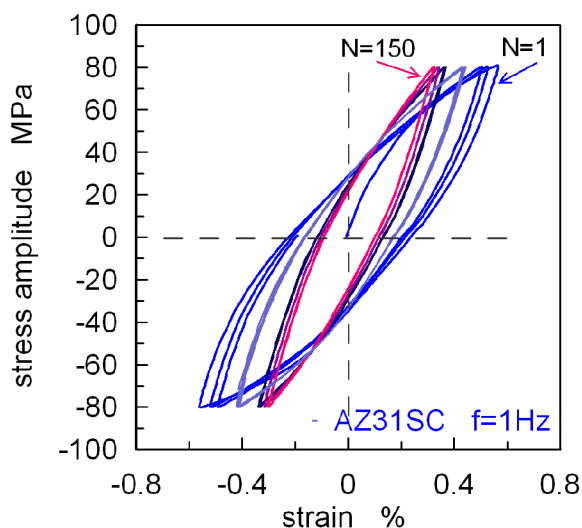
Fig. 6.3.7 Hysteresis loops for AZ31SC at σ_a = 80 MPa and f = 1 Hz.
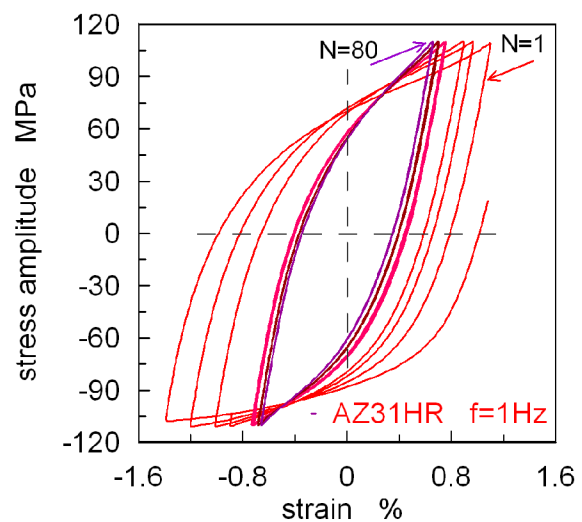
Fig. 6.3.8 Hysteresis loops for AZ31HR at σ_a = 110 MPa and f = 1 Hz.
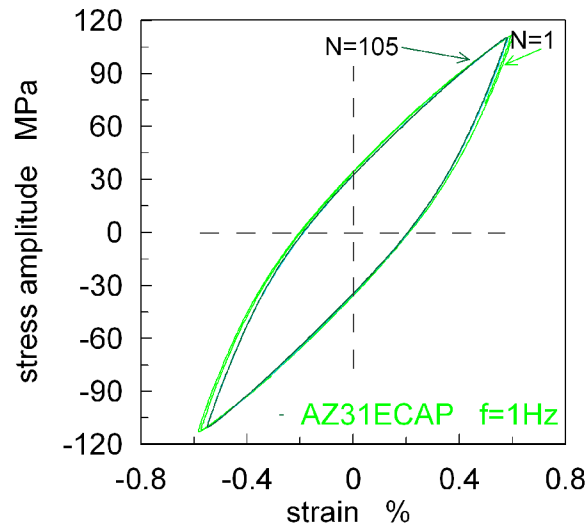
Fig. 6.3.9 Hysteresis loops of AZ31ECAP at $\sigma_a = 110$ MPa and f = 1 Hz.

ECAP material was tested only at one load amplitude of 100 MPa. The result of this test is shown in Fig. 6.3.9. Compared to the SC and HR conditions, the ECAP material shows only very small cyclic hardening. During the first hundred cycles the width of the hysteresis loops remains practically constant.

The general finding is that in all three conditions of AZ31 the cyclic hardening was observed. The strongest effect was found for HR material and the weakest one for ECAP material.

6.3.2   S - N curves, fatigue endurance of smooth and notched specimens, influence of frequency on fatigue behaviour

From the fatigue tests resulting in a very broad interval of number of cycles to failure ranging from low-cycle fatigue up to gigacycle fatigue, the following material characteristics were obtained.

1. Fatigue endurance and fatigue strength of smooth specimens for the three conditions of AZ31.

2. Fatigue endurance and fatigue strength of notched specimens for the three conditions of AZ31. Notched specimens with different notch geometries and different stress concentration factors were used for the tests.

3. Fatigue notch factor K_f was determined for all three conditions. Two ways of establishing the fatigue notch factor were applied. The direct way is calculating the notch factor according to the definition from experimentally determined fatigue strength of smooth and notch specimens, Eq. 6.4.

$$K_f = \sigma_{c, \text{smooth}} / \sigma_{c, \text{notch}} \qquad , \qquad (6.4)$$

where: $\sigma_{c,\text{smooth}}$ is the fatigue limit of a smooth specimen [MPa] and $\sigma_{c,\text{notch}}$ is the fatigue limit of a notched specimen [MPa].

The second way is based on fracture mechanical considerations and laws of fatigue crack propagation. The fatigue notch factor can be expressed by means of theoretical stress concentration factor K_t and material parameter according to Eq. 6.5 [206]:

$$K_f = K_t / (1 + 4.5 (a_0 / r))^{1/2} \quad , \qquad (6.5)$$

where K_t is the theoretical stress concentration factor, r is the notch radius [mm] and a_0 is the critical crack size (taken as a material constant), [mm].

4. The notch sensitivity factor q for all three conditions of AZ31 was determined according to Eq. 6.6.

$$q = (K_f - 1) / (K_t - 1) \qquad . \qquad (6.6)$$

If q = 0 => the notch has no influence on fatigue behaviour.
If q = 1 => full theoretical effect of the notch on the fatigue lifetime.

5. The effect of loading frequency was studied and the frequency influence on fatigue behaviour of the three material conditions was examined. The data for particular conditions were compared and discussed. Fatigue tests on smooth and notched specimens were conducted at three frequencies: 20 Hz, ~ 100 Hz and 20 kHz. S – N curves for all three material conditions, for both types of specimens were established at 20 and ~ 100 Hz. Additionally, the S – N curve for smooth SC specimens tested at frequency of 20 kHz was determined as well.

The fatigue tests performed at loading frequencies of 20 and 100 Hz terminated at 10^7 cycles. The fatigue strength was defined on the basis of 10^7 cycles. Only the ultrasonic tests run till higher number of cycles, namely up to the region of 10^9 cycles.

6. Fracture surface observations were conducted on all conditions of AZ31 with the aim to describe fracture mechanisms and to recognize the differences in behaviour of particular structures.

S – N curves of smooth specimens for AZ31SC, HR and ECAP

The S – N curves for SC material were established in a broad interval of stress amplitudes in the range of 70 – 35 MPa. Examples of fatigue behaviour at three loading frequencies of 20 Hz, ~ 100 Hz and 20 kHz are presented in Figs. 6.3.10 –6.3.12.

In Fig. 6.3.10, the S – N curves for smooth SC specimens loaded at frequencies of 20 and 100 Hz are shown. It can be seen that the specimens fail either after a relatively low number of cycles (of the order of 10^5) or remain unbroken for more than 10^7 cycles, independently on the loading frequency. This effect points out the existence of inherent defects in the material (casting defects) or of a highly inhomogeneous distribution of cyclic plastic deformation leading to a scatter in the conditions for the fatigue crack initiation.

The fatigue strength of 40 MPa was determined at 10^7 cycles and at frequency of 20 Hz from three unbroken specimens. The descending part of the S - N curve (20 Hz) was fitted by Eq. 6.7 with the correlation coefficient of 0.84:

$$\sigma_a = 420 \, N_f^{-0.18} \qquad , \qquad (6.7)$$

where: σ_a is stress amplitude [MPa] and N_f is the number of cycles to fracture.

The S – N curve determined at frequency of 100 Hz is presented in Fig. 6.3.10. It can be seen that the fatigue endurance at 100 Hz is higher than that at frequency of 20 Hz. This is the case in low and high cycle regime. The fatigue strength of 45 MPa at 10^7 cycles was determined at 100 Hz. The descending part of the S - N curve is described by the Eq. 6.8 with the correlation coefficient for the fit being 0.85,

$$\sigma_a = 286 \, N_f^{-0.12} \qquad \qquad (6.8)$$
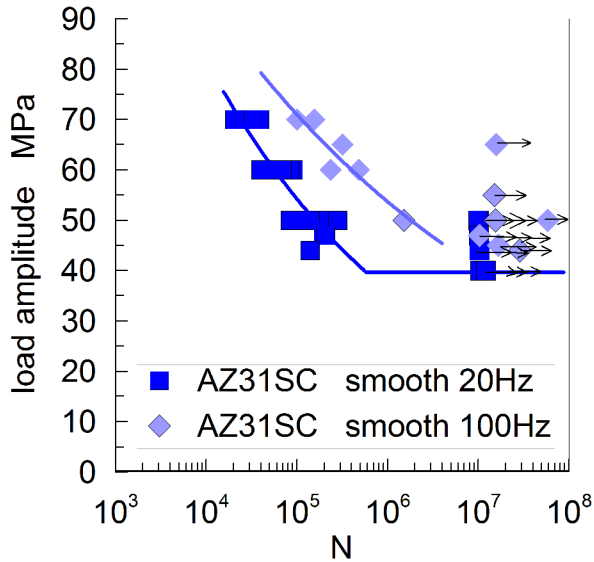
Fig. 6.3.10 S - N curves of smooth specimens of AZ31SC at 20 and 100 Hz.
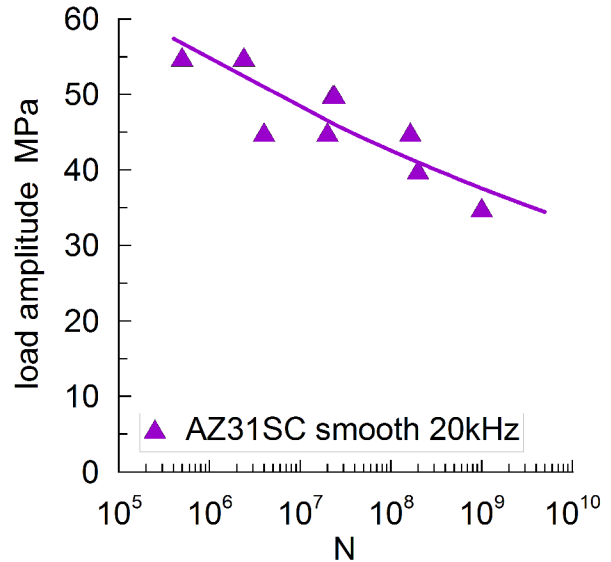
Fig. 6.3.11 S - N curves of smooth specimens of AZ31SC at 20 kHz.
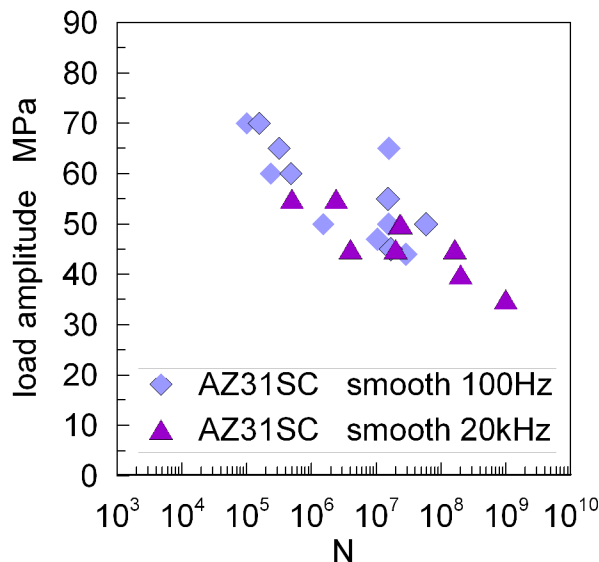
Fig. 6.3.12 S - N curve of smooth specimens of AZ31SC at 100 Hz and 20 kHz.

The gigacycle region of the S – N curve for smooth SC specimens is shown in Fig. 6.3.11. For these tests the ultrasonic frequency of 20 kHz was used. The experimental results are fitted by Eq. 6.9,

$$\sigma_a = 116 \, N_f^{-0.054} \qquad\qquad . \qquad\qquad (6.9)$$

The correlation coefficient in the case of Eq. 6.9 is 0.76.

In Fig. 6.3.12 a compound plot combining results for 100 Hz with those for 20 kHz is presented. It is clearly visible from the figure that the ultrasonic experimental data confirm the decreasing tendency of the S - N curve for 100 Hz up to the gigacycle region. This gives evidence for the fact that the fatigue limit based on 10^7 cycles does not mean an infinite fatigue endurance. Fatigue limit of this alloy has to be defined as the endurance limit or the fatigue strength at certain number of cycles. In the case of this work 10^7 cycles was taken as the decisive number.

Smooth specimens of hot rolled material were tested at two frequencies, namely at 20 and 100 Hz. The results of these tests are shown in Fig. 6.3.13. Also here, similarly to the case of SC material, an interval of stress amplitudes at which the specimens failed after a relatively low number of cycles or remained unbroken (run out specimens) after a high number of cycles ($\sim 10^7$) is observed. This indicates existence of internal defects in material. From comparison of results of testing at two different frequencies it can be concluded that the frequency did not have any influence on fatigue behaviour. The experimental data for both frequencies overlaps quite well. The endurance limit of the HR material for 10^7 cycles is 95 MPa. Fitting of all data by a power law results in Eq. 6.10:

$$\sigma_a = 218 \, N_f^{-0.058} \qquad\qquad . \qquad\qquad (6.10)$$

The correlation coefficient of this fit is 0.52.
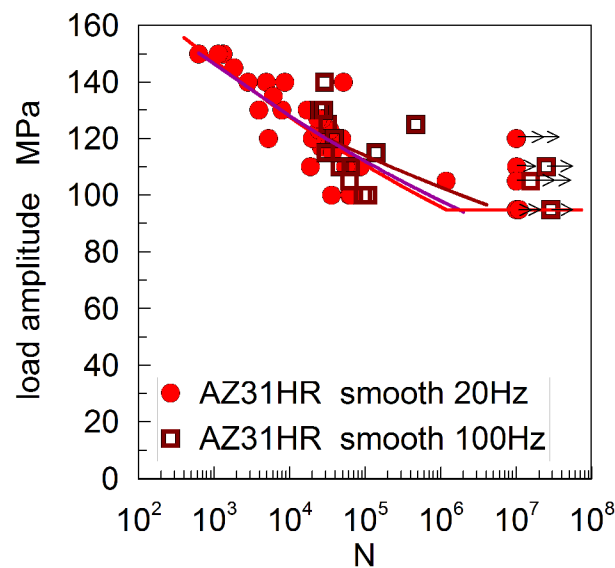
Fig. 6.3.13 S - N curves for smooth specimens of AZ31HR at 20 and 100 Hz.
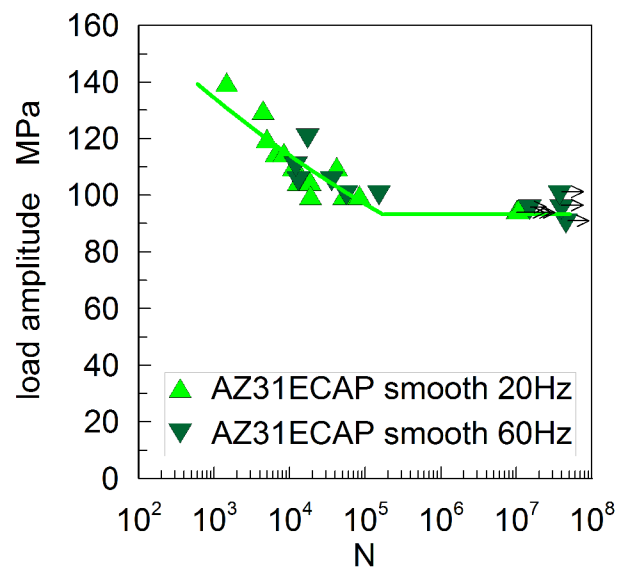
Fig. 6.3.14 S - N curves for smooth specimens of AZ31ECAP at 20 and 60 Hz.

Experimental results of fatigue behaviour of smooth ECAP specimens tested at two frequencies (20 and 60 Hz) are presented in Fig. 6.3.14. Also in this case no frequency effect was found. The experimental data points corresponding to both frequencies overlap very well. This holds both for low-cycle and high-cycle region. The decreasing part of the S − N curves is described by Eq. 6.11.

$$\sigma_a = 219 \ N_f^{-0.07} \qquad . \qquad (6.10)$$

The correlation coefficient is 0.72. The fatigue strength at 10^7 cycles is 95 MPa for both frequencies.

S – N curves of notched specimens for AZ31SC, HR and ECAP

The S – N curves for notched SC specimens are presented in Fig. 6.3.15. Specimens with a theoretical stress concentration factor $K_t = 2.8$ were used for the testing. The specimens were loaded at frequencies of 20 and 100 Hz. A broad scatter of experimental data at different stress amplitudes is observed, Fig. 6.3.15. The decreasing parts of the S – N curves tested at a frequency of 20 Hz and 100 Hz were fitted by power laws, Eqs. 6.11 and 6.12. The corresponding correlation coefficients are 0.61 and 0.88, respectively.

$$\sigma_a = 165 \ N_f^{-0.092} \qquad (6.11)$$

$$\sigma_a = 183 \ N_f^{-0.093} \qquad (6.12)$$

No significant difference in fatigue behaviour for the specimens tested at two frequencies was observed. The experimental points in LCF and HCF create one broad scatterband. The fatigue strength of the squeeze cast notched AZ31 corresponding to 10^7 cycles is 40 MPa.
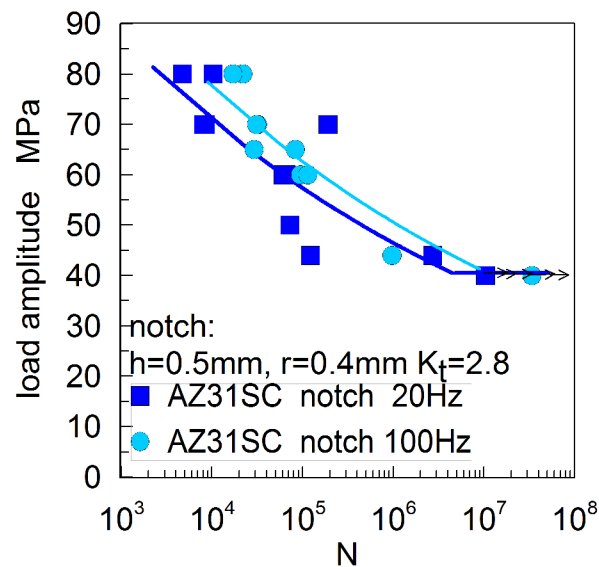
Fig. 6.3.15 S - N curves of notched SC specimens at 20 and 100 Hz.
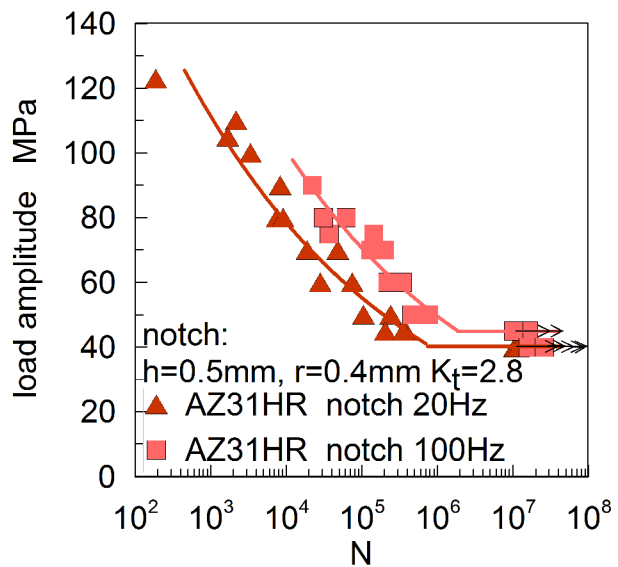
Fig. 6.3.16 S - N curves of notched specimens of AZ31HR at 20 and 100 Hz.

The notched HR specimens with a stress concentration factor of 2.8 were tested at two frequencies; 20 and 100 Hz. Results of fatigue behaviour are presented in terms of S - N curves in Fig. 6.3.16. A small increase of fatigue endurance with increasing frequency can be deduced from the data. The decreasing part of the S – N curve for 20 Hz is described by a power law, Eq. 6.13 and for 100 Hz by Eq. 6.14. The correlation coefficient for Eq. 6.13 is 0.94 and for Eq. 6.14 it is 0.85.

$$\sigma_a = 318 \, N_f^{-0.15} \qquad\qquad\qquad (6.13)$$

$$\sigma_a = 415 \, N_f^{-0.15} \qquad\qquad\qquad (6.14)$$

The fatigue strength at 10^7 cycles at the frequency of 20 Hz for notched HR specimens was found to be 40 MPa and at 100 Hz slightly higher, 45 MPa. The experimental points of notch specimens exhibit substantially smaller scatter as compared to the smooth specimens.

The ECAP notched specimens were tested at two frequencies of 20 Hz and 60 Hz. The specimens with a stress concentration factor of 2.5 were tested at frequency of 20 Hz and the specimens with a stress concentration factor of 2.0 were tested at frequency of 60 Hz. The results of determination of lifetime are shown in Fig. 6.3.17. The ECAP specimens with smaller stress concentration factor and tested at higher frequency show better fatigue endurance and fatigue strength as compared to specimens with higher stress concentration factor tested at lower frequency. The fatigue strength for specimens with $K_t = 2.5$ is 45 MPa, while for specimens with $K_t = 2$ it is 80 MPa. The decreasing part of the S - N curve for specimens with $K_t = 2.5$ tested at 20 Hz is described by the Eq. 6.15 with a correlation coefficient of 0.93. The decreasing part of the S - N curve for the notched specimens with $K_t = 2$ is described by Eq. 6.16 with the correlation coefficient of 0.7.

$$\sigma_a = 359 \, N_f^{-0.16} \qquad\qquad\qquad (6.15)$$

$$\sigma_a = 153 \, N_f^{-0.039} \qquad\qquad\qquad (6.16)$$
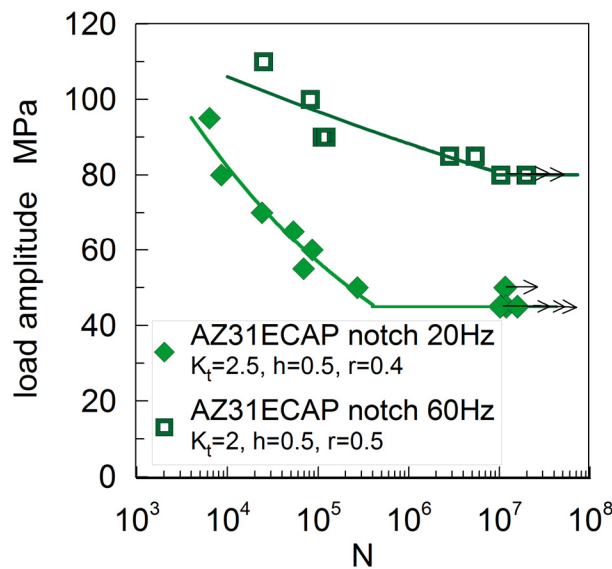
Fig. 6.3.17 S - N curves of notched specimens of AZ31ECAP at 20 and 60 Hz

Fatigue notch factor, fatigue notch sensitivity and critical crack size

When fatigue behaviour of smooth SC specimens at frequency of 20 Hz is compared with results of notched SC specimens it is possible to conclude that there is no notch effect, cf. Figs. 6.3.10 and 6.3.15. The fatigue strength of smooth specimens as well as notched specimens is nearly the same and equal to 40 MPa. Thus, the fatigue notch factor K_f calculated by Eq. 6.4 is 1. Consequently, the fatigue notch sensitivity is zero according to

Eq. 6.6. This result means full notch insensitivity of SC material. The results are summarized in Tab. 6.5.

The situation is very similar when results of smooth SC specimens and notched SC specimens tested at frequency of 100 Hz are compared. The fatigue strength of smooth specimens tested at frequency of 100 Hz is 45 MPa. This value is slightly higher when compared to results of notched SC specimens with fatigue strength of 40 MPa. In this case, the fatigue notch factor is 1.13. The corresponding fatigue notch sensitivity is 0.07, Tab. 6.5. Taking into account the scatter of experimental data, it can be concluded that the SC material is practically insensitive to notches with theoretical stress concentration of about 2.8.

The critical crack size for non-propagating cracks for smooth and notched specimens of SC material was calculated according to Eq. 6.5. In the case of the SC specimens tested at 20 Hz the critical crack size is 60 μm. The critical crack size for SC specimens tested at 100 Hz is 51 μm, Tab. 6.5. The critical crack size in both cases differs not too much. With respect to the accuracy of the experimental determination of lifetime data the critical crack size of 55 ± 5 μm can be considered as representative value for SC material. However, this size is much smaller than the average grain size, which indicates that influence of inherent defects in SC material may shield the effect of artificial notch with $K_t = 2.8$.

Tab. 6.5 Fatigue notch factor, notch sensitivity and critical crack size

	AZ31					
	SC	**SC**	**HR**	**HR**	**ECAP**	**ECAP**
Frequency, f (Hz)	20	100	20	100	20	60
Radius below the notch, d (mm)	7	7	7	7	6	6
Notch depth, h (mm)	0.5	0.5	0.5	0.5	0.5	0.5
Notch radius, r (mm)	0.4	0.4	0.4	0.4	0.4	0.5
Fatigue strength of smooth sp., $\sigma_{c,s}$ (MPa)	40	45	95	95	95	95
Fatigue strength of notched sp., $\sigma_{c,n}$ (MPa)	40	40	40	45	45	80
Fatigue notch factor, K_f	1	1.13	2.38	2.11	2.11	1.19
Stress concentration factor, K_t	2.8	2.8	2.8	2.8	2.5	2.0
Critical crack size, a_0 (mm)	0.060	0.051	0.0076	0.013	0.0078	0.033
Notch sensitivity, q	0	0.07	0.76	0.62	0.74	0.19

The significant decrease of fatigue life and fatigue strength of notched HR specimens is observed when compared to smooth specimens, cf. Figs. 6.3.13 and 6.3.16. It means high notch sensitivity of HR material. The fatigue notch factor K_f for specimens tested at a frequency of 20 Hz is 2.38. This value was determined as the ratio of fatigue strength of smooth specimens (95 MPa) and notched specimens (40 MPa), Tab. 6.5. The fatigue notch factor K_f of 2.11 was determined for specimens tested at frequency of 100 Hz. In this case the fatigue strength of smooth specimens was 95 MPa and the fatigue strength of notched specimens was 45 MPa. The fatigue notch factor is slightly higher at lower frequency when compared to fatigue notch factor at higher frequency. The notch sensitivity factor is 0.76 for loading with frequency 20 Hz and 0.62 for loading at frequency 100 Hz. Both values are far from zero and thus they prove a significant notch sensitivity of HR material.

The non-propagating crack size of 7.6 μm was determined for specimens tested at 20 Hz and 13 μm for specimens tested at 100 Hz. These values are well comparable with the grain size of the HR material, ranging between 5 and 20 μm. It suggests that the grain size

may be the responsible structural parameter from the point of view of fatigue damage and the fatigue strength. The notch with the radius of 0.4 mm and the depth of 0.5 mm and its stress concentration field is much larger than the grain size and thus the artificial surface notch is expected to have significant effect on fatigue performance of HR material.

The fatigue strength of smooth ECAP specimens tested at frequency of 20 Hz is 95 MPa, Fig. 6.3.14. The fatigue strength of ECAP notched specimens with $K_t = 2.5$ tested at 20 Hz is 45 MPa, Fig. 6.3.17. Consequently, the fatigue notch factor K_f is 2.11, Tab. 6.5. In this case the notch sensitivity is 0.74. This value of notch sensitivity indicates a high notch effect in the case of ultrafine grained material. The situation was slightly different when the smooth specimens and notched specimens with $K_t = 2.0$ made from of ECAP material were tested at frequency of 60 Hz. In this case the fatigue notch factor K_f is 1.19 and the notch sensitivity factor q is 0.19. The comparison of K_t and K_f values Tab. 6.5 shows that the notch geometry and also frequency of loading influences the notch sensitivity of ECAP material.

The calculated critical non-propagating crack size of 7.8 μm was determined from observation on specimens with $K_t = 1.0$ and 2.5 tested at a frequency of 20 Hz, Tab. 6.5. From observations on the specimens with $K_t = 1.0$ and 2.0 tested at 60 Hz, a critical crack size of 33 μm was determined. The value of $a_0 = 33$ μm is higher than that in the previous case ($a_0 = 7.8$ μm, $K_t = 2.5$), see Tab. 6.5. The size of the critical crack is larger than the grain size (2.5 μm) of ECAP material. Thus, in ECAP material the grain size itself cannot be directly considered as a limiting factor for non-propagating cracks.

6.3.3 Fractographic examination

From the observation of fracture surfaces of SC, HR and ECAP AZ31 loaded at different stress amplitudes some generalising conclusions can be drawn. In this chapter, by reason of better transparency, only few representative pictures of each material condition are presented.

Squeeze cast material

The overview picture of a fracture surface of the SC specimen, tested at $\sigma_a = 70$ MPa and run until fracture at $N_f = 139\ 978$ cycles, is shown in Fig. 6.3.18. In the case of SC specimens, mostly a multiple fatigue crack initiation from the specimen surface was observed. Detail of a crack initiation site is shown in Fig. 6.3.19 for a specimen loaded at $\sigma_a = 80$ MPa and fractured at $N_f = 12\ 186$ cycles. The fatigue crack initiated on the specimen surface and macroscopically propagated towards the specimen centre. However, microscopically, just after initiation in this case the crack propagated along the cylindrical specimen surface, as can be inferred from the fracture markings, resembling striations. Typically, the crack does not follow one specific direction, but it grows in more directions simultaneously. This is documented in Fig. 6.3.20. Fatigue fracture of SC material had a transcrystalline character. The detailed analysis of the fracture surface of three neighbouring grains (one of them is very close to the specimen surface) is shown in Fig. 6.3.21.
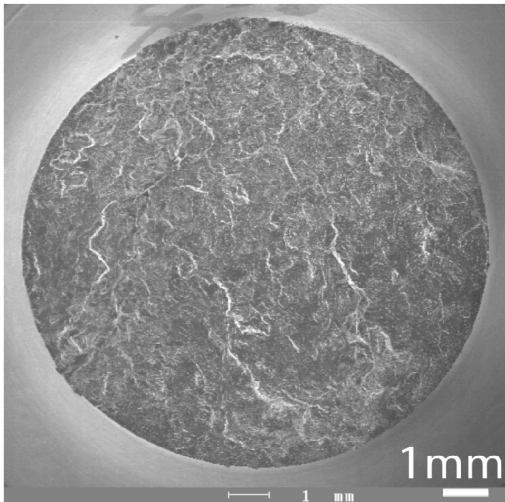
Fig. 6.3.18 Macro view of AZ31SC, multiple crack initiation, $\sigma_a = 70$ MPa, N_f = 139 978 cycles.
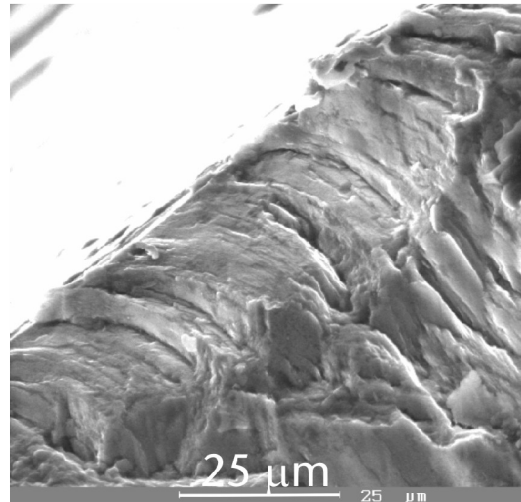
Fig. 6.3.19 Initiated crack from specimen surface follows the circumference of specimen surface, $\sigma_a = 80$ MPa, N_f = 12 186 cycles.
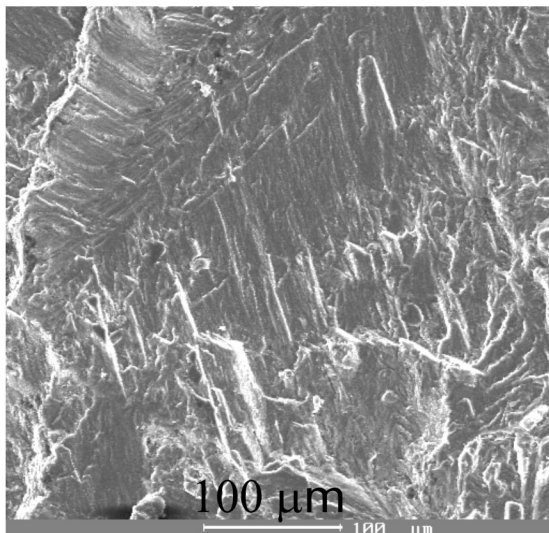
Fig. 6.3.20 Different directions of crack propagation in AZ31SC, $\sigma_a = 80$ MPa, N_f = 12 186 cycles.
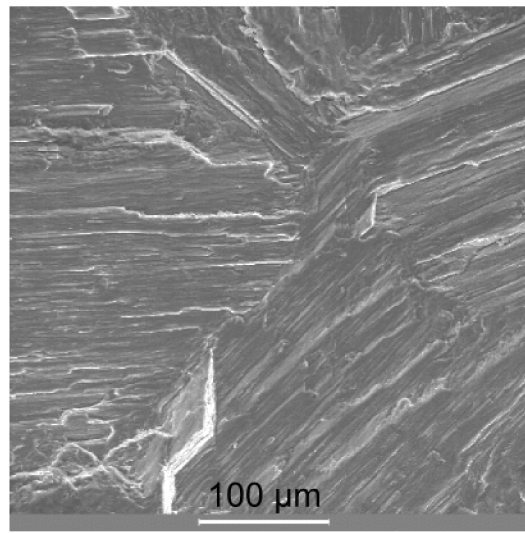
Fig. 6.3.21 Three neighbouring fractured grains of AZ31SC, $\sigma_a = 70$ MPa, N_f = 139 978 cycles.

Hot rolled material

An overview of a typical fracture surface of HR material is shown in Fig. 6.3.22. The roughness of the surface is substantially lower than that of SC material. The cracks initiated on the specimen surface. Generally, a multiple crack initiation sites are observed. The fracture surface with surface markings, striations, indicating the direction of the crack propagation is shown in Fig. 6.3.23. The fracture surface corresponds in this case to low-cycle fatigue and high crack propagation rate.
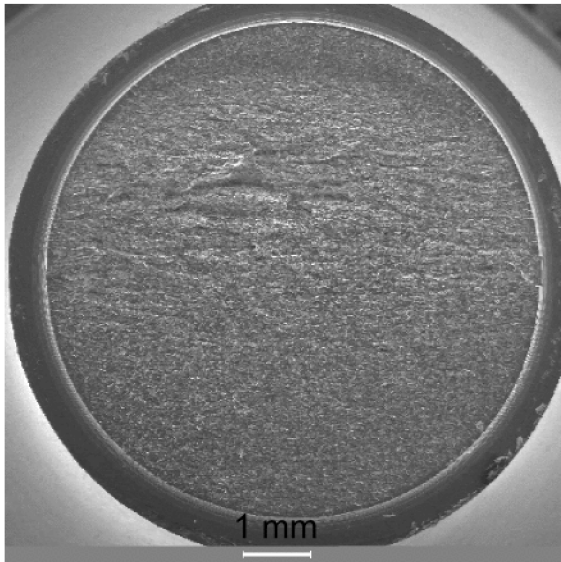
Fig. 6.3.22 Overview of fatigue fracture on the notch specimen, AZ31HR; σ_a = 60 MPa, N_f = 28 172.
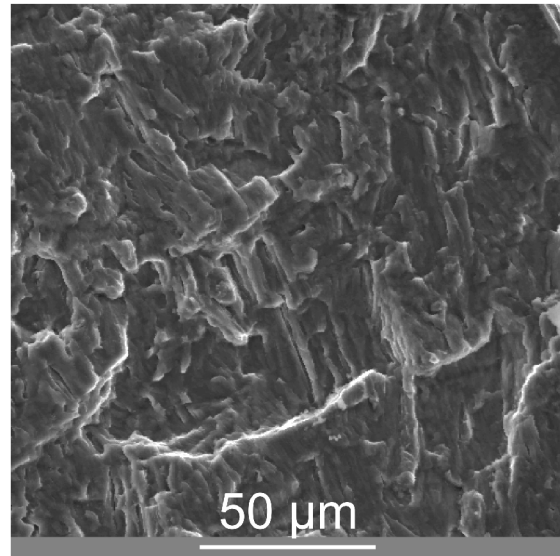
Fig. 6.3.23 Crack propagation from the upper right corner of the picture, AZ31HR, σ_a = 150 MPa, N_f = 622 cycles.

ECAP material

Overview of the fracture surface of the ECAP material tested at stress amplitude of 110 MPa is shown in Fig. 6.3.24. The significant segmentation of the fracture surface is clearly visible. Multiple crack initiation was often observed. An example of crack initiation site is presented in Fig. 6.3.25. A high number of secondary cracks was observed. Multiple crack initiation along the shear planes of the last ECAP plane can be seen on the gauge length of the specimen, Fig. 6.3.26. These cracks were tilted about 45° away from the loading direction. Detail of one such a crack is shown in Fig. 6.3.27.
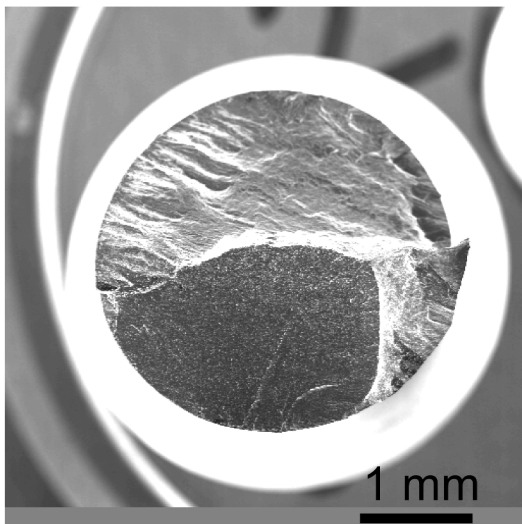
Fig. 6.3.24 View of a fracture surface of AZ31ECAP, segmentation of the fracture surface, σ_a = 110 MPa, N_f = 11 162 cycles.
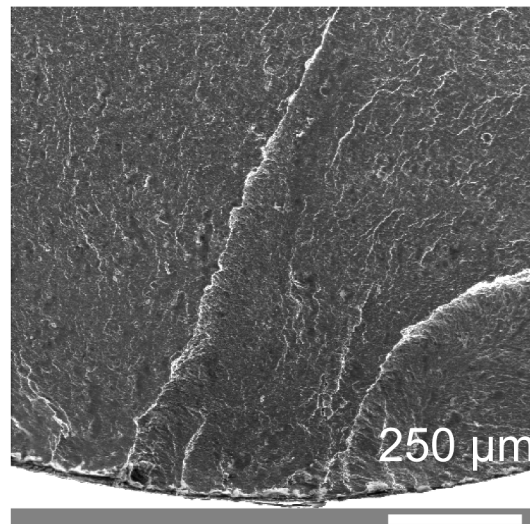
Fig. 6.3.25   Crack   initiation   site   in AZ31ECAP, σ_a = 110 MPa, N_f = 11 162 cycles.
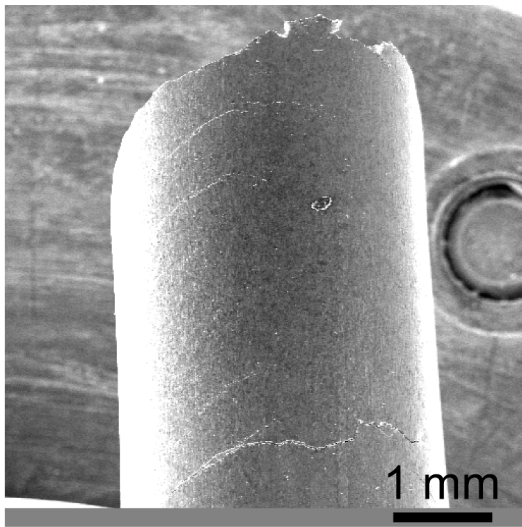
Fig. 6.3.26 Smooth specimen after fracture, several cracks on the body of smooth specimens, AZ31ECAP, σ_a = 100 MPa, N_f = 84 025 cycles.
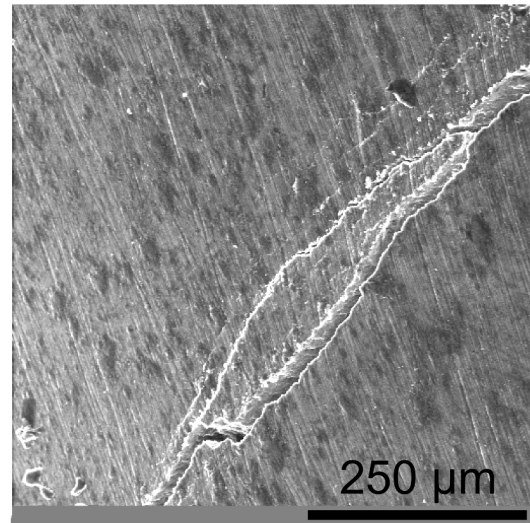
Fig. 6.3.27 Splitting of a crack on the specimen surface, AZ31ECAP, σ_a = 100 MPa, N_f = 84 025 cycles.

7   Discussion and conclusions

The first task in this work was to process the magnesium alloy AZ31 by equal channel angular pressing. Various processing conditions, differing in pressing temperature, pressing speed and lubricants were examined. The optimal pressing parameters for producing AZ31 by ECAP were found: temperature of 200°C and a pressing speed of 5 mm/min. At these conditions bulk specimens were produced without any cracks and defects. This was a crucial step for further progress of this work, because the main task of this research was comparison of fatigue behavior and performance of AZ31 Mg alloy in different conditions including state after ECAP.

An important achievement of this part of the research is the finding that with sufficient experience and with suitably defined process parameters, Mg alloy AZ31 can be well processed by ECAP, though its hexagonal structure. The resulting microstructure exhibits fine-grain size.

Microstructure and texture

From the data published in the literature, it is obvious that microstructure and texture are influenced by the processing route. Magnesium alloy AZ31 was produced by squeeze casting, hot rolling and equal channel angular pressing. The three conditions of AZ31 examined in this work show strong differences in microstructure and texture. These differences result from the processing details of each production technique. Generally, a coarse microstructure is observed in the material produced by squeeze casting. It is because Mg-Al alloys have no reliable grain refiner. The squeeze cast AZ31 presented in this work shows a coarse dendrite microstructure with random texture. This result is in full agreement with literature data where the coarse grained microstructure of cast magnesium alloys is reported. Actually, after gravity casting, a grain size of 1800 μm was observed and after continuous casting the grain size was 350 μm [51]. Similar results were found in [53, 72, 75, and 207].

The materials produced by hot rolling show smaller grain size than materials produced by squeeze casting. For example, grain sizes of 10 μm [208] and 9 μm [63] were observed in rolled AZ31. A grain size of 58 μm with very large grains up to 250 μm were observed for rolled AZ31 by Bohlen et al. in [71]. Grain sizes of 50 μm [29, 72] and 60 μm [75] were determined for AZ31; a grain size of 40 μm for AZ91 [89, 209]. In some microstructures twins were observed [63]. However, the grain size and twins occurrence strongly depend on the rolling temperature. In the present work the grains of HR material are equiaxed and well developed. It indicates that the recrystallization took place as a consequence of elevated process temperature. The grains have a character of high angle boundaries. Texture observations of HR alloy proved typical texture after hot rolling process. The basal planes were parallel to the last rolling direction. The origin of this texture could be explained in the following way. When the deformation degree in one direction is higher than in the other one, then the basal planes prefer to align in the higher deformation direction. It means that the rolling could be understood as a compression perpendicular to the sheet plane and as a tension in the rolling direction. Consequently, basal planes during rolling are oriented parallel to the sheet plane. These results, following from this study, are in good agreement with literature data. The basal texture was observed for rolled AZ31, AZ61 and AM60 in [59, 73, 185 and 209]. However, the texture of Mg alloys where the basal planes are tilled ± 15 to 25 and 7 − 8 degrees away from the normal direction towards the rolling direction was found as well [63,

74, 75 and 209]. It is evident that the literature data are not comprehensive and discrepancies can be often found. Thus, a further detailed study of microstructure is necessary. In this context it is significant that the strain rate and temperature of the rolling as well as chemical composition of the magnesium alloy have a strong influence on the microstructure and texture [65, 69 and 75].

It was stated in literature that the grain size of ECAP alloy is about 1 –2 μm [29 and 59]. For example a grain size of 1.4 μm was observed for AZ31ECAP [68] and in AZ91 it was 1 μm [210, 211]. This finding is in full correspondence with the results of the present work where a grain size of 2.4 μm was determined for ECAP material. Since the ECAP process is performed at elevated temperature, it is basically not possible to obtain a considerably finer microstructure, let us say in the order of hundreds of nanometers. It is a consequence of DRX at elevated temperature that is not possible to suppress or exclude. It is important that the ECAP grains show a high angle boundary character. ECAP alloy shows definitely higher amount of high angle boundaries than hot rolled material. On the other hand, coarse grains of the size 15 – 50 μm surrounded by grains of 2.5 μm were observed for ZK60ECAP by Stoica et al. [90]. These inconsistencies in literature data may, according to our experience with ECAP technique, result from different parameters of ECAP process. Temperature and strain rate have a very strong influence on resulting microstructure. There is very limited information data base on texture of ECAP magnesium alloys in literature. The majority of texture observations was done on cubic metals, such as Al, Cu, Fe and their alloys [33, 59, 72 and 90]. However, in the literature reports about Mg alloys processed by ECAP the texture with basal planes parallel to the shear plane was observed by many authors [31, 42, 50, 59, 81 - 84, 95]. This texture, where the basal planes lay parallel to the shear plane of ECAP, was observed also for the ECAP material studied in this work. With other words, the basal planes are inclined by about 45° to the pressing direction. Thus the ECAP texture is a combination of basal and prismatic planes being inclined about 45° to the pressing direction. Also in this case a correlation between the direction of a high deformation and the basal plane orientation could be detected.

Further, the texture intensity of ECAP material is stronger when compared to the HR one. This is in good agreement with literature data dealing with texture intensity. Agnew et al. [83] and Kim et al. [84] reported that the texture intensity in magnesium alloys produced by ECAP is higher than that in extruded or rolled alloys. The highest intensity of ECAP texture can be explained by the lowest processing temperature (200°C) as compared to the hot rolling (~ 370°C) and casting. The next reason for higher texture intensity of ECAP alloy is a larger strain involved during the deformation process as compared to hot rolling. These conclusions are in very good agreement with known literature data.

It is not surprising and could be expected that the three different microstructure and texture conditions of tested AZ31 influence substantially the mechanical properties of the AZ31 alloy. Considering the Hall-Petch relation the ECAP material should have the best mechanical properties. Surprisingly, the behaviour of ECAP material was found to be not as expected. The ECAP material does not exhibit an improvement of the mechanical properties in such extend as it was expected. On the contrary, in many cases deterioration of the material properties was observed. The explanation of this finding will be given later in the discussion of results.

Tensile behaviour

The literature data show that the tensile properties of magnesium alloys strongly depend on the material condition, Sec. 3. Texture and microstructure influence the material properties. Materials with strong textures (extruded and rolled) show in many cases anisotropy of the mechanical properties [51, 53 and 65]. Agnew et al. [83] stated that the orientation of the tensile specimen with respect to the initial texture significantly influences the tensile behaviour. The highest yield stress and tensile strength was observed for the 0°-specimen with c-axis perpendicular to the loading direction, Sec.3. The same effect was observed also in the present work. HR material with c-axis perpendicular to the tensile loading direction showed the highest tensile strength and yield stress. High values can be explained by unfavorable texture orientation for easy activation of slip or twinning mechanisms. The Schmidt factor, related to the easiness with which deformation by glide can occur, is close to zero. Contrary to these observations, other authors demonstrated different behaviour [51, 53, 63, 74 and 212]. A higher yield stress and ultimate tensile stress were observed for the 90°-specimens when compared to the 0°-specimen. These differences were explained by initial texture variability as in the case of rolled AZ31 [74], where the basal plane was tilted ± 15° to the rolling direction. Further, Wendt et al. reported in [208] any plane anisotropy of mechanical properties in different directions for hot rolled AZ31. Isotropy of the tensile properties was also observed for rolled AZ31 by Kim et al. [79].

In the case of texture inclined 45° to the loading direction, simulating ECAP texture, a low yield stress and improved ductility was observed by Yi [65]. Mukai et al. [81] showed that material with texture favourable for basal slip showed higher ductility over that having unfavourable texture for basal slip. The improvement of ductility by a factor of about 2 -3 for AZ31ECAP over the non-ECAP condition was reported in [72 and 82]. Identical results were observed for AZ31ECAP in [59, 71, 81 and 83]. These results support also the present work, where the ECAP alloy showed an enhanced ductility when compared to the hot rolled and cast condition. Further, a lower yield stress and tensile strength was observed for AZ31ECAP when compared to the HR material but not to the SC one. Similar behaviour was also found by Watanabe et al. [95] for extruded AZ31 vs. ECAP one, even the ECAP alloy had a smaller grain size. These results could be explained by favourable texture orientation (c-axis 45° to the loading direction) for easy basal slip at the beginning of the loading. The Schmidt factor is high, approx. m = 0.5. Further, Agnew et al. [72] suggested that the ductility improvement is due to the randomization of the originally strong extrusion texture. Contrary to this, subsequent work of Agnew et al. [83] showed that the ECAP texture was stronger than the original extruded texture, rather than weaker. Thus, the improvement of the ductility for AZ31 is due to a positive change in texture [83]. Results of this work confirm this statement, because also here a higher texture intensity was found for ECAP material when compared to hot rolled alloy. Next, any difference in ultimate strength between AZ31ECAP and AZ31ECAP+annealing was observed by Mukai et al. in [81] and by Komado et al. in [213]. However, a strong discrepancy of the results can be found in relevant literature. First, ECAP magnesium alloys with enhanced elongation and enhanced strength when compared to the extruded and cast alloy were reported by Watanabe et al. and del Valle et al. [95 and 59]. This behaviour was confirmed for AZ31B-ECAP+annealed [66], $Mg_{97}Zn_1Y_2$ ECAP [31] and further for Mg and Mg-9Al (ECAP *vs.* cast [48]) and AS21 (EX-ECAP *vs.* HPDC [125]). Second, enhanced ductility, but not enhanced strength, was reported for ECAP magnesium alloys when compared to the extruded one. It means that the ductility and the strength are not always improved with decreasing grain size simultaneously. A higher ductility and lower strength of ECAP material when compared to the extruded one was reported for ZK60 [90, 126], AZ61 [84] and AZ31 [83]. Also the results of this work belong to this category. The

third case is when enhanced strength but not enhanced ductility of ECAP material (when compared to cast one) is reported. So it was for example in the case of AM60ECAP when compared to the cast alloy [97]. These differences among the literature results are due to the differences in the texture and microstructure resulting from the big variations in production techniques conditions regarding temperature, speed, strain etc.

The ECAP material exhibits the highest hardening during tensile loading when compared to the SC and HR condition. This observation is in full agreement with results published in [83, 213], where a higher hardening response was reported for AZ31ECAP than for the non-ECAP alloy. The high hardening of fine-grained alloy observed in this work is possible to explain by additional intensive twinning and dislocation pile-ups. Consequently, the ECAP material shows the highest plastic ability during tensile loading. The lowest hardening when considering the stress increment between the yield and the ultimate tensile stress, σ_{UTS} - σ_{YS}, was determined for SC material. The cast alloy with random texture means that some grains are favourably oriented for activation of deformation modes and other grains are not. This may lead to a variation of the Schmid factor. Generally, SC alloys with random texture do not exhibit any anisotropy of tensile properties. These data show that the texture has an important influence on the tensile properties of wrought Mg alloys.

The texture is, however, not the sole mechanism influencing the material properties. Also the grain size is expected to influence the tensile properties. From general knowledge it follows that higher tensile properties are expected for fine-grained material [50, 81 and 122]. The tensile results of the present work show that the squeeze cast alloy with coarse grains exhibits, according to expectation, the lowest tensile strength and ductility, which is in full agreement with literature results described in Sec. 3. A low tensile elongation was reported for the die cast AZ91 (8 %) and AM60 (11 %) [81] and cast AM60 [59]. The low tensile properties of SC alloy result from the coarse grained structure, hcp-lattice with restricted slip systems, slip anisotropy, difficulty of cross-slip within the grains [123] and by deteriorate effect of cast defects [124].

Wrought magnesium alloys, after rolling and extrusion, have smaller grain size and thus also better mechanical properties [64 and 122]. The same tendency was expected for ECAP material due to its fine microstructure [48, 72 and 98]. In the present work the hot rolled material with grains of 15 μm has higher tensile strength than the ECAP material with grain size of 2.4 μm. Additionally, the ECAP alloy has a slightly lower tensile strength than the hot rolled material. Thus, the Hall-Petch relation is obviously not valid for AZ31ECAP vs. AZ31HR. The ECAP alloy has higher ductility when compared to other tested conditions. The explanation of this effect may be based on the influence of unfavourable HR texture and favourable ECAP texture for activation of deformation modes. To activate the deformation modes in HR material is more difficult and thus high stresses are necessary. It is just the opposite to the compressive behaviour, where for this lattice orientation of HR material a low yield stress was observed [214]. It results from the favourable orientation of hcp lattice for twinning in compression mode. It is very important to distinguish between the loading directions. From these results is evident that it is not possible to conclude that the tensile properties of ECAP alloy depend only on the grain size. The texture plays a certain role too.

The results of this work show that the materials with unfavourable texture for slip show a higher yield stress and ultimate tensile strength when compared to materials with favourable texture for slip deformation, almost independently on the grain size. Contrary to that, a higher ductility is found in the materials with texture favourable for slip deformation, as it is in the case of ECAP materials.

The results of this work provide new evidence regarding the effect of grain size and texture on the tensile properties of magnesium alloys. The texture effect appears to be predominant in the fine grained alloys and the grain size effect looks to be stronger in coarse grained SC alloy. However, the quantitative determination of particular contributions of the two effects to the materials strength is rather difficult. The results of the present study make it clear that it is necessary to carefully consider which condition of Mg alloy is to be used for a particular application and what processing route is to be chosen to produce the appropriate combination of grain structure and texture. New problems for engineering are opened because these results point out that a "small-grained material" does not automatically means the best strength characteristics of the material as it is expected on the basis of the Hall-Petch relation. Further, it is clear that the grain size is not the sole material parameter influencing the tensile properties. Additionally, results of this work play up the high significance of texture influence.

Fatigue behaviour

Generally, fatigue properties of materials with fine microstructure are better than those with coarse microstructure, except of threshold values for propagation of long fatigue cracks. Thus, it is expected that ECAP materials should exhibit better fatigue endurance than materials prepared by conventional methods and having conventional grain size. However, the results of this work show that this general trend is confirmed only partially for magnesium alloy AZ31. The general trend was confirmed only for magnesium alloys prepared by conventional techniques as squeeze casting and hot rolling. Research papers dealing with fatigue properties of ECAP magnesium alloys are completely missing in the literature. Thus, this work provides the first fatigue data on ECAP magnesium alloy AZ31. That is why the research was focused on conducting basic fatigue experiments, on determination of cyclic plastic response, fatigue endurance, notch sensitivity and frequency influence.

Cyclic plastic response. From literature data, cf. Sec. 3 it follows that the cyclic hardening is typical behaviour of cycled magnesium alloys [161, 188]. This was confirmed also by the results of this work. Cyclic hardening was observed for all three conditions of AZ31. However, significant differences were detected among the cyclic plastic responses of these three conditions. The cyclic hardening is related to the increasing dislocation density during repeated loading. The cyclic hardening in Mg alloys results from pinning of dislocations on incoherent precipitates and on the grain boundaries [55, 132]. Magnesium alloy AZ31 does not have sufficient amount of secondary particles, thus the hardening is most probably related to dislocation pinning on the grain boundaries. The higher hardening is expected in materials with small grains due to the higher amount of grain boundaries and thus having more places for dislocation pinning. Contrary to these expectations, the ECAP material with the smallest grain size showed the smallest cyclic hardening. The width of hysteresis loops remains practically constant from the beginning of cycling. Contrary to that, the HR and SC material show a pronounced hardening. Taking this into account, the explanation based on the grain size effect solely is not sufficient. The additional explanation could be sought in texture. ECAP material has strong texture with the majority of the grains oriented in one direction. The c-axis of hcp is tilted 45° to the loading direction. As it was already explained above, this is a very favourable position for slip. Since the grains have the same orientation, the dislocations could pass easily from one grain to another. Relative easiness of cyclic slip and the reversibility of dislocations glide upon unloading results in very small hardening of ECAP alloy at the beginning of cyclic loading.

The situation is different for SC and HR material. SC material has large grains which mean fewer possibilities for dislocation pinning. On the other hand, SC alloy has a random texture. Some grains are favourably oriented for easy deformation by slip and twinning and other grains are unfavourably oriented. The dislocation movement from one grain to another is obstructed by the neighbouring grains with the unfavourable orientation for glide as well as for twinning formation. Since twins are also obstacles for dislocation movement, they lead to hardening of the material, too.

The situation is a bit more complicated in the case of HR material, where an intensive cyclic hardening was observed. HR material has a grain size that efficiently arrests the dislocation movement that leads to hardening. However, the hardening of HR material was not uniform when tensile and compressive characteristic are compared. This effect has to be related with texture influence. Texture effect on the cyclic plastic response is more complex and not easy to explain. The c-axis of HR material is perpendicular to the loading. This hcp orientation means an unfavourable orientation for slip and twinning in tensile loading. On the other hand, this orientation is extremely favourable for twinning in compression loading. This was confirmed by comparison of yield stresses in compression and tension reported in [214]. The yield stress of HR material was much smaller in compression than in tension. It means that in compression loading the twinning is easily activated; even in the tension the deformation is difficult. Twinning in compression rotates the grains. This rotation causes a more favourable orientation of grains for easier initiation of deformation modes in tensile loading. Simultaneously, twinning and high among of grain boundaries mean obstacles for dislocation movement. It leads to extensive cyclic hardening of HR material. Thus higher cyclic hardening of HR material when compared to ECAP and SC alloy could be explained by more efficient pinning of dislocations.

To the author's knowledge this is the first study focused on the cyclic plastic response under fatigue loading of ECAP magnesium alloy, no such data being available in literature.

S – N characteristics. In Sec. 3 it was shown that the fatigue endurance increases with decreasing grain size [150]. It is valid at least for conventionally produced materials. However, this behaviour was not proved for ECAP magnesium alloys [146]. It is necessary to stress that fatigue data dealing with ECAP magnesium alloys are extremely limited. The results of the present work confirm that the coarse grained SC material has the lowest fatigue endurance and so also the lowest fatigue strength when compared to the ECAP and HR material. This behaviour was found in LCF and HCF. In the LCF, the HR alloy has the highest fatigue endurance. Thus, ECAP material with the smallest grains did not lead to improvement of the fatigue properties over the HR one. However, in the area of HCF, the fatigue strength is identical for both HR and ECAP material. Thus, no improvements of fatigue properties of ECAP material when compared to HR material were found, but on the other hand, also no their deterioration. The explanation of poor fatigue properties of SC material could be sought in the coarse structure with its inherent defects. On the other hand, the fatigue response of HR and ECAP material is not fully clear. The literature data dealing with this problem are very scarce [146, 167]. It is clear that the explanation of lower fatigue resistance of ECAP material could not be based only on the grain size effect. Texture has to play an important role too. A certain similarity of fatigue behaviour of ECAP and HR material could be found in tensile behaviour. Due to not yet known reason, the crack initiation and propagation is faster in ECAP material than in HR. Since the basal planes of ECAP materials are favourably oriented for easy deformation under loading, this could lead to easy crack propagation. All grains have identical orientation; thus they can not effectively hinder the dislocation movement and crack propagation. In the case of HR material, the texture orientation is unfavourable for easy deformation under tensile loading. On the other hand,

twinning is activated easily under compression loading. Thus, twins play as obstacle for dislocation movement. Consequently, due to the difficulty of dislocation movement, the crack initiation and propagation is slowed. Thus, it appears that the texture effect has bigger influence on fatigue behaviour of HR and ECAP material than grain size effect. However, to fully confirm these assumptions, a further, more extensive study is required.

From the literature data is obvious that S − N curves of magnesium alloys show a knee point in the range of 10^5 − 10^6 numbers of cycles [131]. It describes a transient from LCF to HCF. Such a transient area was found also for S − N curves in the present work. A knee point was determined for all three tested conditions of AZ31. Thus, results of this work are in good correlation with the general trend for magnesium alloys described in literature [164], Sec. 3.

Frequency effect on fatigue behaviour of three conditions of AZ31 was evaluated in this work. Since the loading frequency may significantly influence the fatigue endurance, these data are interesting from the point of practical applications. However, no critical frequency effect on fatigue behaviour was reported in the literature. The literature knowledge is based only on cast magnesium alloys and hot rolled material, ECAP alloys were not studied at all. Thus, results of this work are important for a complete knowledge of the fatigue behaviour of different conditions of magnesium alloys under loading at different frequencies. The experimental results for all three conditions of AZ31 tested at frequencies of 20 Hz, 100 Hz and 20 kHz, did not provide any evidence of a frequency effect on fatigue behaviour. So, these results are in a very good agreement with the literature data. However, a small discrepancy among the results for the SC material tested at 20 and 100 Hz is visible. It is necessary to mention when considering the experimental data for 20 Hz and 100 Hz that the specimens used for testing were machined from two different castings. The metallographic analysis brought evidence that the grain size of about 450 μm was the characteristic dimension for specimens tested at 20 Hz and the grain size of about ~150 μm was typical for 100 Hz testing. Consequently, the observed lower fatigue resistance at lower loading frequency reflects most probably the general trend of an increase of fatigue strength with decreasing grain size than any frequency effect. Therefore, it is not possible to unequivocally conclude if the observed effect assigns to the loading frequency or to microstructure of cast alloy. However, when fatigue behaviour of notched SC specimens at different frequencies is compared, then it could be seen that the frequency does not have any influence on fatigue behaviour of cast AZ31. (Fatigue behaviour of notched specimens will be discussed in more detail below). Thus the deterioration effect on fatigue behaviour of smooth SC specimens at a loading frequency of 20 Hz could be prescribed to the microstructure of the material and not to the frequency effect. No frequency influence on fatigue behaviour of smooth HR and ECAP specimen was observed. However, the notched HR specimens show slightly higher fatigue endurance at higher frequency of 100 Hz than at frequency of 20 Hz. This is not the case when smooth HR specimens are tested. The reason of this behaviour is not clear yet and more intensive study has to be done to fully confirm if this is really a frequency effect or not.

Generally, results of this work together with literature data, give information about negligible effect of loading frequency on the fatigue endurance of magnesium alloys, independently on the material condition.

To conclude these results, the following could be stated. The HR material has the best fatigue resistance in LCF region of all. In the HCF, the fatigue strength of HR and ECAP material is the same. Thus, fine-grained ECAP material does not lead to further improvement of fatigue properties of the magnesium alloy AZ31. The SC alloy shows the lowest fatigue endurance. The loading frequency in the frequency range investigated does not have any negative or positive effect on the fatigue behaviour of the magnesium alloy AZ31.

Notch sensitivity. Since in the engineering applications irregular parts with stress concentrators are very often used, the issue of notch influence on fatigue endurance is extremely important [186 and 195]. Unfortunately, the literature data regarding notch sensitivity of magnesium alloys are mostly missing. From known literature data it is obvious that a notch may have a negative effect on the fatigue performance [131]. The notch effect is more pronounced in the fine grained materials than in coarse ones [197]. This was confirmed also by results of the present study. The notch sensitivity factor of SC alloy at frequency of 20 Hz was zero. It means that coarse grained material is insensitive to the artificial surface notch. For the SC material tested at frequency of 100 Hz, a very small notch sensitivity q of 0.07 was found. This value is insignificant and it again confirms the practical notch insensitivity of SC material. The notch insensitivity of cast AZ31 may be explained in the following way. The existing inherent defects in the cast material have a stronger influence on the fatigue endurance than the surface circumferential notches, having theoretical stress concentration factor up to 2.8. The notch insensitivity of cast magnesium alloys is also confirmed by Berger et al. and Renner et al. in [186, 191]. Also here the notch insensitivity was assigned to the effect of internal defects of the cast microstructure. Contrary to that, a strong notch sensitivity of cast magnesium alloys was reported by Sonsino et al. [131]. Thus, it is seen that the literature data are not really uniform. Just opposite to the SC material notch insensitivity observed in this work, both HR and ECAP AZ31 show significant notch sensitivity. The notch sensitivity of ECAP material was found to be higher than that of the HR material. Not only the fine-grained ECAP material shows worse fatigue resistance in LCF and HCF region than HR material, but it also has higher notch sensitivity. The experimentally determined notch sensitivity factor of the HR material is 0.76 for 20 Hz loading and 0.62 for 100 Hz loading. This proves a relative high notch sensitivity of the HR material. The situation is a bit more complicated in the case of ECAP alloy. In this case, notch specimens with two different stress concentration factors were used for testing at two frequencies of 20 and 100 Hz. The ECAP specimens with K_t of 2.5 tested at 20 Hz show the fatigue notch sensitivity of 0.74. By contrast, the ECAP specimens with K_t of 2.0 tested at 100 Hz show a substantially lower fatigue notch sensitivity of 0.19. This effect could be theoretically assigned to the frequency effect. However, no frequency effect was observed when smooth ECAP specimens were tested. Thus, it looks quite improbable that the frequency effect would be so strong in the case of notched ECAP specimens. The big difference in notch sensitivity of ECAP material is possible to assign to the effect of the stress concentration factor. The specimens with lower stress concentration factor show better fatigue endurance than the specimens with higher stress concentration. Identical tendency was also found in the literature reported by Sonsino et al. [131] for the magnesium alloy AZ91.

Tab. 7.1 Stress concentration factor and notch sensitivity

	f [Hz]	K_t	q
HR	20	2.8	0.74
ECAP	20	2.5	0.76

From the experimental results it follows that HR and ECAP alloys have substantially higher fatigue resistance than SC material. However, the SC alloy is notch insensitive. The fatigue lifetime of HR and ECAP alloys decreases with increasing K_t. Additionally, in Tab 7.1 the notch sensitivity of HR and ECAP material is compared. The notch sensitivity values for both materials are approximately the same. But the stress concentration factors are different. For the same notch sensitivity, the ECAP material has a lower stress concentration factor than the HR material. Hypothetically, if the ECAP material would have the same K_t as the HR

material, then the value of notch sensitivity of the ECAP material would be higher than that of the HR material. It proves a higher notch sensitivity of the ECAP alloy. Thus, it is seen that the notch sensitivity of AZ31 depends strongly on the material condition. The literature data concerning the notch sensitivity of magnesium alloys are extremely scarce. The data obtained in this work bring some light on the notch sensitivity of HR and ECAP Mg alloy AZ31. The data of this kind were missing in the literature till now. Because the fatigue notch sensitivity is an important material property/indicator necessary for safe engineering design of cyclically loaded components, further study of this problem is desirable.

The critical size defect at the endurance limit is an important material parameter, characterizing the fatigue behaviour. Unfortunately, no data of this kind exist in the literature for magnesium alloys. In the present work the Klesnil – Lukáš equation [206] was used for the evaluation of non-propagating crack size at the fatigue strength for all three conditions of AZ31. The critical defect size is sought to be in a close relation to the decisive structural parameter of a particular material. The results of this work show that the critical defect size differs in dependence on material condition. A critical defect of 60 μm was calculated for SC material tested at a frequency of 20 Hz and at a frequency of 100 Hz it was 51 μm. Both values are much smaller than the grain size of the SC material. Thus, the grain size can not be the decisive structural parameter for non-propagating cracks at the fatigue strength of SC alloy. Therefore, other microstructural parameters must be responsible for short crack propagation. It supports the idea of large inherent defects, the dendrite size or porosity that influence the short crack propagation and hence the fatigue life more significantly than the grain boundaries. In the SC alloy inherent defects larger than 60 μm have to be present and therefore the influence of artificial surface notch with K_t of 2.8 is shielded. In the case of HR material, the situation is completely different. The calculated non-propagating crack size at the frequencies of 20 and 100 Hz was 7.6 μm and 13 μm, respectively. These values are in good correlation with the grain size of HR material. It indicates that the grain size could be the responsible structural parameter from the point of view of fatigue damage at the endurance limit. The artificial surface notch size is larger than the grain size of HR material. The situation is again different for ECAP material. The critical defect size at a frequency of 20 Hz was 7.8 μm, while at a frequency of 100 Hz it was 33 μm. These values are obviously larger than the grain size of ECAP alloy. Consequently, in the ECAP material, similarly to the SC alloy, the grain boundaries itself cannot be directly considered as decisive obstacles for non-propagating (short) cracks. As it was pointed out above, no data of critical crack size of magnesium alloys are available from literature. The only possible comparison can be made with the results determined for ultrafine-grained copper by Lukáš et al. [170]. However, this comparison is not fully appropriate, because of completely different crystallographic structure and different slip mechanisms in Cu.

Obtained results on the critical defects enable the following considerations. AZ31 produced by the conventional method of hot rolling shows good correlation between the critical crack size and the grain size. This is not valid for conventionally prepared squeeze cast material due to inherent microstructural defects. Further, the correlation between the critical crack size and grain size was not confirmed for fine-grained ECAP material. The critical defect is much larger than the grain size. The explanation of this behaviour is missing. A more detailed study of the mechanisms of crack initiation, slip band formation and conditions for crack propagation in fine-grained Mg alloys is necessary for better understanding of this observation.

8   Summary

The first task of this work was to process magnesium alloy AZ31 by equal channel angular pressing (ECAP). For that the proper processing conditions had to be found. Further, the fatigue properties of AZ31 processed by ECAP were examined and later on the results were compared with fatigue properties of the conventionally prepared AZ31, i.e. by squeeze casting (SC) and hot rolling (HR).

ECAP technique has been chosen due to its positive impact on the mechanical properties resulting from ultra-fine grained microstructure. However, due to the hexagonal structure of magnesium alloy, an elevated processing temperature had to be used and thus the outcoming microstructure was not in ultra-fine range but rather fine-grained one.

The microstructure and texture of the three conditions of AZ31 were examined. It was found that these three conditions significantly differ in microstructure and texture corresponding to the three different production techniques. The SC material shows a coarse microstructure and random texture, while the HR material shows equiaxed grains with a size of 15 μm. The HR material has a strong basal texture. It was proved that ECAP leads to production of a fine-grained microstructure with grain size of 2.4 μm. The texture of ECAP material differs from that of HR and SC. The basal planes are tilted 45° to the ECAP pressing direction.

From general knowledge it was expected that a small grained material will have superior mechanical properties. Thus, the influence of the microstructure and texture on tensile and fatigue properties was examined. Surprisingly, the highest tensile strength and yield stress were not observed for fine-grained ECAP material but for the HR one. On the other hand, the highest ductility was detected for ECAP material over the HR and SC one. The lowest tensile properties were found for coarse grained SC material. It was shown that the hypothesis based on Hall-Petch relation was not confirmed when properties of HR and ECAP material were compared. The fine grained ECAP material did not lead to an improvement of the strength characteristics over the HR material. From the results of this work it could be stated that texture effect predominates over grain size effect regarding to tensile properties.

Cyclic hardening of all three conditions of AZ31 is a characteristic feature of cyclic stress - strain response. The strongest cyclic hardening was observed for HR material, while very weak hardening was measured for ECAP material. This behaviour was explained by the texture and grain size influence.

The best fatigue resistance in LCF was observed for HR material and not for ECAP one. However, the HR and ECAP material showed identical fatigue strength in HCF region. The lowest fatigue strength was determined for SC material. On the other hand, the SC material is notch insensitive while HR and ECAP material show significant notch sensitivity. Additionally, the notch sensitivity in ECAP material is even higher than that of HR material. The ECAP material has not the best fatigue endurance, as it expected; simultaniously it exhibits the highest notch sensitivity. The fatigue strength of SC material is the same for smooth specimens as well as for notched specimens. This implies that the fatigue strength determined for smooth SC specimens can be used for fatigue life assessment even for bodies with stress concentrators. However, this is not the case of HR and ECAP material. The fatigue strength of notched HR and ECAP specimens was of same magnitude as for the fatigue strength of coarse grained SC material. Thus, in the case of HR and ECAP materials their fatigue notch sensitivity should be carefully evaluated in structural applications exposed to cyclic loads.

All three conditions of AZ31 show transcrystalline fatigue fracture surfaces. However, the significant differences in the roughness of fatigue fracture surfaces of AZ31 squeeze cast, hot rolled and ECAP specimens were observed. Additionally, a strong segmentation of the fracture surface of the ECAP material was observed.

The experimental outcomes of this work have demonstrated that the properties of AZ31 depend strongly on the manufacturing route applied. Surprisingly, the ECAP process did not bring any improvement of the tensile and fatigue properties of magnesium alloy AZ31. However, it is generally not possible to say which of the three conditions of AZ31 have the 'best' overall properties. Each material condition is suitable for different applications. Thus, a proper material condition has to be considered on the foundation of the specific requests. This work offers a first information base to make such decision.

9 List of own publications

Published works

[1] Y. Estrin, H. Wang, H. Fu, G. Song, **Z. Zuberova**: The effect of mechanical processing on the bio.corrosion and fatigue resistance of Mg alloy AZ31, TMS 2008 (The Minerals, Metals & Materials Society)

[2] H.-G. Brokmeier, W. Gan, M. Zheng, **Z. Zuberova**, Y. Estrin: Development of extrusion and rolling textures during ECAP of Mg-alloys, Materials Science Forum, Vols. 584-586, 2008, 748-753

[3] H. Wang, Y. Estrin, **Z. Zúberová**: Bio-corrosion of a magnesium alloy with different processing histories, Materials Letters, Vol. 62, 16, 2008, 2476-2479

[4] Y. Estrin, S.B. Yi, H.-G. Brockmeier, **Z. Zúberová**, S.C. Yoon, H.S. Kim, R.J. Hellmig: Microstructure, texture and mechanical properties of magnesium alloy AZ31 processed by ECAP, International Journal of Material Research, 99 (1), 50-55, Jan. 2008, 1862-5282

[5] T.V. Ivleva, J. Göken, I.S. Golovin, **Z. Zuberova**, M. Maikranz-Valentin, K. Steinhoff: Damping in AZ31 ECAP-processed alloy, In: Golovin, I.S.; Levin, D. M.: Interaction between Defects and Anelastic Phenomena in Solids. Solid State Phenomena, Volume 137, Zürich, Trans tech publication inc. 2008, 181-189.

[6] H. Wang, Y. Estrin, H.M. Fu, G.L. Song, **Z. Zúberová**: The effect of pre-processing and grain structure on the bio-corrosion and fatigue resistance of magnesium alloy AZ31, Advanced Engineering Materials, Vol. 9, No.11, 2007, 967-972

[7] L. Kunz, P. Lukáš, **Z. Zúberová**: Fatigue of ultrafine-grained materials, Materials Degradation 2003, (Degradácia konštrukčných materiálov), EDIS - ŽU Žilina, Slovak Republic, 2007

[8] **Z. Zúberová**, Y. Estrin, T.T. Lamark, M. Janeček, R.J. Hellmig, M. Krieger: Effect of equal channel angular pressing on the deformation behaviour of magnesium alloy AZ31 under uniaxial compression, Journal of Materials Processing Technology 184, 2007, 294-299

[9] **Z. Zuberova**, L. Kunz, T.T. Lamark, Y. Estrin, M. Janecek: Fatigue and tensile behaviour of cast, hot rolled and severely plastically deformed AZ31 magnesium alloy, Metallurgical and Materials Transactions, Vol. 38, 9, 2007, 1934-1940

[10] D. Canadinc, P. Gabor, H. Maier, R. Hellmig, **Z. Zuberova**, Y. Estrin: The influence of zirconium on the low-cycle fatigue response of ultrafine-grained copper, Metallurgical and Materials Transactions, Vol. 38, 9, 2007, 1916-1925

[11] Y. Estrin, R.J. Hellmig, M. Janeček, T.T. Lamark, **Z. Zúberová**, R.Y. Lapovok and M.V. Popov: Effect of ECAP on the mechanical properties of Mg alloys,.In: Ultrafine Grained Materials IV. Edited by Y.T. Zhu, T.G. Langdon, Z. Horita, M.J. Zehetbauer, S.L. Semiatin, and T.C. Lowe. TMS (The Minerals, Metals & Materials Society), 2006, pp. 381-388

[12] L. Kunz, P. Lukáš, Y. Estrin, **Z. Zúberová**: Notch sensitivity of cast AZ31 magnesium alloy, Materials Engineering, Vol. 12, 3, EDIS – ŽU Žilina, Slovak Republic, 2005, 88-92

[13] **Z. Zúberova**, O. Bokůvka: Railway track renovation by welding methods (Renovácia koľajníc technológiami navárania), Nowe technologie i osiagniecia w metalurgii i

inzinierii materialowej, Czestochowa, Poland, Metalurgia Vol. 39, 1, 2004, 408

[14]   L. Kunz, **Z. Zúberová**, Y. Estrin: Measurement of crack growth rate in magnesium alloy AZ31SC, (Šíření dlouhých únavových trhlin v Mg slitině AZ31SC), Sommer School – Fatigue of Materials, (Letná škola únavy materiálov 2004), Conference, Zuberec – Roháče, Slovak Republic, EDIS ŽU Žilina, Vol. 7, 2004, 160 – 165

[15]   **Z. Zúberová**, L. Kunz, R.J. Hellmig, T.T. Lamark: The influence of loading frequency on high cycle fatigue of magnesium alloy AZ31-SC. (Vplyv frekvencie zaťažovania na vysokocyklovú únavu zliatiny AZ31-SC), Materials Degradation 2003, (Degradácia konštrukčných materiálov), EDIS - ŽU Žilina, Slovak Republic, 2003, 36 - 42

Non-published presentations

[16]   **Z. Zúberová**, T.T. Lamark, R.J. Hellmig, L. Kunz: Fatigue properties of squeeze cast AZ31, Frühjahrstagung der Deutschen Physikalischen Gesellschaft DPG, 08.03. – 12.03.2004, Regensburg, Germany

[17]   L. Kunz, **Z. Zúberová**, R.J. Hellmig, J. Estrin: Measurement of crack growth rate of magnesium alloy AZ31, Frühjahrstagung der Deutschen Physikalischen Gesellschaft DPG, Berlin, Germany

[18]   **Z. Zúberová**, Y. Estrin, T.T. Lamark, M. Janeček, R.J. Hellmig, M.G. Krieger: Effect of equal channel angular pressing on the deformation behaviour of magnesium alloys AZ31 under uniaxial compression, Frühjahrstagung der Deutschen Physikalischen Gesellschaft DPG, Dresden, Germany

10 References

[1]   J.F. Shackelford: Introduction to materials science for engineers, 2005 Pearson Education, Inc. ISBN: 0-13-127619-0

[2]   Y. Saito, N. Tsuji, H. Utsunomiya, T. Sakai, R.G. Hong: Ultra-fine grained bulk aluminum produced by accumulative roll-bonding (ARB), Scripta Mater. 39, 1998, 1221-1227

[3]   M. Richert, H. Petryk, S. Stapkiewicz: Grain refinement in AlMgSi alloy during cyclic extrusion compression: experiment and modeling, Archives of metallurgy and materials, Vol. 52, 1, 2007, 49-55

[4]   J.-Q. Su, T.W. Nelson, C.J. Sterling: Journal of Materials Research. 18, 2003, 1757-1764

[5]   R.Z. Valiev, I.V. Alexandov Y.T. Zhu, T.C. Lowe : Strength and ductility of nanostructured SPD materials, Journal of Mater. Researches, 17, 7, 2002, 279

[6]   Proc. Of Symposium of TMS Annual Meeting of Ultrafine Grained Materials III, Charlotte, North Carolina 2004, Y.T. Zhu et al. (Eds), TMS Warrendale, ISBN 0-87339-571-9, p. 686

[7]   G.A. Salishchev, R.M. Galeyev, S.P. Malysheva, M.M. Myshlyaev: Nanostructured Materials, Vol. 11, 1999, 407-414

[8]   Ghosh, Huangl: in Investigation and Application of Severe Plastic Deformation, Lowe & Valiev, ed., Kluwer Academic Publishers, Dordrecht. p. 29, 2000.

[9]   J.Y. Huang, Y. T. Zhu, H. Jiang, T. C. Lowe : Microstructures and dislocation configurations in nanostructured Cu processed by repetitive corrugation and straightening, Acta Materialia, 49, 2001, 1497 -1505

[10]   S. Firstov, M. Brodnikovsky, M. Danylenko and Yu. Podrezov: Nanocrystalline structure formation under severe plastic deformation and its influence on mechanical properties, Rev. Adv. Mater. Sci. 4, 2003, 155-162

[11]   N. Tsuji, Y. Saito, H. Utsunomiya, S. Tanigawa: Ultra-fine grained bulk steel produced by accumulative roll-bonding (ARB) process; Scripta Materialia, 40, 7, 1999, 795-800

[12]   H. Jiang, Y.T. Zhu, D.P. Butt, I.V. Alexandrov, T.C. Lowe: Microstructural evolution, microhardness and thermal stability of HPT-processed Cu; Materials Science and Engineering A290, 1-2, 2000, 128-138

[13]   A. P. Zhilyaev, G. V. Nurislamova, B. -K. Kim, M. D. Baró, J. A. Szpunar: Experimental parameters influencing grain refinement and microstructural evolution during high-pressure torsion T. G. Langdon: Acta Materialia, 51, 2003, 753-765

[14]   Y.T. Zhu, H. Jiang, J. Huang, T.C. Lowe: A new route to bulk nanostructured metals; Metallurgical and Materials Transactions A32, 6, 2001, 1559-1562

[15]   D.H. Shin, J.-J. Park, Y.-S. Kim, K.-T. Park: Constrained groove pressing and its application to grain refinement of aluminium; Materials Science and Engineering A 328, 1-2, 2002, 98-103

[16]   M.Y. Huh, J.P. Lee, J.C. Lee, J.W. Park, Y.H. Chung: Evolution of annealing textures and microstructures in AA 3103 after cold rolling and repeated shear deformation; Materials Science Forum. 396, 2002, 479

[17]   Y. Saito, H. Utsunomiya, H. Suzuki, T. Sakai: Improvement in the r-value of aluminum strip by a continuous shear deformation process; Scripta Materialia 42, 12, 2000, 1139-1144

[18]   J.H. Han, H.K. Seok, Y.H. Chung, M.Ch. Shin, J.Ch. Lee: Texture evolution of the strip cast 1050 Al alloy processed by continuous confined strip shearing and its formability evaluation, Materials Science and Engineering A323, 1-2, 2002, 342-347

[19]   J.C. Lee, H. -K. Seok, J. -Y. Suh: Microstructural evolutions of the Al strip prepared by cold rolling and continuous equal channel angular pressing ; Acta Materialia, 42, 2002, 4005-4019

[20]   G.J. Raab, R. Z. Valiev, T.C. Lowe, Y.T. Zhu: Continuous processing of ultrafine grained Al by ECAP–Conform; Materials Science and Engineering A328, 1-2, 2004, *30-34*

[21]   R.Z. Valiev, Y. Estrin, Z. Horita, T.G. Langdon, M.J. Zechetbauer, Y.T. Zhu: Producing bulk ultrafine-grained materials by severe plastic deformation, JOM Journal of the Minerals, Metals and Materials Science, Vol. 58, 4, 2006, 33-39

[22]   T.C. Lowe, R.Z. Valiev: Producing nanoscale microstructures through severe plastic deformation, Journal of Metals, 52, 4, April 2000, 27-28

[23]   G. Langdon, M. Furukawa, M. Nemoto, Z. Horita: Using equal-channel angular pressing for refining grain size, Journal of Metals 52, April 2000, 30-33

[24]   R.Z. Valiev, T.C. Lowe, A.K. Mukherjee: Understanding the unique properties of SPD-induced microstructure, Journal of Metals, April 2000, 37-40

[25]   T. Ungár, I. Alexandrov, M. Zehetbauer: Ultrafine-grained microstructures evolving during severe plastic deformation, Journal of Metals, April 2000, 34-36

[26]   M. Furukawa, Z. Horita, M. Nemoto, T.G. Langdon: Review processing of metals by equal-channel angular pressing, Journal of Materials Science 36, 2001, 2835-2843

[27]   M. Furukawa, Z. Horita, M. Nemoto, T.G. Langdon: The use of severe plastic deformation for microstructure control, Materials Science and Engineering A324, 1-2, 2002, 82-89

[28]   R.Z. Valiev, R.K. Islamgaliev, I.V. Alexandrov: Bulk nanostructured materials from severe plastic deformation, Progress in Materials Science 45, 2, 2000, 103-189

[29]   S.R. Agnew, G.M. Stoica, L.J. Chen, T.M. Lillo, J. Macheret, P.K.

Liaw: Equal channel angular processing of magnesium alloys, Ultrafine Grained Materials II; Edited by Y.T. Zhu, T.G. Langdon, R.S. Mishra, S.L. Semiatin, M.J. Saran, and T.C. Lowe. TMS (The Minerals, Metals & Materials Society), 2002, 643-652

[30]   T.G. Langdon: The principles of grain refinement in equal-channel angular pressing; Materials Science and Engineering A 462, 1-2, 2007, 3-11

[31]   Ch. Yongjun, W. Qudong, P. Jianguo, Z. Chunquan: Improving the mechanical properties of AZ31 Mg alloy by high ratio extrusion, Materials Science Forum, Vols. 503-504, January 2006, 865-870

[32]   Y. Estrin: Effect of severe plastic deformation: Mechanical properties and beyond, Materials Science Forum, Vols. 503-504, January 2006, pp. 91-98

[33]   J.A. del Valle, M.T. Pérez-Prado, O.A. Ruano: Texture evolution during large-strain hot rolling of the Mg-AZ61 alloy, Materials Science and Engineering A355, 1-2, 2003, 68-78

[34]   M. Furukawa, Z. Horita, T.G. Langdon: Processing by equal channel angular pressing: Applications to grain boundary engineering; Journal of Materials Science 40, 2005, 909-917

[35]   G.M Stoica, P.K. Liaw: Progress in equal-channel angular processing, Journal of Metals, 53, 3, March 2001, 36-40

[36]   S.L. Semiatin, D.P. Delo, E.B. Shell: The effect of materials properties and tooling design on deformation and fracture during equal channel angular extrusion, Acta Materialia 48, 8, 2000, 1841-1851

[37]   H.S. Kim, M.H. Seo, S.I. Homg: Plastic deformation analysis of metals during equal channel angular pressing, Journal of Materials Processing Technology 113, 2001, 622-626

[38]   V.M. Segal: Equal channel angular extrusion: from macromechanics to structure formation, Materials Science and Engineering A271, 1-2, 1999, 322-333

[39]   F.J. Humphreys, P.B. Prangnell, J.R. Bowen, A. Gholinia, C. Harris: Developing stable fine-grain microstructures by large strain deformation, Philosophical Transactions: Mathematical, Physical and Engineering Sciences, (Phil. Trans. R. Soc. Lond. A), Vol. 357, No. 1756, Deformation Processing of Metals, 1999, 1663-1681

[40]   B.Q. Han, T.G. Langdon: Improving the high-temperature mechanical properties of a magnesium alloy by equal channel angular pressing, Materials Science and Engineering A 410-411, 2005, 435-438

[41]   K.N. Braszcynska: Possibilities of ECAE of magnesium alloy, Magnesium – Alloys and Technology, Ed. K.U. Kainer, Wiley-VCH Verlag, 2003, 236-241

[42]   V.M. Segal: Materials processing by simple shear, Materials Science and Engineering A197, 2, 1995, 157-164

[43]   H.S. Kim: Prediction of temperature rise in equal channel angular pressing, Materials Transaction, Vol. 42, No. 3, 2001, 536-538

[44]   Y. Iwahashi, J. Wang, Z. Horita, M. Nemoto, T.G. Langdon: Principle of equal-channel angular pressing for the processing of ultra-fine grained materials Scripta Materialia 35, 2, 1996, 143-146

[45]   M. Furukawa, Z. Horita, T.G. Langdon: Factors influencing the shearing patterns in equal channel angular pressing, Materials Science and Engineering A332, 1-2, 2002, 97-109

[46]   S. Kamado, T. Ashie, Y. Ohshima and Y. Kojima: Tensile properties and formability of Mg-Li alloys grain refined by ECAE process, Materials Science Forum, Vols. 350-351, 2000, 55-62

[47]   S. Yoshimoto, Y. Miyahara, Z. Horita and Y. Kawamura: Mechanical properties and microstructure of Mg-Zn-Y alloys processed by ECAE, Materials Science Forum, Vols. 503-504, January 2006, 769-774

[48]   A. Yamashita, Z. Horita, T.G. Langdon; Improving the mechanical properties of magnesium and a magnesium alloy through severe plastic deformation, Materials Science and Engineering, A300, 1-2, 2001, 142-147

[49]   I.J. Palmer; Light alloys – From traditional alloys to nanocrystals, Fourth edition, Elsevier, 2006

[50]   H. Watanabe, T. Mukai, K. Ishikawa: Effect of temperature of differential speed rolling on room temperature mechanical properties and texture in an AZ31 magnesium alloy, Journal of Material Processing Technology, 182, 1-3, 2007, 644-647

[51]   F. Kaiser, J. Bohlen, D. Letzig, K.-U. Kainer, A. Styczynski, C. Hartig; Influence of rolling condition on the microstructure and mechanical properties of magnesium sheet AZ31, Advanced Engineering Materials, 5, No.12, 2003, 891-896

[52]   K.U. Kainer, T.U. Benzler: Squeeze casting and thixo-casting of magnesium alloys, Magnesium Alloys and Technology, Ed. By K.U. Kainer, Wiley-VCH, 2003, 56-71

[53]   F. Kaiser, J. Bohlen, D. Letzig, K.U. Kainer, A. Styczynski, Ch. Hartig: A semianalytical sachs model for the flow stress of a magnesium alloy, Proc. 6th Int. Conf. on Magnesium Alloys and Their Applications, Ed. K.U. Kainer, Wiley-VCH Verlag, Germany, 2003

[54]   B. Hadzima, P. Palček, M. Chalupova: The development of the magnesium alloys structure at artificial ageing. Acta Metallurgica Slovaca, Vol.10, Special Issue 1/2004, 2004, 504-509

[55]   C. Potzies, K.U. Kainer: Fatigue of magnesium alloys, Advanced Engineering Materials, Vol. 6, No. 5, 2004, 281-289

[56]   A.K. Dahle, Y.C. Lee, M.D. Nave, P.L. Schaffer, D.H. StJohn: Development of the as-cast microstructure in magnesium-aluminium alloys, Journal of Light Metals 1, 1, 2001, 61-72

[57]   E.F. Emley: Principles of magnesium technology, Pergamon Press Oxford 1966

[58]   M.T. Pérez-Prado, O.A. Ruano: Texture evolution during annealing of magnesium AZ31 alloy, Scripta Materialia 46, 2, 2002, 149-155

[59]   J.A. del Valle, F. Carreno, O.A. Ruano: Influence of texture and grain size on work hardening and ductility in magnesium based alloys processed by ECAP and rolling, Acta Materialia, 54, 16, 2006, 4247-4259

[60]   D.L. Yin, K.F. Zhang, G.F. Wang, W.B. Han: Warm deformation behaviour of hot rolled AZ31 Mg alloy, Materials Science and Engineering A392, 1-2, 2005, 320-325

[61]   G. Gottstein: Physikalische Grundlagen der Materialkunde, Springer-Verlag, Berlin, u.a., 1. Aufl., 1998

[62]   G. Gottstein: Physical foundations of materials science, Springer-Verlag Berlin Heidelberg 2004

[63]   S.R. Agnew, Ö. Duygulu: Plastic anisotropy and the role of non-basal slip in magnesium alloy AZ31B, International Journal of Plasticity 21, 6, 2005, 1161-1193

[64]   H. Somekawa, T. Mukai: Fracture toughness in ultra fine-grained magnesium alloy, Materials Science Forum, Vols. 503-504, January 2006, 155-160

[65]   S. Yi: Investigation on the deformation behaviour and the texture evolution in magnesium wrought alloy AZ31, Disseratation, TU-Clausthal, 2005

[66]   J. Koike, T. Kobayashi, T. Mukai, H. Watanabe, M. Suzuki, M. Maruyama, K. Higashi: The activity of non-basal slip systems and dynamic recovery at room temperature in fine-grained AZ31B magnesium alloys, Acta Materialia 51, 7, 2003, 2055-2065

[67]   Y.N. Wang, J.C. Huang: The role of twinning and untwining in yielding behaviour in hot-extruded Mg-Al-Zn alloy, Acta Materialia 55, 3, 2007, 897-905

[68]   C.W. Su, L. Lu, M.O. Lai: A model for the grain refinement mechanism in equal channel angular pressing of Mg alloy from microstructural studies, Materials Science and Engineering. A 434, 1-2, 2006, 227-236

[69]   U.F. Koks, C.N. Tomé, H.R. Wenk; Texture and anisotropy – Preferred orientation in polycrystals and their effect on materials properties, Cambridge University Press, 1998

[70]   P. Lukac, Z. Trojanova, A. Rudajevova: Properties of magnesium based composites, International Conference "Advanced metallic materials" 5-7 November 2003, Smolenice, Slovak Republic, 2003

[71]   J. Bohlen, D. Letzig, H.-G. Brokmeier, A. Styczynski, Ch. Hartig, K.U. Keiner: Relationship between microstructure and mechanical properties in magnesium wrought alloy AZ31, In Magneisum Technology 2002. Seattle, WA (USA) 17.-21.02.2002, 169-174

[72]   S.R. Agnew, P. Mehrotra, T.M. Lillo, G.M. Stoica, P.K. Liaw: Texture evolution of five wrought magnesium alloys during route A equal channel angular extrusion: Experiments and simulations, Acta Materialia 53, 1, 2005, 3135-3146

[73]   Q.Jin, S-Y. Shim, S.-G. Lim: Correlation of microstructural evolution and formation of basal texture in a coarse grained Mg-Al alloy during hot rolling, Scripta Materialia 55, 9, 2006, 843-846

[74]   A. Styczynski, Ch. Harting, R. Bormann, F. Kaiser, J. Bohlen, D. Letzig: Texture formation and texture modelling of AZ31 magnesium wrought alloy, Ed. K.U. Kainer, Magnesium, Proceeding of the 6th International Conference: Magnesium Alloys and their Application, Wolsburg 2003, Ed. K.U. Kainer, Wiley-VCH, 2003, 214-219

[75]   A. Styczynski, Ch. Hartig, J. Bohlen, D. Letzig: Cold rolling textures in AZ31 wrought magnesium alloy, Scripta Materialia 50, 7, 2004, 943-947

[76]   S.M. Zhu, J.F. Nie: Serrated flow and tensile properties of a Mg-Y-Nd alloy, Scripta Materialia 50, 1, 2004, 51-55

[77]   S.B. Yi, S. Zaefferer, H.-G. Brockmeier: Mechanical behaviour and microstructural evolution of magnesium alloy AZ31 in tension at different temperatures, Materials Science and Engineering. A424, 1-2, 2006, 275-281

[78]   A. Beck: Magnesium und seine Legierungen, Brlin, Verlag von Julius Springer, 1939

[79]   W.J. Kim, J.B. Lee, W.Y. Kim, H.T. Jeong, H.G. Jeong: Microstructure and mechanical properties of Mg-Al-Zn alloy sheet severely deformed by asymmetrical rolling, Scripta Materialia 56, 4, 2007, 309-312

[80]   P. Yang, Y. Yu, L. Chen, W. Mao: Experimental determination and theoretical prediction of twin orientation in magnesium alloy AZ31, Scripta Materialia 50, 16-17, 2004, 1163-1168

[81]   T. Mukai, M. Yamanoi, H. Watanabe, K. Higashi: Ductility enhancement in AZ31 magnesium alloy by controlling its grain structure, Scripta Mterialia 45, 1, 2001, 89-94

[82]   H. Somekawa, T. Mukai: Fracture toughness in Mg-Al- Zn alloy processed by equal-channel- angular extrusion, Scripta Materialia 54, 4, 2006, 633-638

[83]   S.R. Agnew, J.A. Horton, T.M. Lillo, D.W. Brown: Enhanced ductility in strongly textured magnesium produced by equal channel angular processing, Scripta Materialia 50, 3, 2004, 377-381

[84]   W.J. Kim, H.T. Jeong: Grain size strengthening in equal channel angular pressing processed AZ31 Mg alloys with a constant texture, Materials Transactions, Vol. 46, No. 2, 2004, 251-258

[85]   X. Yang, J. Xing, H. Miura, T. Sakai: Strain-induced grain refinement in magnesium alloy AZ31 during hot forging, Materials Science Forum Vols. 503-504, January 2006, 521-526

[86]   H. Somekawa, H. Hosokawa, H. Watanabe, K. Higashi: Diffusion bonding in superplastic magnesium alloys, Materials Science and Engineering, A 339, 1-2, 2003, 328-333

[87]   H. Takuda, H. Fujimoto, D. Inoue: Effect of warm forming on

mechanical properties of an AZ31 magnesium alloy sheet, Ed. K.U. Kainer, Magnesium, Proceeding of the 6th International Conference: Magnesium Alloys and their Application, Wolsburg 2003, Ed. K.U. Kainer, Wiley-VCH, Weinhem, 2003, 463-468

[88]   J.A. del Valle, M.T. Pérez – Prado, O.A. Ruano: Deformation mechanisms responsible fort he high ductility in a Mg AZ31 alloy analyzed by electron backscattered diffraction; Metallurgical and Materials Transaction A, Vol. 36A, 6, June 2005, 1427-1438

[89]   T. Mohri, M. Mabuchi, M. Nakamura, T. Asahina, H. Iwasaki, T. Aizawa, K. Higashi: Microstructural evolution and superplasticity of rolled Mg-9Al-1Zn, Materials Science and Engineering, A290, 1-2, 2000, 139-144

[90]   G.M. Stoica, L.J. Chen, E.A. Payzant, S.R. Agnew, Y.L. Lu, B.Q. Han, T.G. Langdon, P.K. Liaw; Deformation characteristics of Al and Mg alloys subjected to equal channel angular processing, Magnesium Technology 2001, Edited by J. Hryn, TMS (The Minerals, Metals and Materials Society), 2001, 295-305

[91]   M. Mabuchi, M. Nakamura, K. Ameyama, H. Iwasaki and K. Higashi: Superplastic behaviour of magnesium alloy processed by ECAE, Materials Science Forum Vols. 304-306, 1999, 67-72

[92]   M. Mabuchi, H. Iwasaki, K. Higashi: Low temperature superplasticity processed by ECAE, Materials Science Forum, Vols. 243-245, 1997, 547-552

[93]   R. Lapovok, R. Cottam, P.F. Thomson, Y. Estrin: Extraordinary superplastic ductility of magnesium alloy ZK60, Journal of Materials Research 20, 6, 2005, 1375-1378

[94]   J.C. Tan, M.J. Tan: Superplasticity in a rolled Mg-3Al-1Zn alloy by two-stage deformation method, Scripta Materialia 47, 2, 2002, 101-106

[95]   H. Watanabe, A. Takara, H. Somekawa, T. Mukai, K. Higashi; Effect of texture on tensile properties at elevated temperatures in an AZ31 magnesium alloy, Scripta Materialia 52, 6, 2005, 449-454

[96]   M.V. Popov: Enhancement of mechanical properties of different magnesium alloys due to the grain due to grain refinement by severe plastic deformation processing, PhD thesis, TU-Clausthal 2007

[97]   O.B. Kulyasova, R.K. Islamgaliev, N.A. Krasiulnikov: The influence of the ECAP temperature on microstructure and mechanical properties of a magnesium alloy, Materials Science Forum.; Vols. 503-504, January 2006, 609-617

[98]   K. Mathis, A. Mussi, Z. Trojanova, P. Lukac, E. Rauch: Effect of equal channel angular pressing on mechanical properties of AZ91 alloy, Metallic Materials 41, 5, 2003, 293-299

[99]   R. Kawalla, A. Stolnikov: Deformation behaviour and microstructure development of magnesium AZ31 alloy during hot and semi-hot deformation, Advanced Engineering Materials, 6, No.7, 2004, 525-529

[100]   M.M. Myshlyaev, H.J. McQueen, A. Mwembela, E. Konopleva: Twinning, dynamic recovery and recrystallization in hot worked Mg-

Al-Zn alloy, Materials Sciences and Engineering A337, 1, 2002, 121-133

[101]   Q. Wei, S. Cheng, K.T. Ramesh, E. Ma: Effect of nanocrystalline und ultrafine grain sizes on the strain rate sensitivity and activation volume: fcc and bcc metals, Materials Science and Engineering A 381, 1-2, 2004, 71-79

[102]   D. Caillard, J.L. Martin: Thermally activated mechanisms in crystal plasticity, Pergamon 2003

[103]   J.A. del Valle, O.A. Ruano: Influence of grain size on the strain rate sensitivity in an Mg-Al-Zn alloy at moderate temperatures, Scripta Materialia 55, 9, 2006, 775-778

[104]   H. Vehoff, D. Lemaire, K. Schuler, T. Waschkies, B. Yang: The effect of grain size on strain rate sensitivity and activation volume – from nano to ufg nickel, International Journal of Materials Research, 4, 2007, 259-268

[105]   H. Conrad, K. Jung: On the strain rate sensitivity of the flow stress of ultrafine-grained Cu processed by equal channel angular extrusion ECAE, Scripta Materialia 53, 5, 2005, 581-584

[106]   S.W. Chung, K. Higashi, W.J. Kim: Superplastic gas pressure forming of fine-grained AZ61 magnesium alloy sheet, Materials Science and Engineering A 372, 1-2, 2004, 15-20

[107]   R.C. Picu, G. Vincze, J.J. Gracio, F. Barlat: Effect of solute distribution on the strain rate sensitivity of solid solution, Scripta Materialia 54, 1, 2006, 71-75

[108]   P. Rodriguez, R. W. Armstrong: Strength and strain rate sensitivity for hcp and fcc nanopolycrystal metals, Bulletin of Materials Science, (Bull. Mater. Sci.) Vol. 29, No. 7, December 2006, 717-720

[109]   R.W. Armstrong, P. Rodriguez: Flow stress / strain rate / grain size coupling for fcc nanopolycrystals, Philosophical Magazine 86, Nr. 36, 2006, 5787-5796

[110]   H. Watanabe, T. Mukai, K. Higashi: Grain refinement and superplasticity in magnesium alloys, Ultrafine Grained Materials II; Ed. By Y.T. Zhu, T.G. Langdon, R.S. Mishra, S.L. Semiatin, M.J. Saran and T.C. Lowe, TMS (The Minerals, Metals and Materials Society), 2002, 469-478

[111]   M. Furui, Ch. Xu, T. Aida, M. Inoue, H. Anada, T.G. Langdon: Improving the superplastic properties of a two-phase Mg-8% Li alloy through processing by ECAP, Materials Science and Engineering A 410-411, 2005, 439-442,

[112]   J. May, H.W. Höppel, M. Göken; Strain rate sensitivity of ultrafine-grained aluminium processed by severe plastic deformation, Scipta Materialia 53, 2, 2005, 189-194

[113]   M. Mabuchi, H. Iwasaki, K. Yanase, K. Higashi: Low temperature superplasticity in an AZ91 magnesium alloy processed by ECAE, Scripta Materialia, Vol. 36, No. 6, 1997, 681-686

[114]   P. Zhang, J. Wendt, V. Supik, J. Zhang, F. Holländer: Superplasticity in hot-rolled magnesium alloy AZ31 sheets, Magnesium: Proceedings of the 6th International Conference Magnesium Alloys and Their Applications, 2003, Ed. K.U. Kainer, Wiley-VCH, 2003, 248-253

[115]   Z. Horita, K. Matsubara, K. Makii, T.G. Langdon, A two-step processing route for achieving a superplastic forming capability in dilute magnesium alloys, Scripta Materialia 47, 4, 2002, 255-260

[116]   Y. Estrin and H.S. Kim: Modelling microstructure evolution toward ultrafine crystallinity produced by severe plastic deformation, Journal of Materials Science, 42, 2007, 1512-1516

[117]   Y. Estrin, H.S. Kim and F.R.N. Nabarro: A comment on the role of Frank-Read sources in plasticity of nanomaterials, Acta Materialia, 55, 2007, 6401-6407

[118]   C.H. Cáceres, T. Sumitomo, M. Veidt: Pseudoelastic behaviour of cast magnesium AZ91 alloy under cyclic loading – unloading, Acta Materialia 51, 2003, 6211-6218

[119]   G.E. Mann, T. Sumitomo, C.H. Cáceres, J. R. Griffiths: Reversible plastic strain during cyclic loading-unloading of Mg and Mg-Zn alloys, Materials Sciences and Engineering A456, 1-2, 2007, 138-146

[120]   J. P. Nobre, U. Noster, J. Gibmeier, I. Altenberger, M. Kornmeier, A. Dias, B. Scholtes: Mechanical behaviour and residual stresses in AZ31 wrought magnesium alloy subjected to four point bending, Proc. Mg2000 – International Conference of Mg alloys and their Applications, 26-28 September, Munich, Germany, Ed. K.U. Kainer, Willey-VCH Verlag GmbH, Vol.1, 2000, 336-341

[121]   G.E. Dieter, H. McGraw: Mechanical metallurgy, 1989

[122]   J. Dzwonczyk, N. Hort, K. U. Kainer: Influence of extrusion methods on microstructure and mechanical properties of AZ31 magnesium alloy, Magnesium Alloys and Their Applications, 2003, Ed. K.U. Kainer, Wiley-VCH, Weinhem, 2003, 427-432

[123]   T.M. Yue, H.U. Ha, N.J. Musson: Grain size effect on the mechanical properties of some squeeze cast light alloys, Journal of Materials Science 30, 9, 1995, 2277-2283

[124]   A. Ockewitz, Ch. Schendera, D.-Z. Sun: Deformation and fracture behaviour of magnesium structural components, Magnesium alloys and their applications Proc. Mg2000 – International Conference of Mg alloys and their Applications, 26-28 September, Munich, Germany, Ed. K.U. Kainer, Willey-VCH Verlag GmbH, Vol.1, 2000, 359-364

[125]   T.T. Lamark, R.J. Hellmig, Y. Estrin: Mechanical properties of ECAP processed magnesium alloy AS21X, Materials Science Forum, Vols. 503-504, January 2006, 889-894

[126]   S.R. Agnew, T.M. Lillo, J. Macheret, G.M. Stoica, L. Chen, Y. Lu, D. Fielden, P.K. Liaw: Assessment of equal channel angular extrusion processing of magnesium alloys, Magnesium Technology 2001, Proceeding, 11-15 February 2001, New Orleans, Louisiana, Ed. J. Hryn, TMS (The Minerals, Metals & Materials Society), Warrendale,

PA, 2001, 243-247

[127]   X.-S. Wang, X. Lu, D.-H. Wang: Investigation of surface fatigue microcrack growth behaviour of cast Mg-Al alloy, Materials Science and Engineering A364, 1-2, 2004, 11-16

[128]   H. Mayer, A. Stich, B. Zettl, H.-G. Haldenwanger: High cycle fatigue of magnesium alloys, 6th International Conference: Magnesium Alloys and Their Applications 2003, Ed. K.U. Kainer, Wiley-VCH, 2003, 444-449

[129]   F. Nový, A. Námesný, L. Resetericová, M. Chalupová: Behaviour of AS41 magnesium alloy at cyclic loading, In.: Proc. 24th Danubia - Adria Symposium on Developments in Experimental Mechanics, Sibiu, Romania, 19-22. September 2007, 239-240

[130]   M. F. Horstemeyer, N. Yang, K. Gall, D. McDowell, J. Fan, P. Gullett: High cycle fatigue mechanisms in cast AM60 magnesium alloy, Fatigue and Fracture of Engineering Materials and Structures 25, 11, 2002, 1045-4056

[131]   C.M. Sonsino, K. Dieterich: Fatigue design with cast magnesium alloys under constant and variable amplitude loading, International Journal of Fatigue 28, 3, 2006, 183-193

[132]   L. Chen, Ch. Wang, W. Wu, Z. Liu, G. Stoica, L. Wu, P. Liaw: Low-cycle fatigue behaviour of an as-extruded AM50 magnesium alloy, The TMS Annual Meeting & Exhibition, San Antonio, Texas, March 12-16, 2006

[133]   Bentachfine, L.S. Toth, Z. Azari, G. Pluvinage: Low-cycle biaxial fatigue of a polycrystalline magnesium-lithium alloy, Materials Science, Vol. 31, No. 1, 1995, 11-12

[134]   H.E. Kadiri, Y. Xue, M.F. Horstemeyer, J.B. Jordon, P.T. Wang: Identification and modelling of fatigue crack growth mechanisms in a die cast AM50 magnesium alloy, Acta Materialia 54, 19, 2006, 5061-5076

[135]   T.S. Srivatsan, L. Wei, C.F. Chang: The cyclic strain resistance, fatigue life and final structure behaviour of magnesium alloys, Engineering Fracture Mechanics, Vol. 56, No. 6, 1997, 735-747

[136]   F. Li, Y. Wang, L. Chen, Z. Liu, J. Zhou: Low-cycle fatigue behaviour of two magnesium alloys, Journal of Materials Science 40, 2005, 1529-1531

[137]   Z. Liu, Z.-G. Wang, Y. Wang, L.-H. Chen, H.-J. Zhao, F. Klein: Cyclic deformation behaviour and fatigue crack propagation in AZ91HP and AM50HP, Materials Science and Technology, March 2001, Vol.17, 2001, 264-268

[138]   R.W. Suhr: The high frequency fatigue life of some magnesium alloys used in fuel element application, Journal of Nuclear Materials 20, 1966, 94-103

[139]   H. Zenner, F. Renner: Cyclic material behaviour of magnesium die casting and extrusion, International Journal of Fatigue, Vol. 24, 12,

2002, 1255-1260

[140]   H.W. Höppel, G. Eisenmeier, B. Holzwarth, H. Mugrabi: Cyclic deformation behaviour of the cast magnesium alloy AZ91, Magnesium Alloys and Their Applications, Ed.: K. U. Kainer, Munich, September 26 – 28, 2000, 1-5

[141]   D. Fang, P. Zhang, Q. Duan, S. Wu, Z. Zhang, J. Li, N. Zhao: Fatigue behaviour of Al-Cu alloy subjected to different numbers of ECAP passes, Advanced Engineering Materials, Vol. 9, 10, 2007, 860-866

[142]   M. Papakyriacou, H. Mayer, U. Fuchs, S.E. Stanzl-Tschegg, R.P. Wei: Influence of atmospheric moisture on slow fatigue crack growth at ultrasonic frequency in aluminium and magnesium alloys, Fatigue and Fracture of Engineering Materials and Structures 25, 8-9, 2002, 759-804

[143]   Y. Miyashita, Z.B. Sajuri, T. Umehara, Y. Muton: Fatigue life prediction of magnesium alloys for structural applications, Magnesium Alloys and their Applications 2003, Ed. K.U. Kainer, Wiley-VCH, 2003, 450-455

[144]   Y. Kobayashi, T. Shibusawa, K. Ishikawa: Environmental effect of fatigue crack propagation of magnesium ally, Materials Science and Engineering A234-236, 1997, 220-222

[145]   K. Tokaji, M. Kamakura, Y. Ishiizumi, N. Hasegawa: Fatigue behaviour and fracture mechanism of a rolled AZ31 magnesium alloy, International Journal of Fatigue 26, 2004, 1217-1224

[146]   H.K. Kim, Y.I. Lee, Ch.S. Chung: Fatigue properties of a fine-grained magnesium alloy produced by equal channel angular pressing, Scripta Materialia 52, 6, 2005, 473-477

[147]   A. Bag, W. Zhou: Tensile and fatigue behaviour of AZ91D magnesium alloy, Journal of Materials Science Letters 20, 5, 2001, 457-459

[148]   K. Gall, G. Biallas, H.J. Maier, M.F. Horstemeyer, D.L. McDowell: Environmentally influenced microstructurally small fatigue crack growth in cast magnesium, Material Science and Engineering A 396, 1-2, 2005, 143-154

[149]   H. Mayer, M. Papakyriacou, B. Zettl, S. Vacic: Endurance limit and threshold stress intensity of die cast magnesium and aluminium alloys at elevated temperatures, International Journal of Fatigue 27, 9, 2005, 1076-1088

[150]   Z.B. Sajuri, T. Umehara, Y. Miyashita, Y. Mutoh: Fatigue-life prediction of magnesium alloys for structural applications, Advanced Engineering Materials 2003, 5, No.12, 2003, 910-916

[151]   S.A. Shipilov: Mechanisms for corrosion fatigue crack propagation, Fatigue and Fracture of Engineering Materials and Structures 25. 3, 2002, 243-259

[152]   Y. Uematsu, K. Tokaji, M. Kamakura, K. Uchida, H. Shibata, N. Bekku: Effect of extrusion conditions on grain refinement and fatigue behaviour in magnesium alloys, Materials Science and Engineering A

434, 1-2, 2006, 131-140

[153]   Ch.-S. Chung, D.-K. Chun, H.K. Kim; Fatigue properties of fine grained magnesium alloys after severe plastic deformation, Journal of Mechanical Science and Technology, Vol. 19, No. 7, 2005, 1441-1448

[154]   G. Nicoletto, R. Konecná, A. Pirondi: Fatigue crack paths in coarse-grained magnesium, Fatigue and Fracture of Engineering Materials and Structures, 28, 1-2, 2005, 237-244

[155]   F. Nový, M. Cincala, P. Kopas, O. Bokuvka: Mechanisms of high-strength structural materials fatigue failure in ultra-wide life region, Materials Science and Engineering, A 462, 2007, 189-192

[156]   D.W. Cameron, D.W. Hoeppner: Fatigue properties in Engineering, ASM Handbook, Vol. 19, Fatigue and Fracture, ASTM, 1996

[157]   Y. Chino, T. Furuta, M. Hakamada, M. Mabuchi: Fatigue behaviour of AZ31 magnesium alloy produced by solid-state recycling, Journal of Material Science 41, 11, 2006, 3229-3232

[158]   F. Nový, Z. Zúberová, O. Bokuvka: Fatigue of magnesium alloys at very high numbers of cycles. In: Nowe technologie i osiągnięcia w metalurgii i inżynierii materiałowej : VII międzynarodowa konferencja naukowa, Wydawnictwo Wydziału Inżynierii Procesowej, Materialowej i Fizyki Stosowanej Politechniki Częstochowskiej, Częsztochowa, 2 June 2006, Poland, 419-422

[159]   O. Bokuvka, F. Nový, M. Cincala, M. Chalupová: Ultralong life fatigue of selected structural materials, Materials Engineering, Vol. 14, No. 2, 2007, 1-4

[160]   M. Hilpert, L. Wagner: Enviromental effect on the HCF behaviour of the magnesium alloys AZ31 and AZ80, Magnesium Technology 2000, Edited by H.I. Kaplan, J. Hryn, B. Clow, TMS (The Minerals, Metals and Materials Society) 2000, 375-381

[161]   B. Wolf, C. Fleck, D. Eifler: Characterization of fatigue behaviour of the magnesium alloy AZ91D by means of mechanical hysteresis and temperature measurements, International Journal of Fatigue 26, 12, 2004, 1357-1363

[162]   R. Kwadjo, L.M. Brown: Cyclic hardening of magnesium single crystals, Acta Metallurgica, Vol. 26, 7, 1978, 1117-1132

[163]   T.T. Lamark, F. Chmelík, Y. Estrin, P. Lukác: Cyclic deformation of a magnesium alloys investigated by the acoustic emission technique, Journal of Alloys and Compounds 378, 2004, 202-206

[164]   Z.Y. Nan, S. Ishihara, T. Goshima, R. Nakanishi: Scanning probe microscope observation of fatigue process in magnesium alloy AZ31 near the fatigue limit, Scripta Materialia 50, 4, 2004, 429-434

[165]   A.J. Eifert, J.P. Thomas, R.G. Rateick: Influence of anodization on the fatigue life of WE43A-T6 magnesium, Scripta Materialia Vol. 40, No. 8, 1999, 929-935

[166]   Y. Estrin, R. Hellmig: Improving the properties of magnesium alloys by equal channel angular pressing, Metal Science and Heat Treatment,

Vol. 48, 2006, 504-507

[167]   L. Wu, G.M. Stoica, H.H. Liao, S.R. Agnew, E.A. Payzant, G. Wang, D.E. Fielden, L. Chen, P.K. Liaw: Fatigue-property enhancement of magnesium alloy, AZ31B, through equal-channel-angular pressing, Metallurgical and Materials Transaction A 38, 13, 2007, 2283-2289

[168]   L. Kunz, P. Lukas, M. Svoboda: Fatigue strength, microstructural stability and strain localization in ultrafine-grained copper, Materials Science and Engineering A 424, 1-2, 2006, 97-104

[169]   L. Kunz, P. Lukas, M. Svoboda, O. Bokuvka: Fatigue behaviour of ultrafine-grained copper, Materials Engineering, Vol. 12, No.3, EDIS – ŽU Žilina, Slovak Republic, 2005, 2-6

[170]   P. Lukas, L. Kunz, M. Svoboda: Fatigue notch sensitivity of ultrafine-grained copper, Material Science and Engineering A 391, 1-2, 2005, 337-341

[171]   P. Gabor, D. Canadinc, H.J. Maier, R.J. Hellmig, Z. Zuberova, J. Estrin: The influence of zirconium on the low-cycle fatigue response of ultrafine-grained copper, Metallurgical and Material Transaction A 38, 9, 2007, 1916-1925

[172]   A. Vinogradov, V. Patlan, Y. Suzuki, K. Kitagawa, V.I. Kopylov: Structure and properties of ultra-fine grain Cu-Cr-Zr alloy produced by equal channel angular pressing, Acta Materialia 50, 7, 2002, 1639-1651

[173]   O. Bokuvka, F. Nový, M. Cincala, P. Bojanowicz: Loading frequency influence in giga-cycle fatigue region, Berichte und Informationen, 14, 2/2006, 2006, 11-15

[174]   A. Vinogradov, S. Hashimoto, V.I. Kopylov: Enhanced strength and fatigue life of ultra-fine grain Fe-36Ni Invar alloy, Materials Science and Engineering A355, 1-2, 2003, 277-285

[175]   M. Kamaya, N. Totsuka: Influence of interaction between multiple cracks on stress corrosion crack propagation, Corrosion Science 44, 2002, 2333-2352

[176]   A.Y. Vinogradov, V.V. Stolyarov, S. Hashimoto, R.Z. Valiev: Cyclic behaviour of ultrafine-grain titanium produced by severe plastic deformation, Materials Science and Engineering A318, 1-2, 2001, 163-176

[177]   H.K. Kim, M.I. Choi, Ch.S. Chung, D.H. Shin: Fatigue properties of ultrafine grained low carbon steel produced by equal channel angular pressing, Materials Science and Engineering A 340, 1-2, 2003, 243-250

[178]   A. Vinogradov, A. Washikita, K. Kitagawa, V.I. Kopylov: Fatigue life of fine-grain Al-Mg-Sc alloys produced by equal-channel angular pressing, Materials Science and Engineering A349, 1-2, 2003, 318-326

[179]   C.S. Chung, J.K. Kim, H.K. Kim, W.J. Kim: Improvement of high-cycle fatigue life in a 6061 Al alloy produced by equal channel angular pressing, Materials Science and Engineering A 337, 1-2, 2002, 39-44

[180]   S.N. Liu, Z.G. Wang: Fatigue properties of 8090 Al-Li alloy processed by equal channel angular pressing, Scripta Materialia 48, 10, 2003, 1421-1426

[181]   A. Turnbull, E.R. de los Rios: The effect of grain size on fatigue crack growth in an aluminium magnesium alloy, Fatigue and Fracture of Engineering Materials and Structures, Vol. 18, 11, 1995, 1355-1366

[182]   J. May, M. Dinkel, D. Amberger, H.W. Höppel, M. Göken: Mechanical properties, dislocation density and grain structure of ultrafine-grained aluminium and aluminium-magnesium alloys, Metallurgical and Materials Transaction A 38, 9, 2007, 1941-1945

[183]   J. Petit: Near-threshold fatigue crack path in Al-Zn-Mg alloys, Fatigue and Fracture of Engineering Materials and Structures, 28, 1-2, 2005, 149-158

[184]   K. Gall, G. Biallas, H.J. Maier, P. Gullet, M.F. Horstemeyer, D.L. McDowell, J. Fan: In-situ observations of high cycle fatigue mechanisms in cast AM60 magnesium in vacuum and water vapour environments, International Journal of Fatigue 26, 1, 2004, 59-70

[185]   J. Wendt, M. Hilpert, J. Kiese, L. Wagner: Surface and environmental effect on the fatigue behaviour of wrought and cast magnesium alloys, Magnesium Technology 2001, Eds. By H.I. Kaplan, J. N. Hryn and B.B. Clow, TMS (The Minerals, Metals and Materials Society) 2001, 281-285

[186]   F. Renner, H. Zenner: Fatigue strength of die-cast magnesium components, Fatigue and Fracture of Engineering Materials and Structures. 25, 2002, 1157-1168

[187]   X.S. Wang, J.H. Fan: SEM online investigation of fatigue crack initiation and propagation in cast magnesium alloy, Journal of Materials Science 39, 7, 2004, 2617-2620

[188]   G. Eisenmeier, B. Holzwarth, H.W. Höppel, H. Mughrabi: Cyclic deformation and fatigue behaviour of the magnesium alloy AZ91, Materials Science and Engineering, A319-321, 2001, 578-582

[189]   H. Mayer, M. Papakyriacou, B. Zettl, S.E. Stanzl-Tschegg: Influence of porosity on the fatigue limit of die cast magnesium and aluminium alloys, International Journal of Fatigue 25, 3, 2003, 245-256

[190]   S.E. Stanzl-Tschegg: Fracture mechanisms and fracture mechanics at ultrasonic frequencies, Fatigue and Fracture of Engineering Materials and Structures 22, 7, 1999, 567-579

[191]   C. Berger, B. Pyttel, T. Trossmann: Very high cycle fatigue tests with smooth and notched specimens and screws made of light metal alloys, International Journal of Fatigue 28, 11, 2006, 1640-1646

[192]   F. Nový, M. Chalupová, M. Cincala, Z. Zúberová: Ako je to vlastne s iniciaciou unavovych trhlin?, LSUM – Summer School – Fatigue of Materials, Terchová, Slovak Republic, 2006, 196-203

[193]   Y. Chino, T. Furuta, M. Hakamada, M. Mabuchi: Influence of distribution of oxide contaminants on fatigue behaviour in AZ31 Mg alloy recycled by solid-state processing, Materials Science and

Engineering A 424, 1-2, 2006, 355-360

[194]   L. Kunz, P. Lukáš, Y. Estrin, Z. Zúberová: Notch sensitivity of cast AZ31 magnesium alloy, Materials Engineering, Vol. 12, 3, EDIS – ŽU Žilina, Slovak Republic, 2005, 88-92

[195]   C.M. Sonsino, K. Dieterich, L. Wenk, A. Till: Fatigue design with cast magnesium alloys, Ed. K.U. Kainer, Proceeding of the 6th International Conference: Magnesium Alloys and their Application, 2000, 304-311

[196]   W.D. Pilkey: Peterson`s stress concentration factors, Wiley Interscience Publication, New York, 1997

[197]   M. Tsujikawa, H. Somekawa, K. Higashi, H. Iwasaki, T. Hasegawa, A. Mizuta: Fatigue of welded magnesium alloy joints, Materials Transactions, Vol. 45, 2004, 419-422

[198]   M. Kuffová, F. Nový, M. Chalupová: Fatigue resistance of AZ91D and AZ63HP magnesium alloys at high frequency cyclic loading, Materials Engineering, Vol. 10, No. 4, 2003, 21-28

[199]   Y. Unigovski, A. Eliezer, E. Abramov, Y. Snir, E.M. Gutman: Corrosion fatigue of extruded magnesium alloys, Materials Science and Engineering A360, 2003, 132-139

[200]   A. Eliezer, E.M. Gutman, E. Abramov, Ya. Unigorski: Corrosion fatigue of die-cast and extruded magnesium alloys, Journal of Light Metals 1, 3, 2001, 179-186

[201]   R. Doldon: The fatigue behaviour of magnesium-zirconium and magnesium-aluminium canning materials, Journal of Nuclear Materials 8, No. 2, 1963, 169-178

[202]   F. Nový, P. Palcek, M. Chalupová: Failure of AK 4-1 Al-alloy under creep-fatigue interaction conditions, Kovové materiály, 43, 2005, 447-456

[203]   E.M. Gutman, Y. Unigovski, A. Eliezer, E. Abramov: Mechanoelectro-chemical behaviour of pure magnesium and magnesium alloys stressed in aqueous solutions, Journal of Materials Synthesis and Processing, Vol. 8, 2000, 133-138

[204]   P. Zhang, J. Lindemann: Effect of roller burnishing on the high cycle fatigue performance of the high-strength wrought magnesium alloy AZ80, Scripta Materialia 52, 10, 2005, 1011-1015

[205]   V. Kree, J. Bohlen, D. Letzig, K.U. Kainer: The metallographical examination of magnesium alloys, Practical Metallography, Vol.XLI, May 2004

[206]   M. Klesnil, P. Lukáš: Fatigue of Metallic Materials, Praha 1992, Academia/Elsevier

[207]   M. Svoboda, M. Pahutova, K. Kucharova, V. Sklenicka, T.G. Langdon: The role of matrix microstructure in the creep behaviour of discontinuous fiber-reinforced AZ91 magnesium alloy, Materials Science and Engineering A324, 1-2, 2002, 151-156

[208]   J. Wendt, V. Supik, P. Zhang, J. Zhang: Mechanical properties of hot-rolled magnesium AZ31 sheets, Magnesium: Proceedings of the 6th International Conference Magnesium Alloys and Their Applications, Ed. K.U. Kainer, Wiley-VCH, 2003, 439-443

[209]   M.R. Barnett, M.D. Nave, C.J. Bettles: Deformation microstructure and texture of some cold rolled Mg alloys, Materials Science and Engineering A 386, 1-2, 2004, 205-211

[210]   M. Mabuchi, Y. Yamada, K. Shimojima, C.E. Wen, Y. Chino, M. Nakamura, T. Asahina, H. Iwasaki, T. Aizawa, K. Higashi: The grain size dependence of strength in extruded AZ91 Mg alloy, Magnesium Alloys and their Applications, Ed.: K.U. Kainer, Wiley-VCH, 2000, 280-284

[211]   H.K. Kim, W.J. Kim: Microstructural instability and strength of an AZ31 Mg alloy after severe plastic deformation, Materials Science and Engineering A385, 1-2, 2004, 300-308

[212]   G. Quan, J. Heerens: Analysis of deformation and fracture mechanisms in Mg-AZ31 sheet material, International Conference: Magnesium Alloys and Their Applications 2003, Ed. K.U. Kainer, Wiley-VCH, 2003, 489-494

[213]   S. Kamado, T. Ashie, H. Yamada, K. Sanbun, Y. Kojima: Improvement of tensile properties of wrought magnesium alloys by grain refining, Materials Science Forum Vols. 350-351, 2000, 65-72

[214]   Z. Zúberová, Y. Estrin, T.T. Lamark, M. Janeček, R.J. Hellmig, M. Krieger: Effect of equal channel angular pressing on the deformation behaviour of magnesium alloy AZ31 under uniaxial compression, Journal of Materials Processing Technology 184, 2007, 294-299